A Space Communications Study

Final Report

September 15, 1965 - September 15, 1966

Prepared for

National Aeronautics & Space Administration

Electronic Research Center

under

NASA GRANT NGR-33-006-020

DEPARTMENT OF ELECTRICAL ENGINEERING
POLYTECHNIC INSTITUTE OF BROOKLYN

A Space Communications Study

Final Report

September 15, 1965 - September 15, 1966

Prepared for

National Aeronautics & Space Administration

Electronic Research Center

under

NASA GRANT NGR-33-006-020

Principal Investigators

Kenneth K. Clarke, Professor

Raymond L. Pickholtz, Assistant Professor

Donald L. Schilling, Associate Professor

DEPARTMENT OF ELECTRICAL ENGINEERING
POLYTECHNIC INSTITUTE OF BROOKLYN

TABLE OF CONTENTS

Introduction

This final report summarizes all of the research sponsored by the National Aeronautics and Space Administration under grant NGR - 33 - 016 -020 for the period Sept. 15, 1965 through Sept. 15, 1966. This grant has supported the work of over 30 masters students, and 5 doctoral students. In addition, 4 technical papers have already been published and presented at technical symposia, and several more have been submitted for publication. The work begun under this grant is of great interest to scientists working in the space communication area, and is being continued.

The research supported by this grant deals mainly with the reception of frequency modulated signals passed through deterministic and random time-varying channels. Optimum receivers such as Bayes and maximum likelihood estimation as well as the suboptimum phase lock loop and FM discriminator were studied.

The emphasis has been mainly on the reception of digital data although some novel techniques for processing analog and telemetry type of information have also been investigated. Theoretical and experimental research were simultaneously performed and complemented each other. Some computer studies have been initiated to compare the behavior of optimal and suboptimal receiver structures and initial results of this program have led to improvement in the suboptimal receivers (e.g., spike detection and elimination schemes which lead to reduced threshold are lower error rates).

The theoretical aspects of the research performed under this grant has led to new receiver structures for the demodulation of digital and analog signal and has served as a base for the deeper understanding of communications problems. The experimental research was employed not only to verify our theoretical results, but also led to the discovery of new ideas for improving system performance. This experimental research, in fact, constituted approximately 50% of the total effort.

The participants in this program were:

Professor R. Boorstyn
Professor K. Clarke
Professor P. Crepeau
Professor D. Hess
Professor R. Pickholtz
Professor H. Schachter
Professor D. Schilling
Messrs A. Guida
E. Hoffman
J. Maskasky
E. Nelson
J. Oberst
P. Osborne
M. Unkauf

The final report was prepared by:

Professors K. K. Clarke (Sections III B, C, IV)
R. L. Pickholtz (I A, C, V)
D. L. Schilling (I B, II, III A)

IA Recursive Optimum Detection

IA. 1 Introduction - The classical problem of detection of binary signals in additive Gaussian noise has been treated in various ways. A considerable amount of this theory involves integral equations which are difficult to solve and/or interpret as realizable physical structures. The basic formulation uses the Karhunen-Loeve expansion to express the likelihood ratio (for example, see (1)- (3)). The success of determining the likelihood ratio using the Karhunen-Loeve expansion depends on the type of kernel in the resulting integral equation. It is often a formidable task to compute the likelihood ratio for any but the simplest kernels. (see (1), (2)). Furthermore, even when the integral equation can be solved, the result is not in a form which is suitable for a digital computer mechanization of the detector. The purpose of the investigation is to derive a difference equation for the likelihood ratio so that a real time, recursive computation is available for the detection of digital signals. Recently, Schweppe (4) suggested a different method applied to the detection of random signals. His basic idea of expressing the likelihood ratio into products involving the conditional densities has been exploited further to include the practical problems of non-white noise and known signals. The limiting cases were then developed to yield a differential equation for the likelihood ratio. This equation also, is easily implemented on an analog computer. The advantages of the results are:

(1) A real time computational scheme suitable for a digital (or analog) computer.

(2) The required parameters are based on relatively easily measureable quantities.

(3) Avoiding the problem of solving the integral equations and correspondingly troublesome end conditions.

(4) Results are in a form which makes it relatively easy to investigate the problem of signal selection for minimum probability of error.

IA. 2 Problem Statement and Outline of Solution

One of the two known binary signaling waveforms $S^{(1)}(t)$ or $S^{(2)}(t)$ is transmitted and received imbedded in an additive. Gaussian noise random process, N(t).

$$R(t) = S(t) + N(t) \quad 0 \leq t \leq T \tag{IA-1}$$

T is running time.

To derive the difference equation, N Samples are taken Δ seconds apart such that

$$\Delta = \frac{T}{N} \quad . \tag{IA-2}$$

The likelihood ratio is then written in terms of the conditional probability density functions as follows:

$$\Lambda(n\Delta) = \frac{f_1[r(n\Delta) \mid r(n-1)\Delta|, \ldots, r(\Delta)]}{f_2[r(n\Delta) \mid r(n-1)\Delta, \ldots, r(\Delta)]} \tag{IA-3}$$

If the noise is Gaussian, then

$$f_j[r(n\Delta) \mid r((n-1)\Delta), \ldots, r(\Delta) = \frac{1}{\sqrt{2\pi}\sigma_{n,j}(n|n-1)} \exp$$

$$- \frac{[r(n\Delta) - \overline{R};(n|n-1)]^2}{2\sigma^2_{n,j}(n|n-1)}$$

where $\overline{R};(n|n-1)$ and $\sigma^2_{n,j}(n|n-1)$

are the conditional mean and variance of the received signal given the past data under condition that signal j (1, 2) was transmitted. The logarithm of the likelihood ratio θ_n, at the nth sample time is then given by

$$2\sigma^2_{n,j}[\theta - \theta_{n-1}] = [r(n\Delta) - S^{(2)}(n\Delta) - \overline{R}_1(n|n-1)]^2$$

$$- [r(n\Delta) - S^{(1)}(n\Delta 1 - \overline{R}_2(n|n-1)]^2 \tag{IA-4}$$

The heart of the problem is the computation of the conditional mean and variance of the noise from the auto correlation (or spectrum) of the noise. However, this is particularly simple for Gaussian noise since, by least squares estimation theory the conditional mean in that linear function of the data which minimizes the mean square error (see (5)).

$$\text{or} \quad \overline{R}_1(n|n-1) = S^{(1)}(n\Delta) + \sum_{i=1}^{m} a_i[r(n-i) - S^{(1)}(n-i)] \tag{IA-5}$$

Now the a_i are determined by a set of m simultaneous linear equations whose coefficiencies are the autocorrelation of the noise. In solving for the a_i in a practical situation, use can be made of the markov nature of the noise if it is colored since this noise is often the result of passing white noise through a filter such as an I. F. amplifier. For white noise, the result is particularly simple and the difference equation is given by:

$$\theta_n - \theta_{n-1} = \frac{2}{N}[S^{(1)}(n\Delta) - S^{(2)^2}(n\Delta) + S^{(2)^2}(n\Delta) - S^{(1)^2}(n\Delta)] \tag{IA-6}$$

The mechanization of (IA-6) is shown in figure IA-1 and requires only one unit of memory.

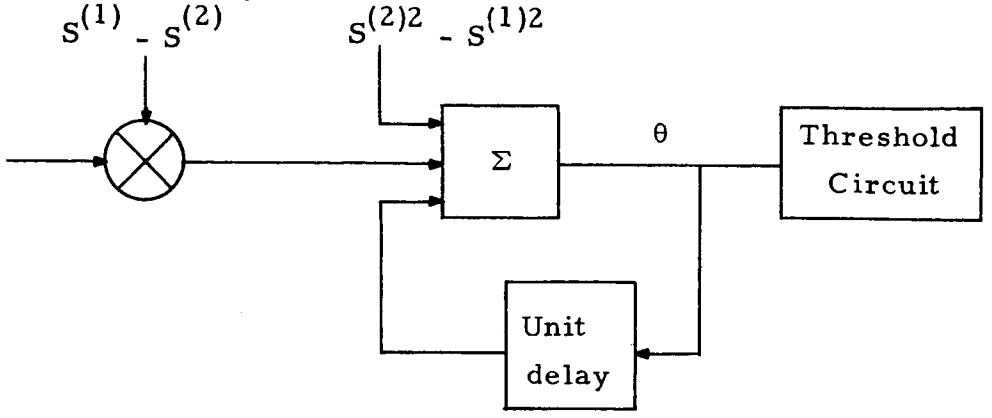

Figure IA-1 - Mechanization for White Noise

The limiting case where the sampling interval Δ shrinks to zero reduces (IA-6) to a differential equation (with zero initial conditions) given by

$$\theta^{1}(t) = \frac{2}{N_o}\, r(t)\,[S^{(1)}(t) - S^{(2)}(t)] + \frac{1}{N_o}\,[S^{(1)}(t)]^{2} - \frac{1}{N_o}\,[S^{(2)}(t)]^{2}$$

which, when integrated is the familiar matched filter solution to the detection problem in white noise.

IB-3 Summary of the General Results

The formulation of the difference equation (IA-4) is perfectly general, the only necessary assumption being the gaussian statistical structure of the received signal. The problem is then to express all entries in the difference equation in terms of the known quantities, i.e. signal and noise covariance. The following canonical structure results

$$2\sigma^{2}[\theta_n - \theta_{n-1}] = 2\,P(r)\,[P(S^{(1)}) - P(S^{(2)})] + P^{2}(S^{(2)}) - P^{2}(S^{(2)})$$

$$P(z) = -\sum_{i=0}^{m} a_i z_i \qquad \text{(IA-7)}$$

The a_i have been worked out in detail for the two most important non-white noise cases with power spectral densities:

(i) $S_n(w) = Q\,\frac{B}{B^{2}+w^{2}}$ [R-c low pass]

or $R_n(\tau) = Q\,e^{-B|\tau|}$

(ii) (ii) $R_n(\tau) = M \cos w_{0}\tau\; e^{-B|\tau|}$ [band pass]

The general mechanization of (IA-7) is shown in figure IA-2. The P-Generator acting on the received signal sequences behaves somewhat like a prewhitening filter (but not quite). The structure operates in real time. For the two cases cited above the coefficients a_i calculate as follows:

(i) $a_o = 1,\ a_1 = e^{-B\Delta}$

all other $a_i = o$

(ii) $a_o = 1,\ a_1 = e^{-B\Delta} \cos w_o\Delta \dfrac{1 - e^{-2B\Delta}\cos 2w_o\Delta}{1 - e^{-2B\Delta}\cos^2 w_o\Delta}$

$$a_2 = e^{-2B\Delta} \frac{\cos^2 w_o\Delta - 1}{1 - e^{-2B\Delta}\cos^2 w_o\Delta}$$

all other $a_i = o$

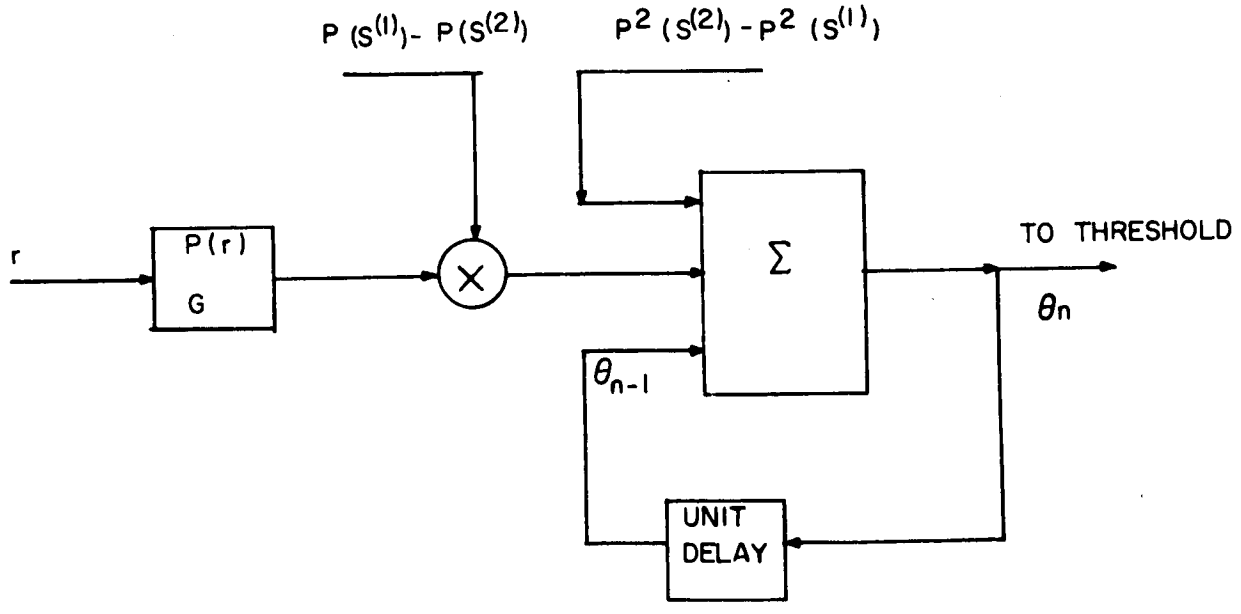

Figure IA-2 General Detector Structure

Further results for any arbitrary rational spectrum can be obtained by solving simultaneous linear equations. Notice that the P-Generators are particularly simple since only two delay elements are needed.

The limiting continuous equations have also been derived [6] for case (i) and together with the boundary conditions, yield results which are consistent with the integral equation solutions in (1).

The signal to noise ratio at the output is given by

$$S = \frac{2}{B^2} \int^{T} [S'(t) - B\,S(t)]^2\, dt \qquad \text{(IA-8)}$$

and the error probability is given by

$$P_e = \frac{1}{2} - \text{erf}\ \frac{S-K}{\sqrt{2S}} \qquad \text{(IA-9)}$$

IA. 3 Optimum Signals

The recursive method tends itself readily to the investigation of signals which, with certain constraints, minimize the Probability of error. Thus, for an "Energy-Bandwidth" constraint on the signals in 1st order noise, the best signals are found by applying the calculus of variations to maximize (IA-8) subject to the constraint that the product of bandwidth and Energy, Ω E (suitably defined) is constant. The result is

$$S(t) = \frac{\Omega}{\pi} \sqrt{2TE}\ \text{Sin}\ \frac{\pi}{T}\ t$$

and under these circumstances, the signal to noise ratio is given by

$$\frac{2\Omega^2 E}{B^2} \left[\left(\frac{BT}{\pi}\right)^2 + 1 \right]$$

IA. 4 Conclusions

The technique of setting up detection problems in the form of difference equations (or differential equations) is not yet fully exploited. There are many important practical communications applications which can benefit from further study. An example is the sequential detector which is ideally suited for deep space communications due to the availability of a relatively noise-free earth-space channel. Another, is the problem of a random channel. Furthermore, the problem and its solution

are formulated in a way which makes the results very compatible with modern digital computer processing of the data. More complicated adaptive techniques shoud be investigated for the problems involving unknown parameters and non-gaussian noise. The results are, of course, applicable to the immediate problems of digitally processing existing data communications such as FSK, biphase and bipolar transmissions; but more important is the possibility of analytically deriving optimum signals for binary (and M-ary) signalling.

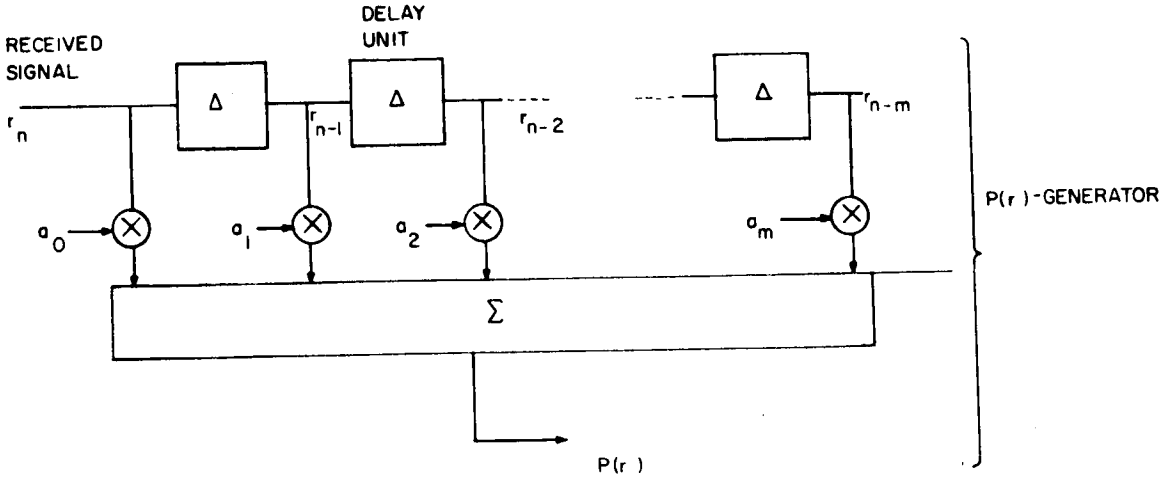

Fig. AI - 2(b) P. Generator

BIBLIOGRAPHY - Section IA

(1). Helstrom, C. W., Statistical Theory of Signal Detection, Pergamon Press, 1960.

(2). Selin, I., Detection Theory, Princeton University Press, 1965.

(3). Middleton, D., An Introduction to Statistical Communication Theory, McGraw-Hill, 1960.

(4). Schweppe, F. C., "Evaluation of Likelihood Functions For Gaussian Signals," IEEE Trans. on Information Theory, Vol. IT-11, No., pp. 61-70; (Jan. 1965).

(5). Papoulis, A., Probability, Random Variables, and Stochastic Processes, McGraw-Hill, 1965.

(6). Kleinberg, L., "Evaluation of Likelihood Ratios" MS Thesis - Polytechnic Institute of Brooklyn, Sept. 1966, R. L. Pickholtz, advisor.

IB Bayes Estimation of F. M. Signals In Randomly Fading Channels

IB. 1 Introduction

This section is concerned with the optimum demodulation of frequency and phase modulated signals which have been trasmitted through random fading channels and corrupted by additive gaussian disturbances. The ultimate objective of this investigation is to derive physically realizable receivers which will yield "best" continuous estimates of transmitted modulating signals. The criterion for optimality is chosen to be the Bayes criterion in which the errors are weighted quadratically.

The problem as stated is related to a vast amount of literature written during the past two decades, a period in which communication theory has taken on a decidedly statistical character. The first significant breakthrough was made by Wiener[1] who in 1944 solved the problem of optimumly filtering signals in noise. In Wiener's approach, only linear operations are used and his results yield a lower mean-squared error than any other linear filter. Subsequently, the question was raised: What might be done if the linearity requirement is dropped and the receiver structure is not determined a priori (as the Wiener's linear filter)? Or again, what possibilities are presented if one replaced the minimum mean-squared error optimality requirement by some other criterion? If so, which one? These are legitimate questions, particularly in view of the fact that the application of linear mean square estimation to FM signals had not then, and still has not, produced meaningful results.

The first important advance toward an optimum demodulation theory was made by Lehan and Parks[2]. They showed how a statistical solution to the FM demodulation problem could be implemented by a phase-locked loop configuration. However their work lacked mathematical rigor, and it remained for Youla[3] to place it on a firm mathematical foundation. In Youla's formulation the minimum mean-square error criterion was replaced by the maximum a posteriori (MAP) likelihood criterion. This approach leads to integral equations, which, when solved, yield optimum receivers.

At about the time that Youla was solving the FM demodulation problem, Thomas[4] was utilizing similar techniques to solve the AM problem. Gradually extensions to these formulations began to appear. The integral equations for the multidimensional FM problem were presented by Thomas and Wong[5]. More recently, Schwartz[6] and Van Trees[7] have extended the Youla MAP solution for the FM problem so as to include the effects of random fading channels. In the random channel problem, Van Trees followed the approach of Youla of expanding the signal process into an orthogonal series having statistically independent coefficients (Karhunen-Loeve expansion). Alternatively, Schwartz solves essentially the same problem employing elegant coordinate free representations which, among other things, enabled him to re-derive Youla's earlier deterministic channel results with extraordinary simplicity.

Aside from the MAP optimizing criterion, another approach which has received recent attention is the Bayes criterion. Middleton[8] has utilized Bayes theory in order to estimate signal waveforms. The main difficulty is, however, that his receiver realizations are composed of filters whose impulse responses are eigenfunction solutions to integral equations. Except in rare instances, his results are impractical.

Pertinent to our problem, Abbate and Schilling[9] have investigated the FM optimum analog demodulation problem in deterministic channels by using Bayes criterion with quadratic weighting of errors as a basis for optimization. Their resulting estimators are realizable as open loop arrangements of matched filters and simple computer operations. These results seem quite promising, but their merit is difficult to evaluate because no crucial comparison has yet been made between MAP techniques and Bayes tehcniques.

In the present work, the Bayes formation as presented by Abbate and Schilling is extended and amplified in order to implement optimum demodulators for FM signals in random fading channels.

IB. 2 Statement of the Problem

The problem will first be stated in its generic form from which a variety of special cases will emerge.

Assume that a set of m antennas receive the following vector signal:

$$\underset{\sim}{\vec{v}}(t) = \underset{\sim}{\vec{x}}\,|t|\cos[w_o t + \underset{\sim}{a}(t)] - \underset{\sim}{\vec{y}}(t)\sin[w_o t + \underset{\sim}{a}(t)] + \underset{\sim}{\vec{n}}(t),\quad 0 \leq t \leq T \quad \text{(IB. 1)}$$

The multiplicative channel fluctuation vectors, $\underset{\sim}{\vec{x}}(t), \underset{\sim}{\vec{y}}(t)$, as well as the additive receiver noise vector $\underset{\sim}{\vec{n}}(t)$ are assumed to be vector gaussian random processes which are statistically independent from each other; however, the components of $\underset{\sim}{\vec{x}}(t)$ and $\underset{\sim}{\vec{y}}(t)$ may be correlated among themselves, and correlation matrices for each are given for each. Furthermore, the noise components of $\underset{\sim}{\vec{n}}(t)$ are assumed to be uncorrelated from each other.

It is desired to estimate, using Bayes criterion with quadratic cost function, the random process $\underset{\sim}{a}(t)$ in the interval (0, T). The relative ease with which $\underset{\sim}{a}(t)$ may be estimated, depends upon the simplifications that one chooses to make in the problem. Specifically, the following sets of alternatives are presented by the foregoing general formulation.

(a) If either x(t) or $\underset{\sim}{\vec{y}}(t)$ is a null vector, the channel introduces amplitude variations only. Otherwise the channel introduces phase fluctuations, and in that case, either a Rayleigh or Rician channel will be assumed. A Rayleigh channel exists for zero-mean processes, $\underset{\sim}{\vec{x}}(t)$ and $\underset{\sim}{\vec{y}}(t)$ and a Rician channel exits when either $\underset{\sim}{\vec{x}}(t)$, $\underset{\sim}{\vec{y}}(t)$ or both, is non-zero mean.

(b) The random processes $\underset{\sim}{\vec{x}}(t)$ and $\underset{\sim}{\vec{y}}(t)$ may represent a channel whose fluctuations are appreciable during the observation interval (0 , T). This is called rapid fading. On the other hand, if the fading rate is slow with respect to this interval, the processes $\underset{\sim}{\vec{x}}(t)$ and $\underset{\sim}{\vec{y}}(t)$ may be replaced by random variables x and $\underset{\sim}{\vec{y}}$. (slow fading)

(c) It might be desired to transmit a constant phase level throughout the interval. In that case, the random process $\underset{\sim}{a}(t)$ is replaced by a random variable θ. The latter possesses the additional alternative of having a probability density which is either a priori discrete or continuous.

(d) If frequency modulation is used instead of phase modulation, $\underset{\sim}{a}(t)$ is simply expressed as the integral $\int_0^t \underset{\sim}{u}(x)\, dx$.

(e) The use of more than one receiving antenna presupposes the use of diversity techniques in order to counteract the deleterious effect of deep fades. If diversity is not required, the use of a single receiver reduces the multidimensional vector problem to a much simpler one dimensional scalar problem.

In the above classification, each entry suggests at least two fundamental situations which might be solved. Clearly this affords a multitude of composite situations. However, in order to avoid gross redundancy, a limited number of selected cases are studied. Within their solutions, however, are inbedded techniques which might be used, at least in principle, to solve any case of the stated problem which might conceivably emerge from a physical situation. A cross-section of these results will now be presented in summary form.

IB. 3 Summary of Results

IB. 31 Bayes Estimators with Quadratic Cost Function

Estimators which are chosen to minimize some average cost of errors are called Bayes estimators. There exist a wide variety of Bayes estimators, depending upon the manner in which cost is assigned to errors. The cost is

is expressed as a function $C(\vec{a}, \vec{a}^*)$ which is assigned to all state space point pairs, $\vec{a}$ and $\vec{a}^*$, , which are respectively the state space vectors representing the signal a(t) (in Eq. IB-1) and its estimate a *(t). When the cost is chosen to be directly proportional to the square of the Euclidean distance between $\vec{a}$ and $\vec{a}^*$, i.e.

$$C(\vec{a}, \vec{a}^*) = C_o(\vec{a} - \vec{a}^*)^2 \qquad \text{(IB-2)}$$

and the resulting Bayes risk is minimized, the Bayes estimator is found to be given by the conditional expectation of $\vec{a}$ given the data v(t).

$$\vec{a}^*_B = E\{\vec{a} | v(t)\} = \int_{\vec{a}} \vec{a} f_{\vec{a}}(\vec{a} | v(t)) d\vec{a} \qquad \text{(IB-3)}$$

Furthermore, it may easily be shown that the Bayes estimator with quadratic cost function given by Eq. IB-3 is also the minimum mean s quare error estimator.

IB.32 Estimation of Discrete Random Variables in Slowly Fading Channels

The objectives of this phase of the study are twofold:

(1) to realize component implementations which will yield the desired Bayes estimators and (2) to decide whether PSK or FSK is more suitable for use in Gaussian, Rayleigh, and Rician multipath channels.

For the case of estimation of phase and frequency discrete random variables in slowly fading channels, the following situations are found to lead to reasonably simple physically realizable results:

(a) PSK in Gaussian amplitude channels

(b) FSK in Rayleigh channels

(c) PSK in Rician channels

In case (a) the problem was considered wherein a signal of known frequency, whose phase is quantized to levels θ_i with a priori probability P_i, is transmitted through a channel whose transmission fact is Gaussianly distributed with variance σ^2 about some known mean value. By evaluating the complicated integrals which arise in this case from Eq. IB-3, the following implementation has been derived (as shown in Fig. IB-1).

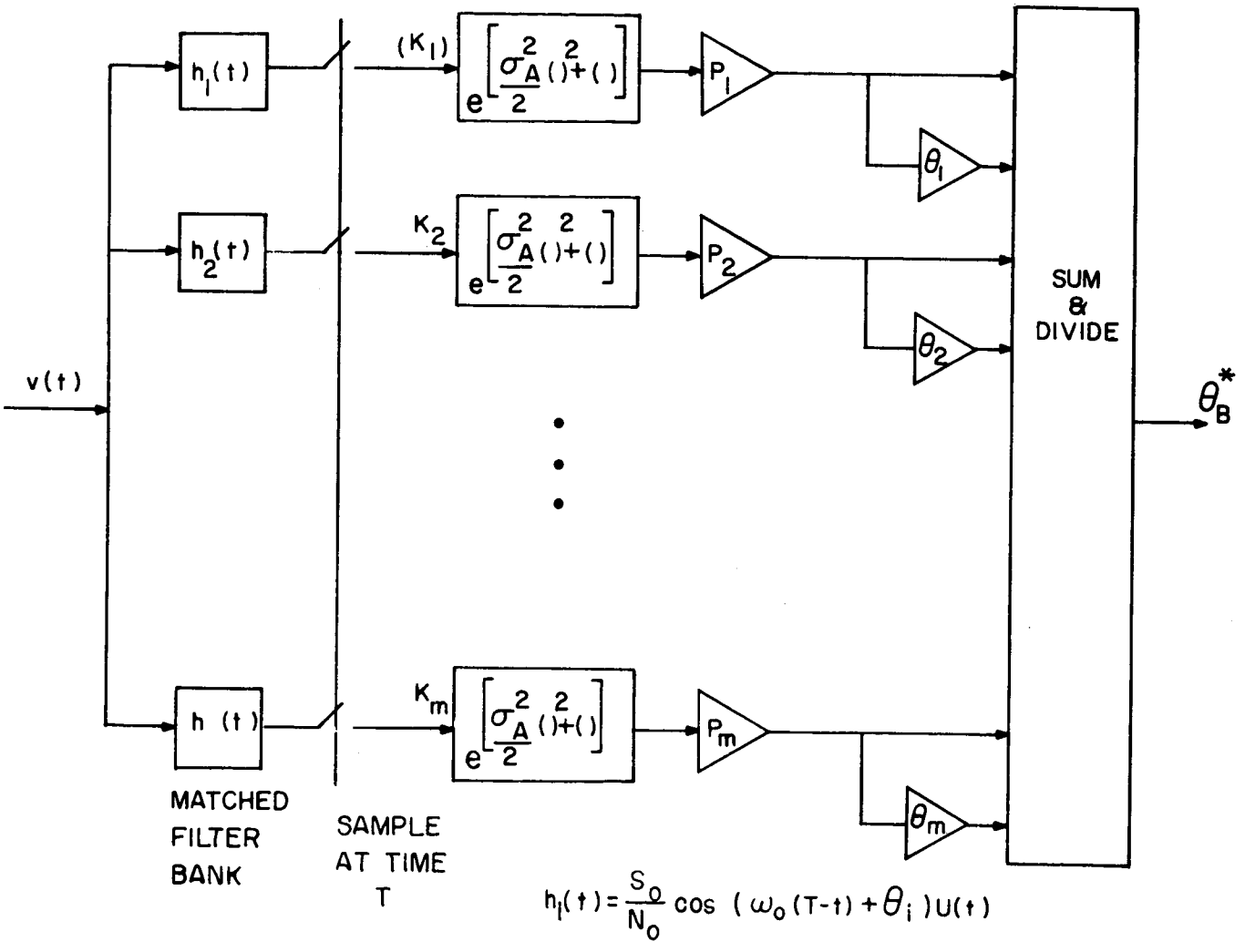

Fig. IB-1

Bayes Estimator for Discrete Phases in Gaussian Amplitude Channel

The implementation illustrated in Fig. IB-1 consists of a bank of matched filters, exponential amplifiers and simple computer elements. It represents a generalization of the Bayes estimator for phase random variables as presented by Abbate and Schilling[9] for the case of deterministic channels. In fact, by letting σ^2 approach zero, the results can be made to coincide identically with those of Abbate and Schilling. Thus the basic effect of channel randomness in this case is to modify the gain of the exponential amplifiers shown in Fig. IB-1.

IB.33 Estimation and Detection

The process of demodulation may be generally regarded as the extraction of information from a received signal which is composed of an information-bearing signal and a corrupting noise signal. The extraction of information may consist of (1) determining the waveshape of the information-bearing signal or determining some unknown parameter of the signal; or (2) deciding which of a finite set of possible alternatives is the true state of the useful signal. The former is a problem of estimation, the latter of detection. In this study detection is accomplished through estimation and accordingly is regarded as a special case of estimation.

The extension of an estimation problem to a detection problem is accomplished by the addition of an ad hoc decision rule which is applied to the estimator output in order to decide upon the true state of the transmitted signal. Suppose, for instance, as in the preceding subsection, that the phase of the signal is an unknown parameter and that it may be transmitted in any of m possible states θ_i, $(i = 1, 2, \ldots m)$, whose a'priori probabilities are known. By using estimating procedures, the "best" estimate θ of the discrete random variable θ_i may be determined. Since θ^* belongs to a continuum of possible values, a decision rule must be introduced in order to assign θ^*. These decisions are denoted by $d(\theta_j)$, by which it is meant that θj was decided upon as the true state. If a particular phase θ_i is transmitted and the decision $d(\theta_j)$ differs from θ_i, then an error of misidentification exists. The conditional probability of this error, given θ_i, is called the probability of error, and this quantity is of great importance

in the comparative evaluation of digital transmission systems.

The decision rule which we have employed consists of selecting the value of θ_j which minimizes the quantity $| \theta_B^* - \theta_j |$, where θ_B^* is the output of the estimator in Fig. IB-1. This is equivalent to constructing decision surfaces which bisect the angles between the a'priori possible transmitted levels. Using this decision rule it has been found that in some cases, the Bayes estimator yields a lower probability of error than the MAP likelihood system, and, in other cases the probability of error is higher than that of MAP. In short, there is no consistent or clear reason for showing the superiority of one estimator over the other.

The need for an ad-hoc decision rule to convert estimated parameters into decisions concerning the true state of a transmitted signal is an inherent disadvantage associated with the use of Bayes estimators in digital systems. For that reason greater attention has been directed toward the use of Bayes estimators in analog modulation systems.

IB.34 Estimation of PM and FM Random Processes Transmitted Through Rayleigh Fading Channels

Consider the scalar case of Eq. IB-1. Assume that ω_o is known and that the process $\underset{\sim}{a}(t)$ is stationary and gaussian with zero mean and variance δ_a^2. The process $\underset{\sim}{a}(t)$ possesses a covariance $R_a(\tau)$ whose Fourier transform $S_a(\omega)$ contains only frequencies which are much less than ω_o. The channel fading processes, $\underset{\sim}{x}(t)$ and $\underset{\sim}{y}(t)$, are also assumed to be stationary, independent, and gaussian with zero mean. Their covariances are identical and denoted by $R_c(\tau)$, and each possess a Fourier transform $S_c(\omega)$ which is also restricted to the region far below ω_o. The noise process $\underset{\sim}{n}(t)$ is assumed to be Gaussian and white, with spectral density N_o watts per cps.

By employing Karhunen-Loeve expansions for all random processes, and using Taylor series expansion techniques for the determination of estimators for the uncorrelated coefficients of the process $\underset{\sim}{a}(t)$, useful results can be obtained over a restricted region of validity. In particular, for

small values of modulating signal power and small values of carrier to noise ratio, first and second order results for Rayleigh channels may be found as shown in Fig. IB-2. These results include both slowly and rapidly fading channels.

The results shown in Fig. IB-2 are particularly useful, in that they are open loop configurations involving multiple filtering operations. Realizability of the filters is insured by incorporating time delays into the system. As a result the estimator output is delayed by some multiple of the observation interval T.

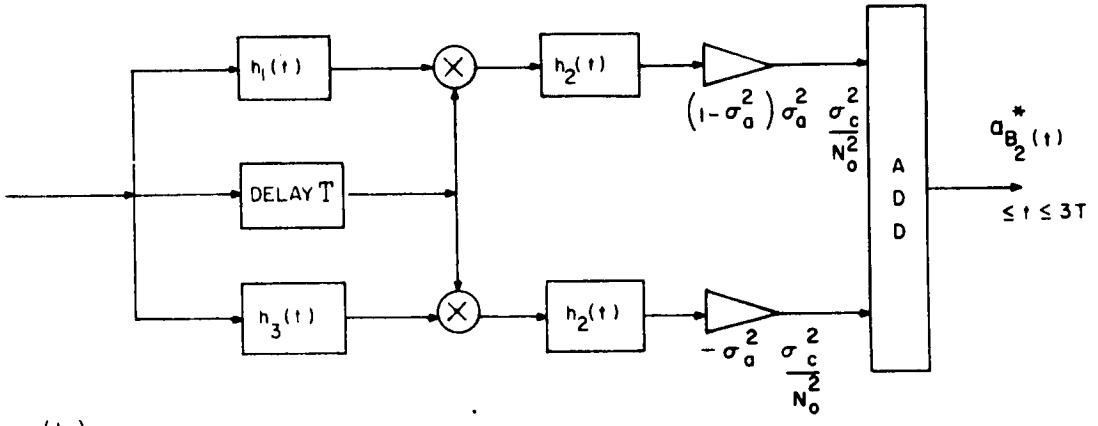

(b)

$$h_1(t) = \begin{cases} \sin w_o(T-t) & \text{- - - - - - - slowly fading channel} \\ \sin w_o(T-t)\, r_c(T-t) & \text{- - - - rapidly fading channel} \end{cases}$$

$$h_2(t) = r_a(T-t)$$

$$h_3(t) = \begin{cases} \sin w_o(T-t)\, r_a(T-t) & \text{- - - slowly fading channel} \\ \sin w_o(T-t)\, r_c(T-t)\, r_a(T-t) & \text{- rapidly fading channel} \end{cases}$$

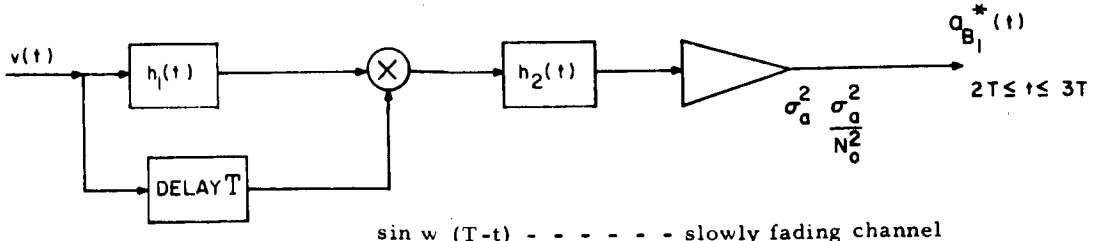

(a)

$$h_1(t) = \begin{cases} \sin w_o(T-t) & \text{- - - - - - slowly fading channel} \\ \sin w_o(T-t)\, r_c(T-t) & \text{- - - rapidly fading channel} \end{cases}$$

$$h_2(t) = r_a(T-t)$$

Fig. IB-2
Approximate Bayes Estimator (a) First Order
(b) Second Order

Bibliography

1. Wiener, N., "Extrapolation, Interpolation, and Smoothing Of Stationary Time Series," MIT Technology Press and John Wiley, New York 1950.

2. Lehan, F.W., and Parks, R.J., Optimum Demodulation, Convention Record of the I.R.E. National Convention, 1953.

3. Youla, D., The Use of the Method of Maximum Likelihood in Estimating Continuous- Modulated Intelligence Which Has Been Corrupted by Noise, Trans. I.R.E., PG IT-3, pp. 90-104, March, 1954.

4. Thomas, J.B., On the Statistical Design of Demodulation Systems for Signals in Additive Noise, Rpt TR-88, August, 1955; Stanford University.

5. Thomas, J.B. and E. Wong, On the Statistical Theory of Optimum Demodulation, I.R.E. PG IT - 7, pp. 420-425, Sept. 1960.

6. Schwartz, M., Maximum A' Posteriori Demodulation of Analog-type Signals Through Random Fading Media, PIB-MRI - 1244-64, December, 1964.

7. Van Tress, H., unpublished paper presented at 1964 IRE WESCON conference.

8. Middleton, D., A Note on the Estimation of Signal Waveform, I.R.E. PGIT - 5, pp. 86-89, June, 1959.

9. Abbate, J., and Schilling D., Optimum Demodulation of Phase and Frequency Modulated Signals by Bayes Criterion, PIB- MRI- 1253-65, June, 1965.

IC Maximum Likelihood demodulation of Signals in Random Channels.

IC.1 Introduction

While the problem in the previous section is concerned with approximating the Bayes solution to the demodulation problem in a random channel, the present chapter treats a more general problem but using the method of maximum likelihood. This includes the very important time dispersive case.

While much of the work on random channels was stimulated by the urgent need to imporve realiability of communications over the ionospheric channel, the results are applicable to a broad class of random channels. Examples of such channels which have come into prominence recently are tropospheric and ionospheric scatter, man-made orbital dipole belts, underwater acoustic transmission and electromagnetic propogation in a turbulent medium. Furthermore, the techniques developed have been used to advance such divers fields as radar astronomy and seismology. It is possible that deep space to earth channels may also fit this category.

The underlying feature of all of the above mentioned work and subsequent work on optimum detection of signals which have been transmitted through a random channel is that it is concerned only with the problem of detection of digital signals. No attempt is made to recover the transmitted waveforms. In contrast, the present work is concerned with the demodulation of continuously modulated waveforms after they have been perturbed by a linear, random channel and additive noise.

The standard method of formulating problems of statistical inference on stochastic processes is to expand the process into a Karhunen-Loeve series with uncorrelated coefficients. Then, by using the properties of the eigenfunctions of the expansion, the results can usually be expressed in terms of integral operations on the observed signal and the eigenfunctions appear nowhere in the result. Thus the eigenfunctions are used only as a coordinate system or basis in an infinite dimensional space. But since the result does not depend on the basis employed, it should be

possible to formulate the problem in its entirety withoug recourse to the eigenfunctions. Several known results have been rederived in a more straight forward and elegant fashion. The basic technique is to treat all signals as points in an abstract vector space and then to define appropriate operations on the vectors without reference to a basis. Using these techniques, the maximum aposteriori probability receiver structures are derived for the case of a non time dispersive channel and for the general time dispersive channel. An application of the results to a modulation scheme using pseudo-noise phase reversals has been worked out. This system is analyzed on the basis of signal to noise ratio and suggests that considerable improvement in performance can be obtained by using the time dispersive effects of the channel in a manner analogous to diversity operation.

The maximum a-posteriori criterion in the case of a purely additive noise channel results in a receiver machanization which may be identified as a phase locked loop. The application of this criterion to more complex channels also results in a phase locked loop, but a more elaborate type. The chief advantage of the maximum a-posteriori criterion for analog demodulation is that it does not presume a particular demodulator structure a-priori and the resulting structures that the results do suggest are practical in a engineering sense.

Only a brief summary of the problem statements and solutions are presented in the following paragraphs. Details may be found in (1).

IC.2 Multiplicative Random Channel

Most physical channels encountered in communications practice affect the transmitted signal amplitude in a manner which is not known

a-priori to the receiver. This "fading" of signals is observed on radio channels as fluctuations in the envelope (and phase) of a transmitted sinusoid. The effect can be represented by multiplying the transmitted signal s(t) by the random process a(t). The received signal is then

$$r(t) = a(t)\, s(t) + n(t) \qquad \text{(IC-1)}$$

where n(t) is the additive noise

The channel represented in this way is a good approximation to a real channel provided that the channel has no memory. In fact, the action of the channel represented by (IC-1)is the most general linear operation without memory that can be performed on input signals s(t). The fact that the channel can only effect the instantaneous signal by multiplication results in a situation where such a channel model cannot account for one of the more troublesome characteristics of real channels, which is the time-dispersive effect on signals. This time dispersion. which results in inter-symbol interference in digital communications and distortion in analog communications can only be accounted for if the channel model includes the effect of memory which clearly (IC-1)does not. Nevertheless, the purely multiplicative channel is, in many cases, a fairly good approximation to a real channel. This would be the case where the channel memory is very small compared to the reciprocal bandwidth of the signals that are transmitted into it. An example is the transmission of very low data rate digital signals say 100 bits/sec. over an H. F. channel using the ionosphere which has a memory no more than a few milli seconds. Then the dispersion of a pulse of duration of tens of milli seconds by one more milli second will hardly effect the reception significantly (unless extremely low error rates are required).

With s(t) modulated by a message signal m(t), and $R_m(s,t)$ and $R_n(s,t)$ the covariance functions of the message and noise respectively, the maximum likelihood condition results in a set of integral equations involving the best estimate of the message m(t) (see [1]). For phase modulation, the integral equations result in a mechanization of an adaptive phase locked loop shown in figure IC-1. The quantatives shown in the figure have been calculated for the case of additive white noise and various types of fading statistics such as Gaussian, Rayleigh and Complex Gaussian (Rayleigh amplitude, uniform phase). In the latter case, the structure shown in figure IC-2 results.

The receiver stuctures in figure IC-1 and figure IC-2 are, in general not realizeable. This is because the low pass filter in the loop has an impulse response $R_m(\tau)$ (stationary case) which is an autocorrelation function of a real random process and there is evein τ. Thus there is response before the impulse is applied and the filter is not casual. It is possible to make the filter itself realizeable if an arbitrarily large delay is permitted. However, the difficulty arises because the filter is inside the loop so that arbitrary delays cannot be tolerated due to stability problems. For large signal to noise ratios, however, the equations defining the loop may be linearized as shown in figure IC-3. Under these conditions the conditional (on a) variance of the loop error may be calculated and averaged over all a (the fading). For gaussian fading, the error variance (power) is given by

$$\frac{\delta_m^2}{\sqrt{2\pi}\ K\delta_a} \exp\frac{1}{4(K\delta_a^2)} K_o \frac{1}{2(K\delta_a)^2}$$

where $K_o(x)$ is the Bessel function of the second kind of zero order. The quantity $(K\delta_a)^2$ is a measure of the averaged (over the fading) signal to noise ratio in the modulation band. The quantities δ_m and $<_a$ are the standard deviations of the message and fading distributions respectively, the result is plotted in figure IC-4. Similar results are plotted in figures IC-5 and IC-6 for the Rayleigh channel and specular channel respectively.

Diversity receiver structures based on maximum likelihood have also been derived (see [1]).

IC-3 Dispersive Channels

For random channels which have a memory comparable to the correlation line of the message signal, one cannot ignore the time dispersive effects produced by the channel. The channel may, for example, have a

"memory" or time spread of the order of several microseconds. This means that if the channel is characterized by a time varying impulsive response $a(t, \tau)$, (the response at time t due to an impulse at time $t-\tau$), then for any t the extend of the response along τ is several microseconds. Such a channel then has a coherent bandwidth of the order of the reciprocal of the total time spread since the time varying transfer function $A(f, t)$ has large effective value for this range of f. The coherent bandwidth sets a limit on the bandwidth of signals which can be transmitted through the ch channel without undue distortion in the case of analog signals or intersymbol interference in the case of digital data transmission. One way of looking at the cause of this distortion is to say that the channel introduces multi-path signals which are scattered from different parts of the channel which interfere with one another. Indeed, when there is a constraint either on the input signal bandwidth or the channel transfer function bandwidth, the channel may be characterized, by the use of sampling theorems, as a tapped delay line structure as in figure IC-7. The various taps may be thought of as multi-path modes.

The RAKE system [?] designed for combating multi-path on the ionospheric channel is essentially a time diversity receiver which, by the use of broadband noise-like transmitting signals allows the receiver to separate the various multi-path returns from the channel by a correlation operation. The original RAKE system as presented by Price and Green, which was designed for digital signals, also included a process for estimating the (complex) channel tap gains. This estimation and particularly the filtering was based on intuitive insight.

We have developed the equations and the receiver mechanizations suggested from them for the reception and demodulation of signals after they have been transmitted through a random, dispersive channel. The technique of maximum a posteriori probability is used and, RAKE receiver structure evolves naturally from the assumed model of the channel. The demodulation problem differs from that of the original RAKE insofar as we are concerned with estimating a message waveform rather than testing the hypothesis that the received signal came from onr or another of a finite ensemble of message symbols (detection). It is assumed that the additive noise component is Gaussian as is the message ensemble. Furthermore, the tap gains on the channel model are assumed to be members of (not necessarily independent) Gaussian

random variables (or processes). For the case of uncorrelated tap gains, the receiver takes on the structure shown in figure IC-8. This can be thought of as a time-diversity maximal ratio combiner [3]. The generalized structures for arbitrary signals and correlated tap gains has been worked out when the tap gain correlation matrix is exponential.

For the case where the transmitted signal is phase-reversal modulated by a pseudo-random binary sequence x(t) with a narrow auto correlation function and the message is phase modulated, it is possible to place the receiver structure into the form shown in figure IC-9. The major advantage here is the removal of the delay line from the loop. The system behaves like a conventional phase locked loop except that the error which drives the loop is diversity derived and combined by what is an essentially a maximal ratio rule.

When the tap gains are uncorrelated, then the SNR improvement in using N taps is N. However, since this is not usually the case, the SNR was calculated when the tap gains are correlated. The result is

$$\mathrm{SNR} = \sigma_a^2 \; \frac{(2N + N^2) + 4\left[\dfrac{N\gamma^2 - \gamma^{2N}}{1-\gamma^2} - \dfrac{\gamma^2 - \gamma^{2N}}{(1-\gamma^2)^2}\right]}{N + 2\left[\dfrac{N-\gamma^N}{1-\gamma} - \dfrac{\gamma-\gamma^N}{(1-\gamma)^2}\right]}$$

This is plotted in figure IC-10 where the parameter CL is a measure of the uncorrelatedness of the taps. $\gamma = \exp - \frac{CL}{N}$. It is seen that the SNR improvement with the number of taps N saturates for rather small N for moderate degrees of correlation. The asymptotic signal to noise ratio improvement is shown in figure IC-11.

IC References

1. Pickholtz, R. L. Demodulation of Signals Transmitted Through a Random Channel", PhD dissertation, Polytechnic Institute of Brooklyn, 1966.
2. Price, R., and Green, P., Jr. "A Communications Technique for Multipath Channels" Proc. I.R.E., Vol. 46 (1958)
3. Van Trees, H.L., Notes for Summer Course in Analog Modulation Theory M.I.T. 1964.

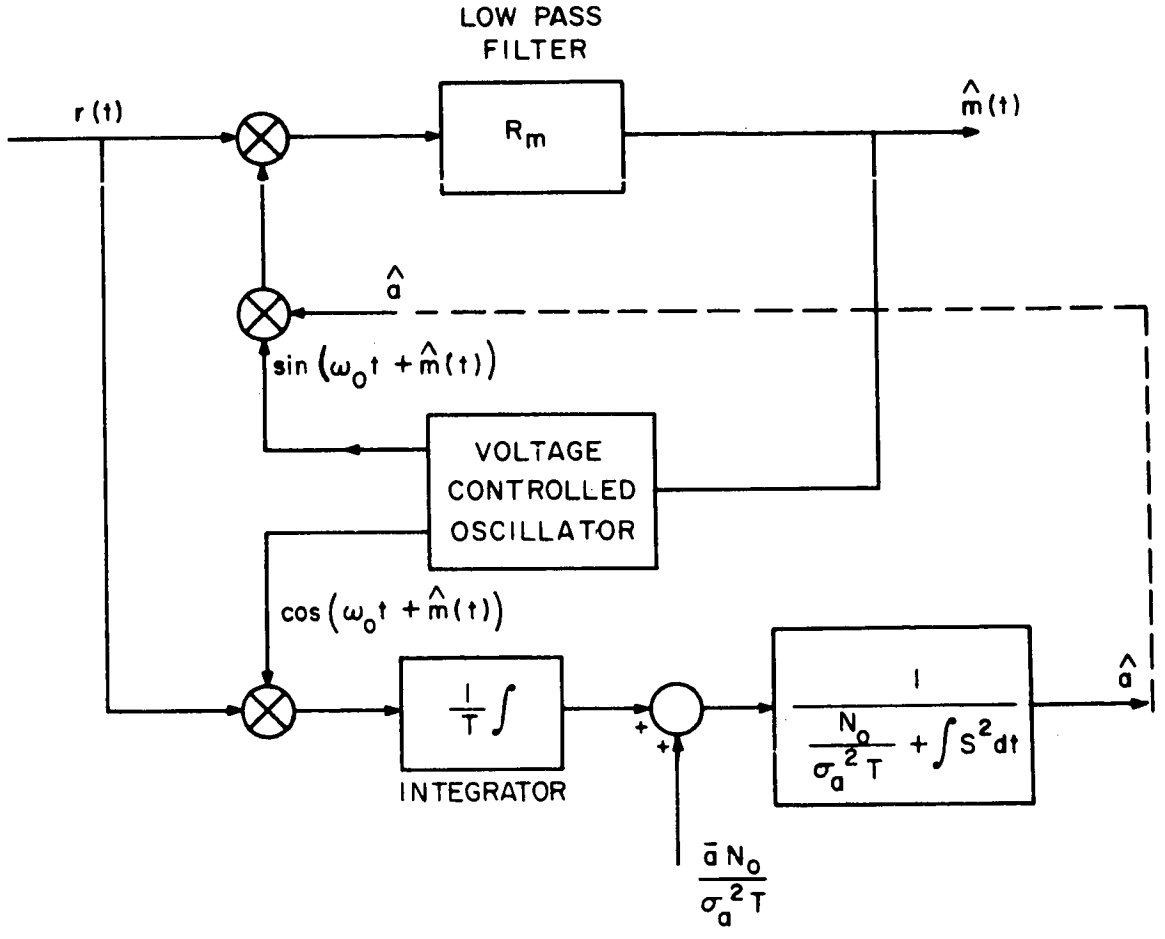

Figure IC-1 Gain Controlled Phase Locked Loop

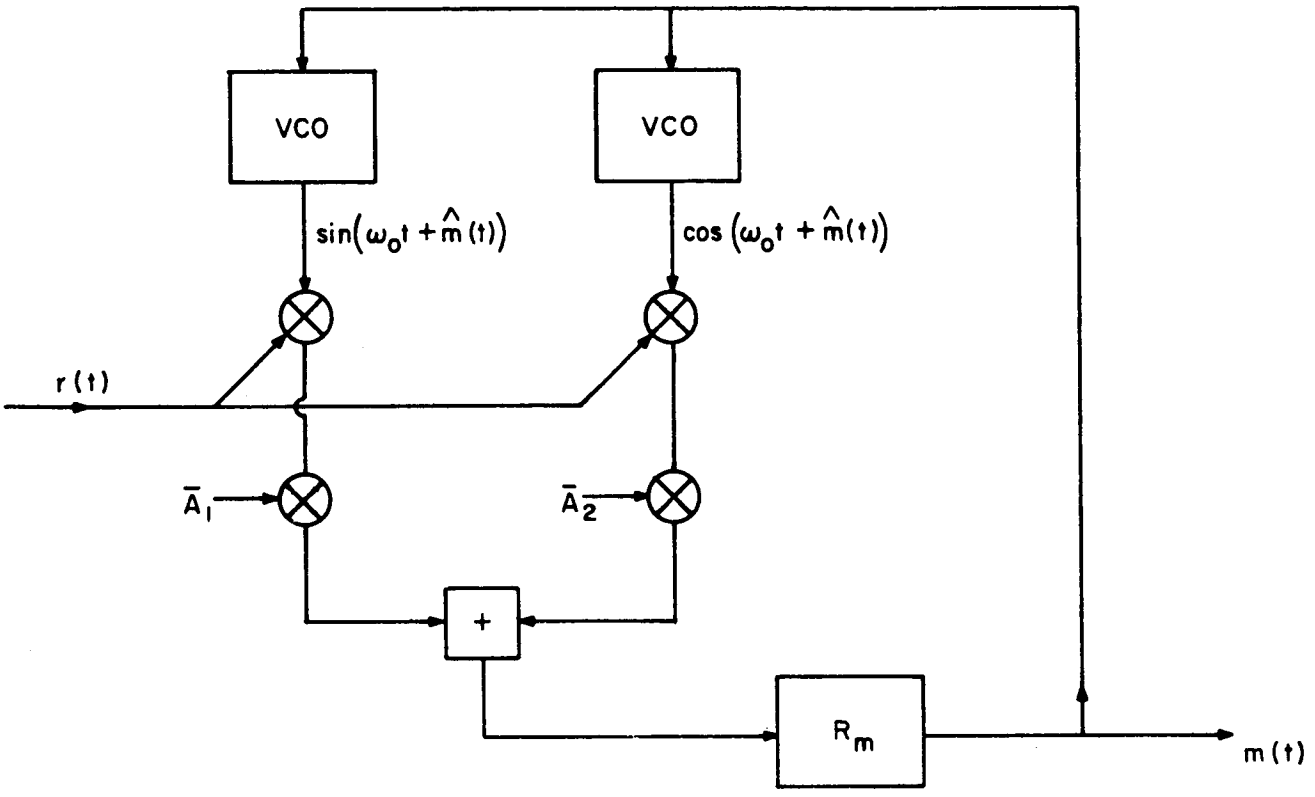

Figure IC-2 Receiver for Fading Amplitude and Phase

The receiver structures in figure IC-1 and figure IC-2 are, in general, not realizeable. This is because the low pass filter in the loop has an impulse response $R_m(\tau)$ (stationary case) which is an autocorrelation function of a real random process and therefore is even in τ. Thus there is response before the impulse is applied and the filter is not casual. It is possible to make the filter itself realizeable if an arbitrarily large delay is permitted. However, the difficulty arises because the filter is inside the loop so that arbitrary delays cannot be tolerated due to stability problems. For large signal to noise ratios, however, the equations defining the loop may be linearized as shown in figure IC-3. Under these conditions the conditional (on a) variance of the loop error may be calculated and averaged over all a (the fading).

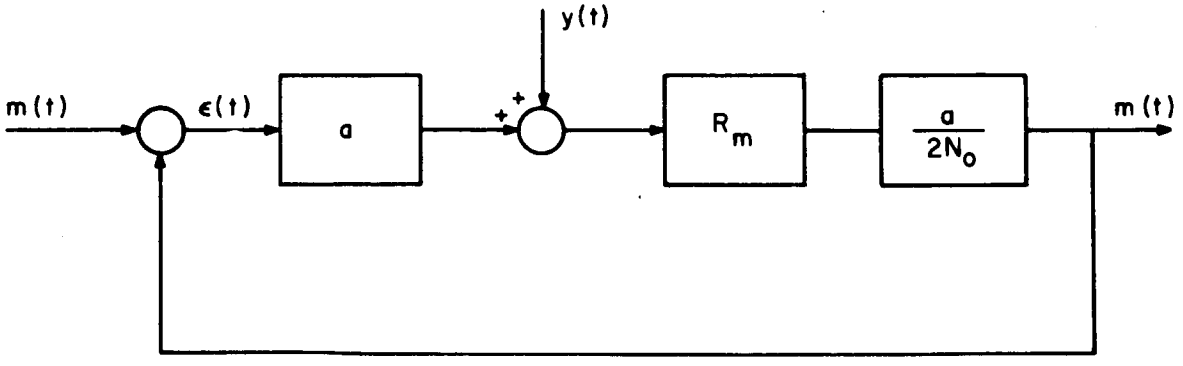

Figure IC-3 Linearized Gain Controlled Phase Locked Loop

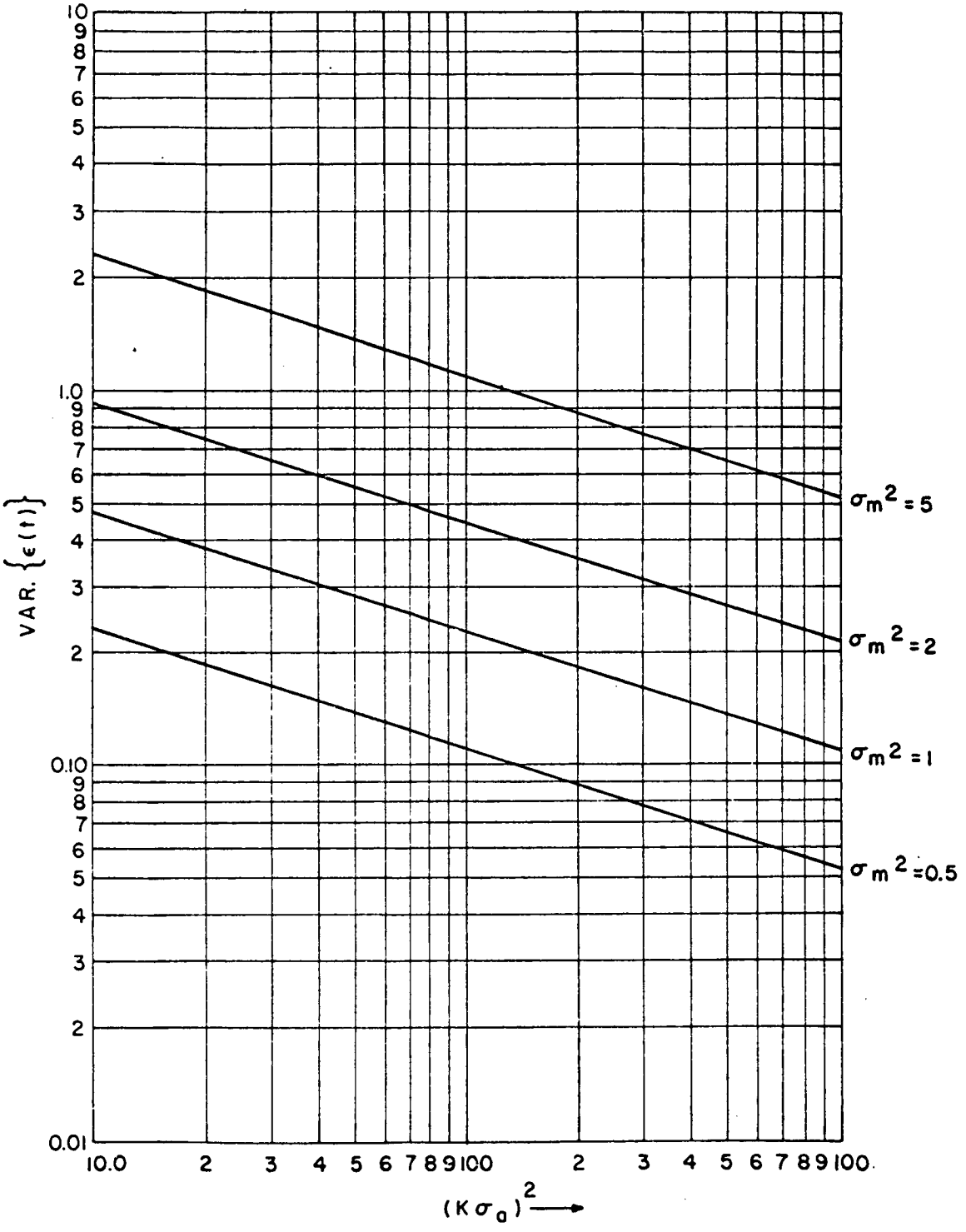

Figure IC-4 Average Error Variance

a is Normal (o, δ_a)

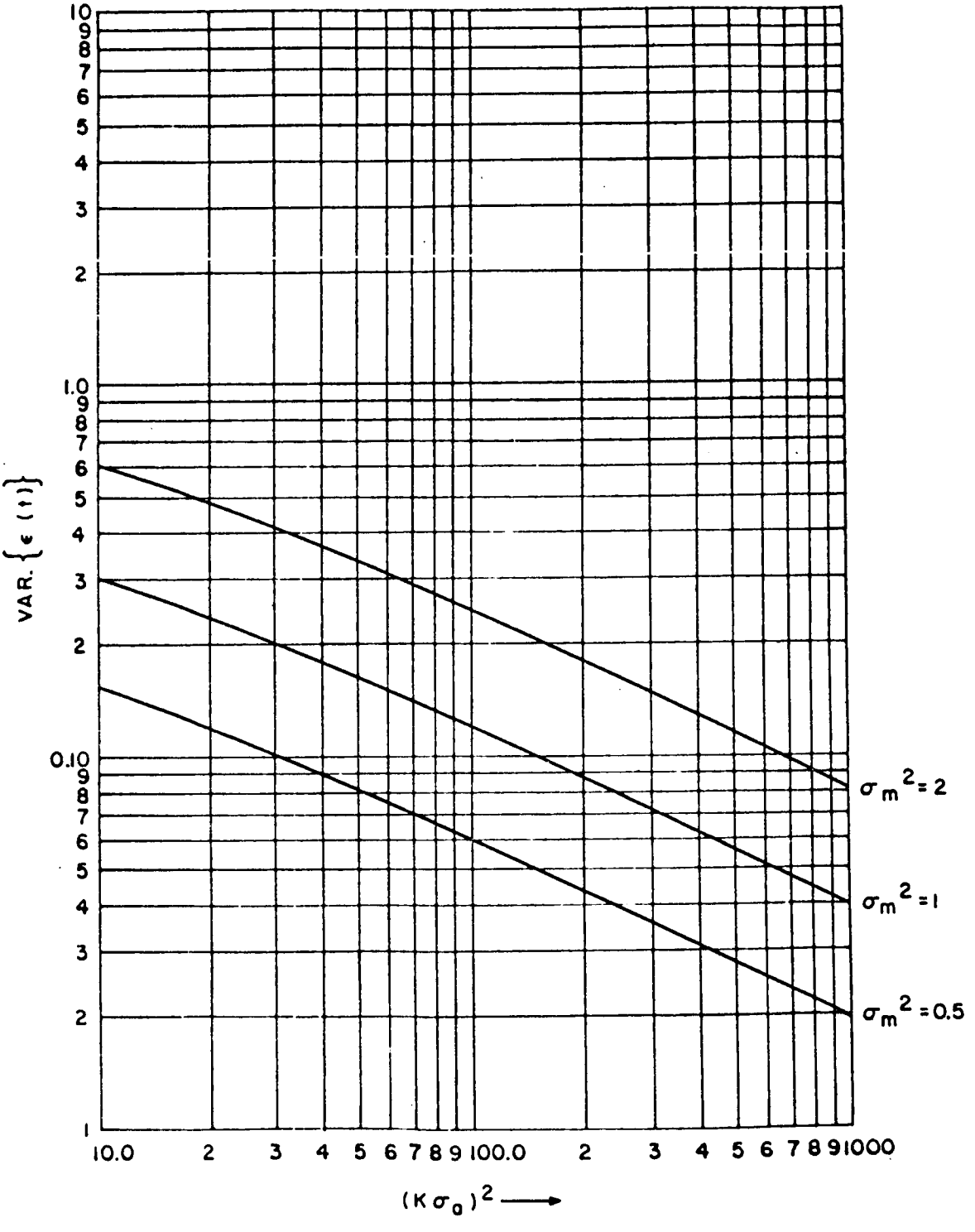

Figure IC-5 Average Error Variance

a is Rayleigh δ_a

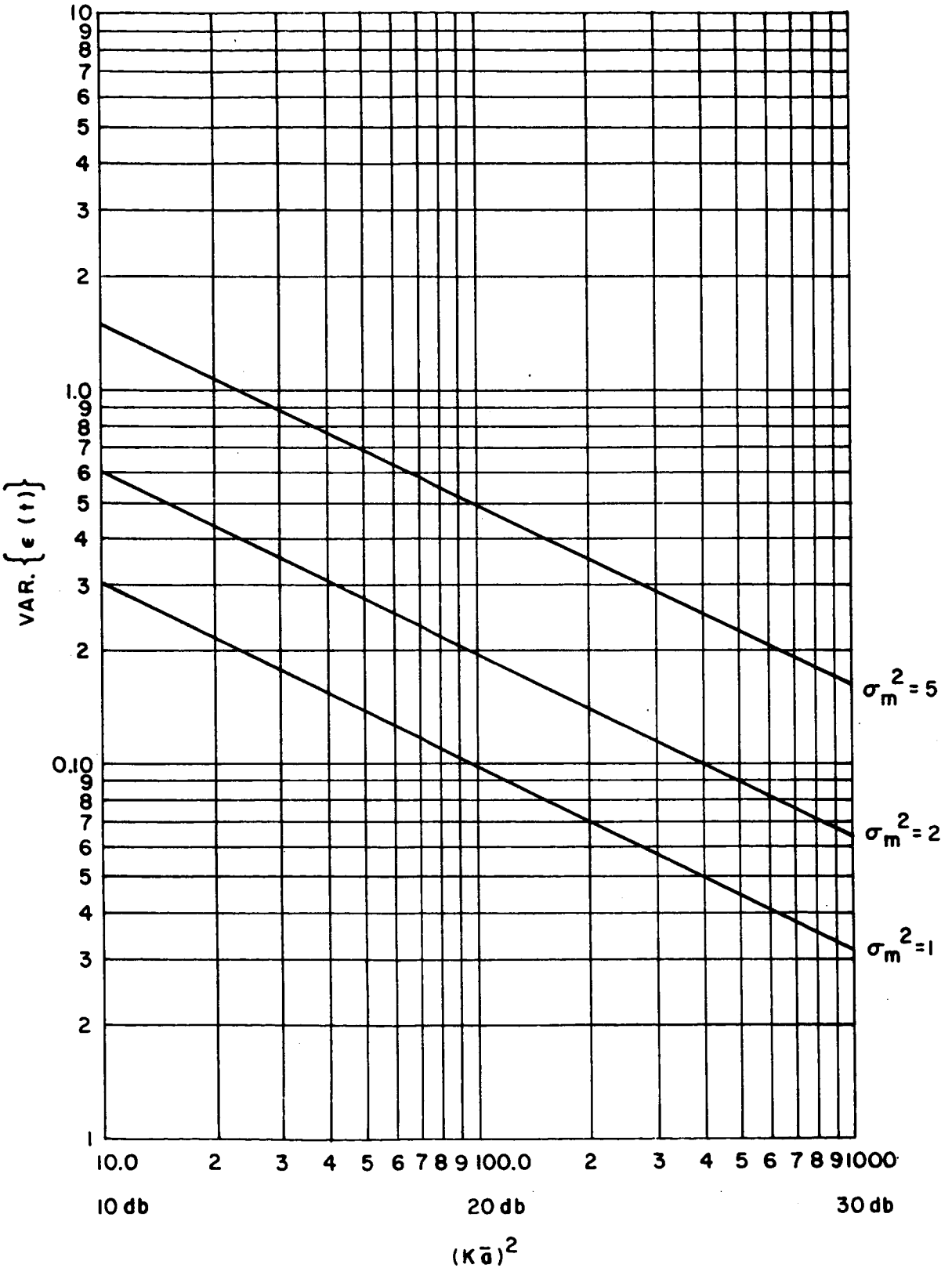

Figure IC-6 Error Variance

Specular Signal Strength $\bar{a}$

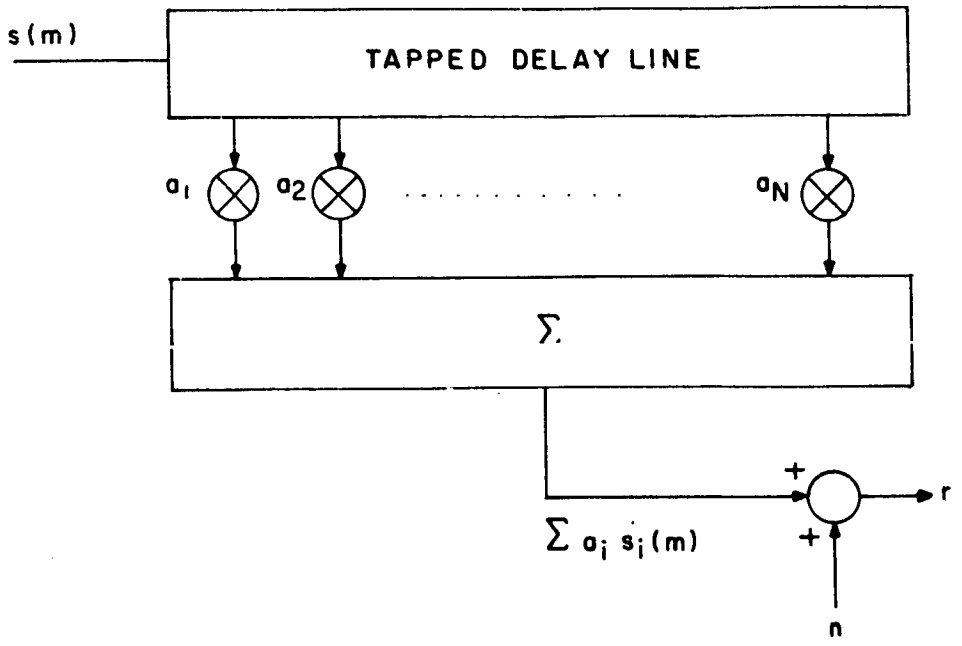

Channel Model

Figure IC-7

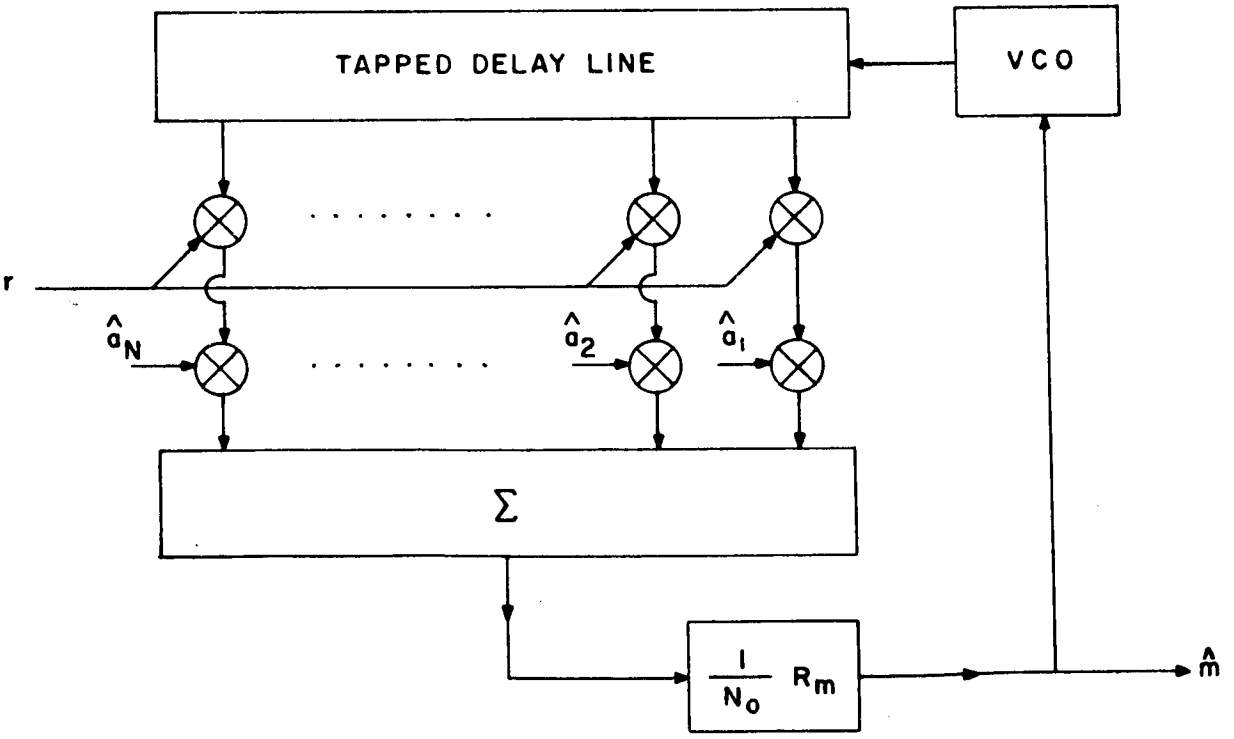

Receiver

Figure IC-8 Channel and Receiver

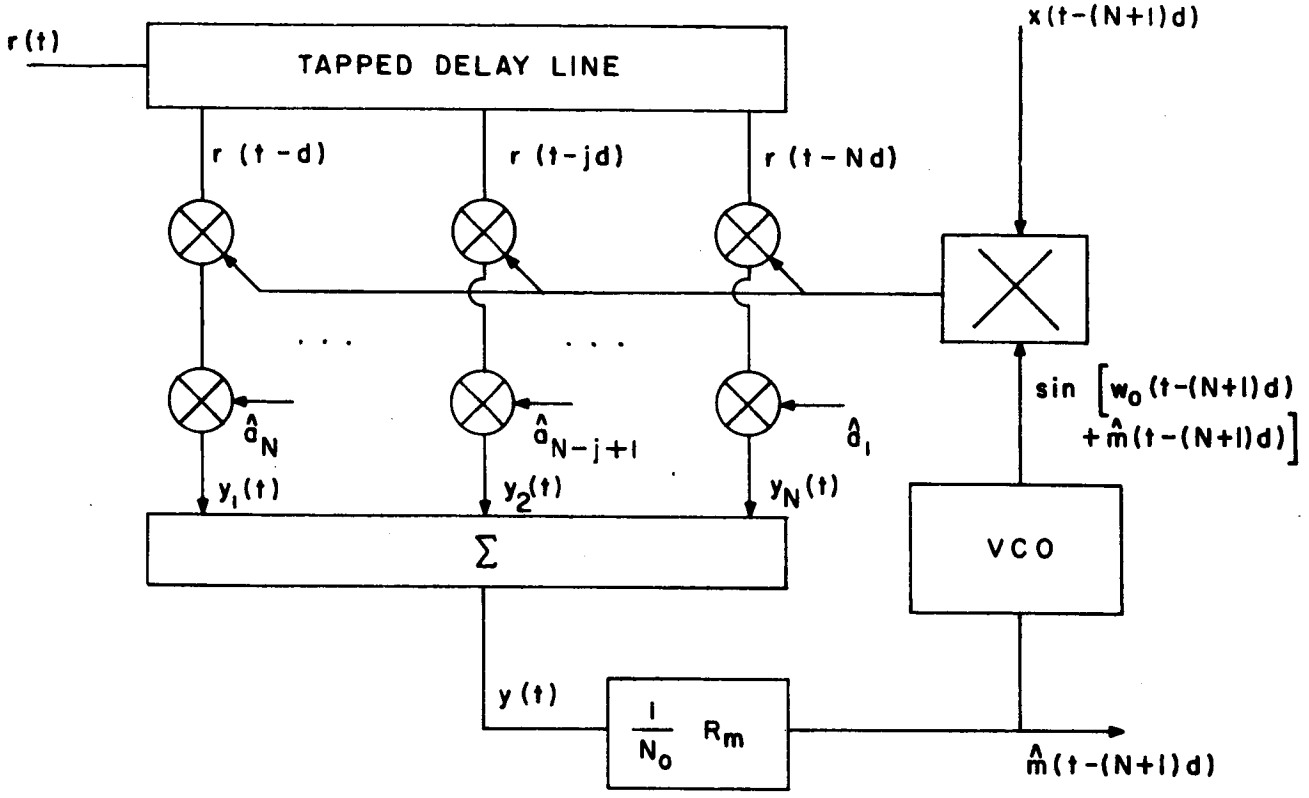

Figure IC-9 Delayed Signal Receiver

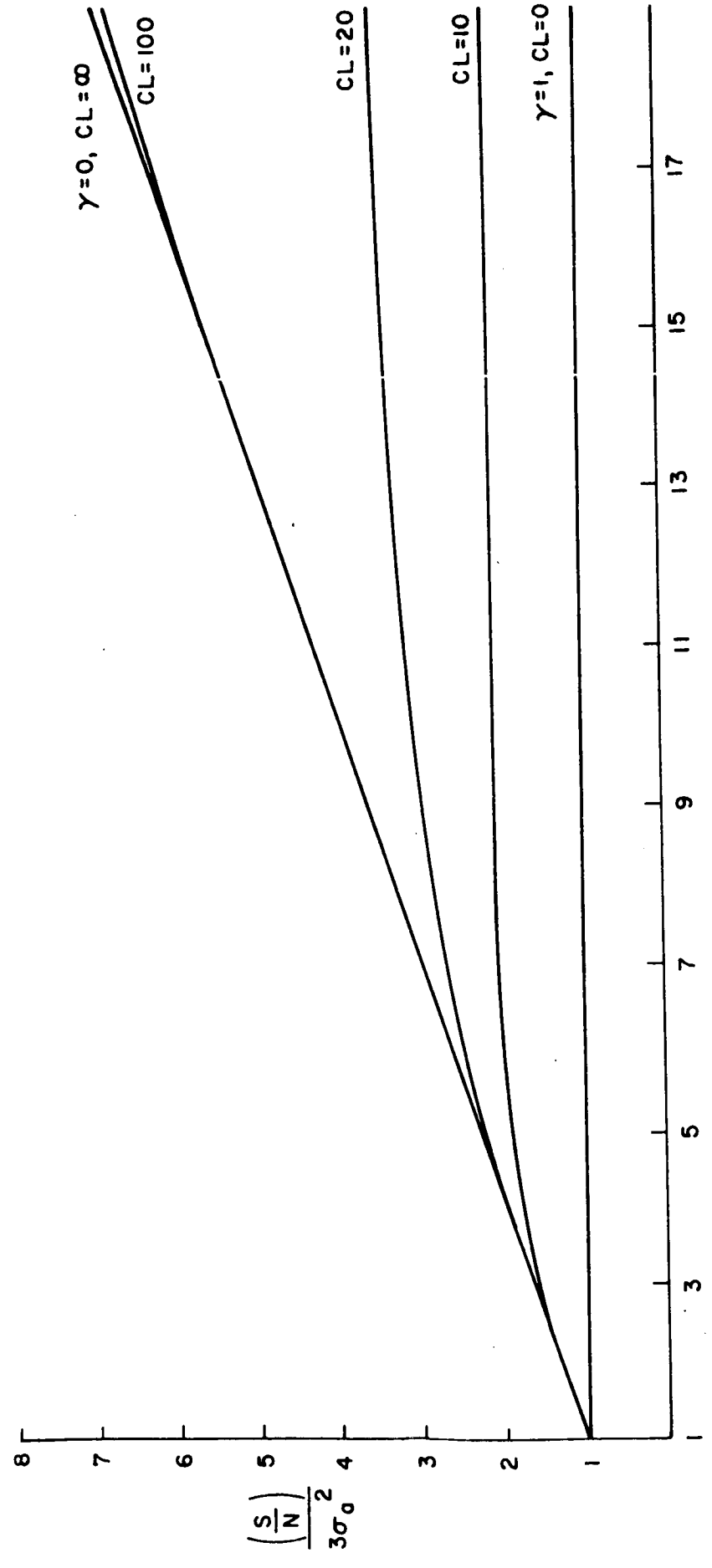

Figure IC-10 Signal to Noise Ratio vs N

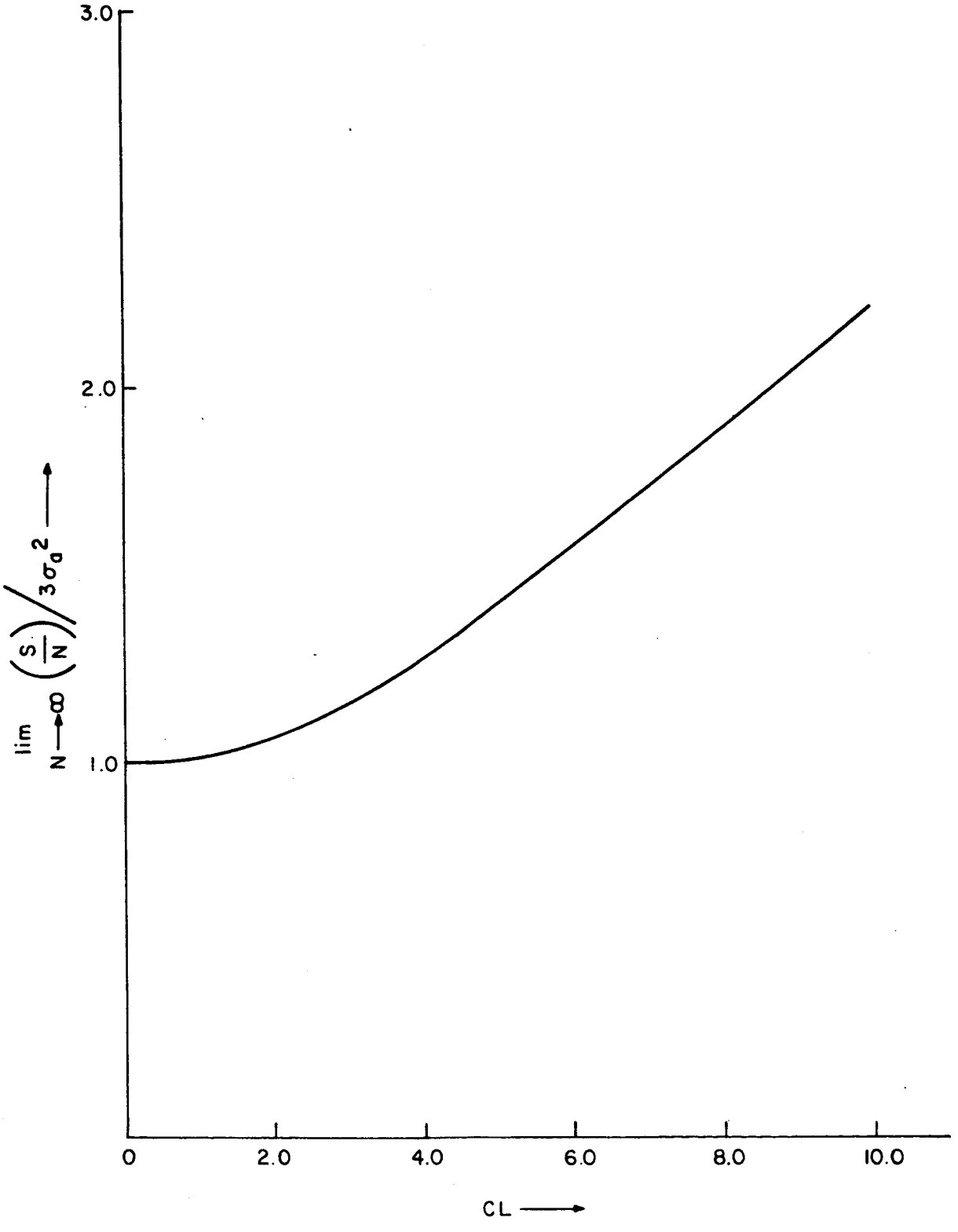

Figure IC-11 Asymptotic Signal to Noise Improvement vs Degree of Correlation of the Channel

II. Phase Locked Loop Studies

Introduction

The studies discussed below deal with the Phase Locked Loop (PLL) Demodulator. This demodulator is suboptimum, i.e. it yields neither the high SNR above threshold nor the low threshold of the Maximum Likelihood or Bayes Estimator discussed in section I. However, it has a threshold which is considerably lower than that obtained using an FM discriminator.

The basic PLL demodulator is shown in fig. 1. It consists of a phase detector, filter, and voltage controlled oscillator (VCO). The output of the VCO and the input signal are multiplied in the phase detector. The output of the phase detector is proportional to the phase difference between the signal and VCO. This output is filtered and returned to the VCO. If the phase of the VCO closely estimates the phase of the input signal, the frequency of the VCO closely estimates the modulation. Since the input to the VCO, e_o, is proportional to the VCO frequency, e_o is proportional to the modulating signal, $e_m(t)$.

When noise is added to the FM signal the PLL output consists of the modulating signal, FM noise, and spike noise. The FM noise has a power spectral density which is parabolic. This noise is easily calculated by linearizing the PLL. The FM noise is in all respects, identical to the FM noise found at the output of an FM discriminator above threshold.

The spike noise is similar to the spike noise seen at the output of an FM discriminator. However, a spike in a PLL can occur in one of two ways. If the PLL followed the phase of the input voltage exactly, it would follow the phase of the noise exactly. Whenever the phase noise rotates 2π radians (causing a spike in a discriminator) the VCO phase would also rotate by 2π radians causing a spike in the PLL. The PLL has a lower threshold than the discriminator because it does it does not follow these large changes. As a result the loop loses 'lock'. Depending on the initial conditions when it loses lock the PLL may relock about zero phase or relock about phase 2π. If the loop relocks about zero phase, it produces a 'doublet' which has zero area. The noise power contributed by this doublet is negligible. If the loop relocks about 2π radians a spike results having an area of 2π radians.

In order to extend the threshold of the PLL the number of spikes occurring per second must be reduced. This can be done by optimizing the design of the phase detector, filter and VCO. In addition, the conditions required for a spike to occur can be determined and whenever a spike is about to occur the PLL can be made to lose lock and relock about zero (alternately one can detect the occurrence of a spike by its rapid rate of change of phase and attempt to cancel the spike).

The reduction and detection of spikes are important, not only in extending threshold but in reducing error rates. It was shown in section I that digital information is transmitted at modulation indices where errors are caused primarily by the spikes. Thus reducing and detecting the spikes can result in an error rate approaching that of a matched filter.

The studies described below are a continuation of studies started here at the Polytechnic Institute of Brooklyn in 1962. We have already obtained thresholds of less than 3db (compared with 10db for the discriminator). See fig. 2. Our attention is now focused on the spike mechanism. Knowing this, a complete theory of operation of the PLL can be developed, error rates and threshold determined, and the spikes can be reduced permitting the error rate to approach the matched filter result and also reducing threshold.

A. Phase Locked Loop Experiments [1-8]

A PLL demodulator has been constructed and thoroughly tested. This report describes the tests performed to insure proper operation of the PLL. Further experiments will establish the probability of occurrence of a spike as a function of the CNR and modulation index, the criteria for occurrence of a spike in a PLL, and the operation of the PLL as a demodulator of digital signals (PSK and FSK).

I. Test Criteria

In addition to the customary tests of Multiplier linearity, VCO sensitivity, and loop locking range, the following tests were found useful in establishing that the PLL was functioning in accordance with theory. It is important to note that the extension of threshold is governed by the degree of which these criteria are met. Loose adherence may well mean only a 3db improvement over the standard FM discriminator.

1. Phase Error

The loop phase error should vary by $\pm \frac{\pi}{2}$ about the value $\frac{\pi}{2}$ over the locking range. A Lissajous pattern between incoming signal and VCO output easily displays this. Any delay in the loop will reduce the obtainable swing. If the loop loses lock at $\pm$ 85^{o} or less the threshold performance is significantly degraded.

2. Critically damped system

The locking range (or loop bandwidth) is largest when the loop is critically damped. Critical damping may best be measured by applying a step in frequency into the system and observing the variation in settling time for the overdamped case, and overshoot in the underdamped case. The critically damped setting corresponds approximately to maximum locking range, see fig. 3.

3. Loop Gain and Loop Bandwidth

The loop gain in a critically damped PLL is equal to its 3db bandwidth (closed loop). The filter in the loop is designed so that its bandwidth is 4 times that of the loop bandwidth. Note, that this filter is not designed to eliminate noise in the loop, but to insure that the loop relocks to zero, rather than to 2π after losing lock.

4. Loop Output vs Input Amplitude

Under noisy or fading conditions, the amplitude of the input signal may greatly vary. It is necessary that the loop output for a given deviation, Δ f, remain constant. Thus, $^{\Delta f}/_{\text{Loop Gain}} \ll 1$.

In addition, no limiting may take place within the loop or the IF filter. Limiting has been found to significantly increase the spike rate (and threshold), see fig. 2.

5. Noise Spectrum

When operating above threshold, the noise spectrum must be parabolic with amplitudes equal to that of the FM discriminator. This test is crucial in that any additional noise or nonlinearity encountered in the system will become apparent during this experiment.

6. VCO Input

Residual ripple transmitted through the power supplies, or ground, in addition to residual carrier and sum-frequency components out of the multiplier, usually presents a serious problem. Any ripple at the VCO input must be kept at a minimum. It adds to the modulation and noise expected. When this sum exceeds the loop gain the loop falls out of synchronism. It was also found experimentally that threshold is very dependent on the minimization of this ripple. The PLL supplies in the system were obtained from batteries to minimize the 60 cycle problem and inductive pick-up.

7. VCO Response

The sensitivity of the VCO must be linear over the operating range. In addition, the VCO sensitivity must remain constant for much higher modulation rates than the maximum signal requirements, since it must respond to a spike.

Since additional gain within the loop is always obtainable, and spectral content and sinusoidal response are most important, the balanced modulator was used in the final configuration. The response of the Balanced Bridge Modulator is shown in Fig. 4 and its spectral characteristics are shown in Fig. 5.

II. System Blocks

1. Multiplier

Three types of multipliers have been tested and compared.

a) Transistor switch (unipolar)

b) FET dual gate

c) Balanced diode bridge

The bases of comparison were:

a) Spectral content

b) Sinusoidal response to two inputs at same frequencies but different phase

c) Multiplier Gain

d) Dynamic range

The results of this test were:

	Spectral Content	Sinusoidal Response	Multiplier Gain	Dynamic Range
Transistor Switch	Poor	Poor	Good	Good
FET dual gate	Poor	Poor	Good	Poor
Balanced Modulator	Good	Good	Poor	Poor

2. Voltage Controlled Oscillator

The VCO employed is a standard astable multivibrator driven by a constant current source driver as shown in fig. 6. The driver (a common emitter stage) is in turn controlled by a control voltage (at the base). The dynamic range is almost 100% of the carrier frequency with less than 0.1% distortion. The sensitivity and center frequency are adjusted by means of the driver emitter bias and the driver emitter resistor.

3. System Design

The design procedure for a PLL which will yield low threshold is given below. It is assumed that the frequency deviation and maximum modulating frequency are specified, then:

(a) Loop Gain $>> \Delta f$

Experimentally a ratio of loop gain to deviation of 3-5 appears to work best. If the ratio is too small, the signal is distorted. When the ratio is too large discriminator type spikes occur (i.e., the PLL does not lose lock and if the input phase rotates 2π radians, the PLL has a spike

(b) 3db frequency of loop filter = 4 (loop gain)

This is the condition for critical damping.

(c) $2f_o >> 4$ (loop gain)

If a balanced phase detector is employed the second harmonic of the carrier is present at the output of the phase detector. To remove this from the input of the VCO the carrier frequency is specified so that the second harmonic can be filtered by the loop filter.

An example of a PLL design is given below.

Center frequency:	455kc
Signal Deviation, Δf:	3kc
Modulation frequency, f_m:	3kc
Modulation Index:	1
Loop gain	$4 \Delta f = 12$kc
Loop filter cut-off	$4G_1G_2A = 48$kc

The configuration of Fig. 6 was utilized. The experimental results for the PLL and an FM discriminator are shown in Fig. 7. Notice a 7db threshold improvement.

B. Digital Computer Simulation of the Phase Locked Loop

This report discusses a digital computer PLL simulation experiment currently in progress. This experiment will determine:

1. the threshold of the PLL
2. the average number of spikes per second produced by the PLL
3. the optimum loop gain
4. the best loop filter
5. the optimum phase detector
6. the effect using of storage to detect and eliminate spikes.

The reason for resorting to a digital computer simulation is that there is no difficulty in determining the least-mean-square error at the output of the phase lock loop whether or not modulation is present; the problem of a carrier reaching the output of the phase lock loop is completely eliminated; the character of the noise, furthermore, can be completely specified, i.e., true Gaussian noise can be simulated. In addition, various components can be put into the simulated phase locked loop which may be impossible to put into an experimental phase lock loop. Two examples are: (1) spike counter and (2) various non-physically realizable feedback filters. One of the results will be the determination of how good the approximation often made of neglecting modulation is with regard to threshold.

As a result of preliminary investigations, we have found that in order to obtain the linear relationship between signal-to-noise output and carrier-to-noise input, modulation which has a rectangular spectrum must be employed. Using any other spectrum, the relationship between these two quantities is not linear but a power function. As the spectrum approaches a rectangular shape, the power function tends to become a linear function. Therefore, only rectangular spectrums and filters are used in the PLL simulation.

The first step in writing a computer program to simulate a 2nd order PLL is to take the differential equation of the PLL and convert it to a differential difference equation, using a parabolic or three-point approximation at each time sample. The required conversion equations are obtained by passing a parabola through three assumed points on the

solution and calculating the first and second derivatives of the solution at the center point as a function of the values at all three points. This type of approximation is the most common approximation used to solve second-order equations and is clearly the simplest.

Once this is done, the next problem is to create on the computer the required modulation data and noise data. These consist of a series of numbers which will become input data for the computer program. In order to provide the desired rectangular spectrums, the noise and modulation have been simulated using the sampling theorem. From the sampling theorem we find that if one uses a string of uncorrelated numbers to represent a signal one can determine correlated intermediate values in such a way as to form a signal whose bandwidth is π divided by the time interval between the original uncorrelated samples. The value of this approach lies in the fact that to take more samples in a given interval of time one need only make more extensive use of the sampling theorem instead of feeding in more uncorrelated numbers. In each case, that is, the number of uncorrelated numbers required is a constant. In addition, the sequence of random numbers is chosen to be Gaussian so that a true band-limited Gaussian noise and Gaussian modulation is obtained. The required Gaussian random numbers are obtained from the extensive tables [9].

For the case of sine-wave modulation, the construction of the modulation is, of course, obtained simply by taking the sine of a linearly increasing angle. By correctly choosing the rate of increase of the angle, we obtain the desired frequency for the sine-wave modulation.

As a result of the well-known investigation by Rice[10], we have included in this PLL simulation a spike counter. The spike counter, in effect, indicates the number of times that the phase angle of the PLL switches to a point 2π away from the integral of the modulation with respect to time. The spike counter is a simple yet extremely useful addition to the PLL simulation as we shall see shortly.

The program includes two techniques to determine the output SNR. The first procedure is to subtract the true modulating signal from the PLL output. The difference represents noise (including distortion). The noise power is then obtained by squaring and averaging the noise. An alternate

way to obtain the output signal-to-noise ratio is to take the number obtained by the spike counter, determine the noise power contribution of the spikes based on this number, and add to it the Gaussian noise power (which we would expect to pass through a linear version of the PLL). This procedure yields the output noise power. The closeness of the output noise power obtained using each technique is an indication of how accurate a picture of the PLL can be formulated using the concept of spikes.

Whenever, a spike occurs the time at which it occurs is recorded. This is very significant. By running a second program in which an FM discriminator is simulated, and again count spikes and determine their time of occurrence, we can find if there is any connection between the spikes at the output of a PLL and spikes of the output of an FM discriminator.

Since the study of these spikes is so important to the understanding of the operation of the PLL we have also undertaken simulation of specific noise inputs to the loop. These inputs have been chosen to create spikes in the FM discriminator every time they occur. The question is, do these noise sequences also cause spikes in the PLL? This second kind of simulation seems to be particularly useful in giving us further insight into the mathematics of the threshold of the PLL.

I. Assumptions and Approximations

The accuracy of any digital simulation of a physical process depends a great deal on the number of sample points chosen to represent a physical function in a given interval of time. In the PLL program we have used a differential difference equation to approximate a differential equation. A method of estimating the accuracy of this approximation consists of locating the roots of the characteristic equation associated with the differential difference equation. From the theory of differential difference equations, we find that the equation has a divergent solution if the magnitude of any one of the roots of the associated characteristic equation is larger than one, otherwise the solution is convergent.

For the simulation program, the magnitude of the largest root occurs when the loop gain is a maximum, and for the highest gains considered in the first PLL simulation program, the magnitude of this root is equal to .5774. For loop gains less than the maximum the magnitude of the largest root of the characteristic equation is proportionally less. A check on this

method will be the use of a PLL program with five times as many samples as the first program. If we find that the results of programs one and two are comparable where program two has five times as many samples as one for the same time interval, we will assume that we have satisfactorily approximated the solution to the differential equation. The second assumption used in the program is that we can use the sampling theorem with a finite number of terms. The complete sampling theorem requires that any intermediate sample be obtained from an infinite set of uncorrelated numbers. Our approximation is to base each intermediate sample on six uncorrelated numbers. While six is considerably less than infinity, it turns out that this is still not unreasonable because the weighting function in the sampling theorem ($\sin x/x$) falls off rapidly enough after six samples. A second application of the sampling theorem in the program is in the output filtering. Here the theorem calls for the use of an infinite number of cycles of the $\sin x/x$ function. We have chosen instead to approximate with four cycles of the $\sin x/x$ function. Again we can show that the error in failing to use all of the cycles of the $\sin x/x$ function is sufficiently small. These approximations will be checked out again by future programs in which we will use more samples and more cycles of $\sin x/x$ in applying the sampling theorem.

A third approximation, known as the Monte-Carlo approximation, is that a sufficient number of Gaussian random numbers has been used to simulate the noise. As in every Monte-Carlo simulation process, this is only an approximation, since every possibly sequence of Gaussian random numbers is not present in the finite sequence used in the simulation. In order to check on the validity of this approximation, we have a simple procedure that can be followed. In as much as the random numbers are punched on IBM cards all we have to do is shuffle the cards to create a different noise sequence. We will run programs with the shuffled cards to determine if there is any significant difference in the results.

A fourth approximation is that the computer simulated noise is bounded, i.e., the largest amplitude the noise can have is limited to a constant times the rms value of the complete set of noise samples (σ). Usually "3σ" noise is used. An elementary calculation shows that, with the peak noise limited to 3σ, no spikes can occur if the input carrier to

noise ratio (CNR) is greater than 9.55 db. Since the threshold of the FM discriminator is approximately 10db, the use of 3σ noise is unsatisfactory for threshold calculations of a discriminator, but certainly sufficient to determine the threshold of a PLL.

II. Results

Although no significant results are available yet on the basic problem (output SNR versus input CNR), some results are available on the following secondary problems:

1. Formation of a more complete explanation of the operation of the PLL.

It has been found that the number of spikes at the output of a PLL is less than the number at the output of an FM discriminator. When a spike occurs in a PLL they also occur in the FM discriminator.

When a spike occurs in the discriminator but not in the PLL, the PLL produces a "doublet", i.e., two spikes of different polarity having zero average area and, thus, are removed by the low-pass-filter (LPF) which follows the PLL. The spikes which do occur have the 2π area expected and are not removed by the low-pass-filter. Since spikes are the cause of threshold in both the FM discriminator and the PLL, this indicates why the PLL has a lower threshold then the FM discriminator.

2. Checking of the known PLL theorems.

Using the computer simulated PLL we have obtained data to confirm the theorem that the performance is deteriorated by using a limiter at the input to the PLL. The results so far indicate that the PLL spikes equal the discriminator spikes and are all of area 2π if a hard limiter is used before the PLL. Thus, the overall device acts like an FM discriminator and there is no threshold improvement.

Conclusions

During the next two years the study of the phase locked loop will be continued and expanded.

We are presently constructing an analog computer simulation of the PLL. This simulation will be extended to consider the FMFB and other threshold extension devices. The analog and digital computer simulations complement each other. The analog computer can take data over a long period of time which is prohibitively costly to do with a digital computer. The storage capability in a digital computer is a great advantage not enjoyed by the analog computer.

The response of a PLL to an FM signal which is fading or which is in the presence of an interfering signal will be studied.

A PLL used to detect PSK-TDM signals is being studied. In addition, synchronization problems will be investigated.

A comparison of TDM and FDM systems has also been undertaken. Initial results indicate that when using an FM discriminator, FMFB, or PLL the TDM system results in a lower error rate in each channel.

References

1. "The Response of an APC System to FM Signals and Noise" Proc. IEEE, Oct. 1964

2. "On the Threshold Extension Capabilities of the PLL and the FDMFB" (with J. Billig) Proc. IEEE Correspondence, May 1964

3. "A Comparison of the Threshold Performance of the FDMFB and the PLL" (co-author) J. Billig, PIBMRI Report 1207-64.

4. "Threshold Extension Using the PLL and the FDMFB" with J. Billig, presented at the ICMCI Conference in Tokyo, September 1964.

5. "Error Rates in FSK Using the PLL Demodulator" IEEE Trans. of First Annual Communication Technology Convention, Globecom 7, June 1965, (with J. Billig and D. Kermisch).

6. "Phase Locked Loop Threshold" - Correspondence of Proc. IEEE, October 1965.

7. "Threshold Comparison of the Phase Locked Loop and the Frequency Demodulator Using Feedback" - presented at 1965 International Space Electronics Symposium, November 1965.

8. "Intermodulation Distortion of a Phase Locked Loop Demodulator" (with M. Smirlock), Fourth Canadian Symposium on Communications, Octobe r 1966.

9. One million random digits, Rand Corporation

10. Rice - Noise in FM Receivers, Chapt 25, Time Series Analysis, edited by Rosenblatt, Wiley 1963.

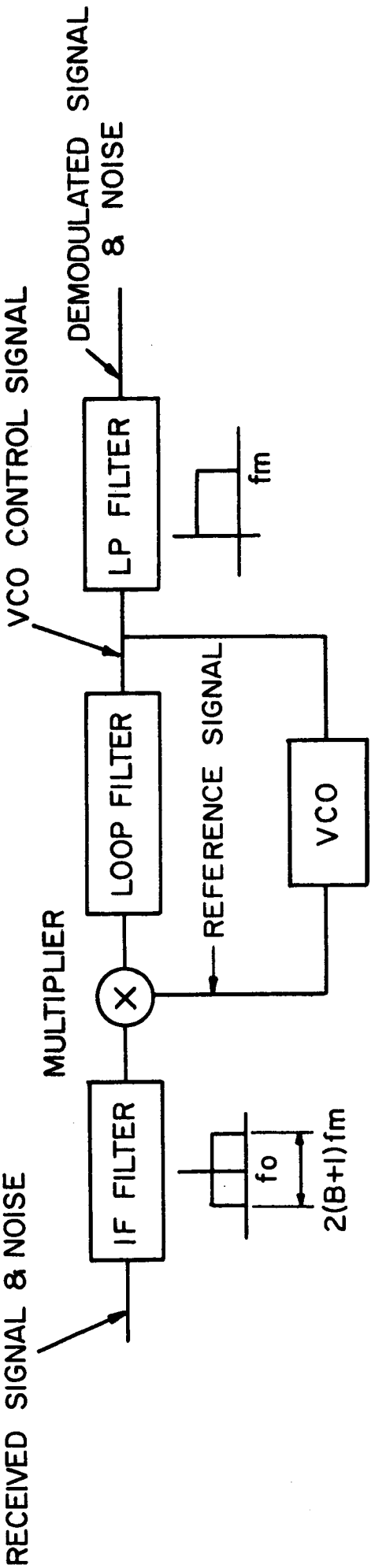

Fig. II-1 PLL Demodulator Block Diagram

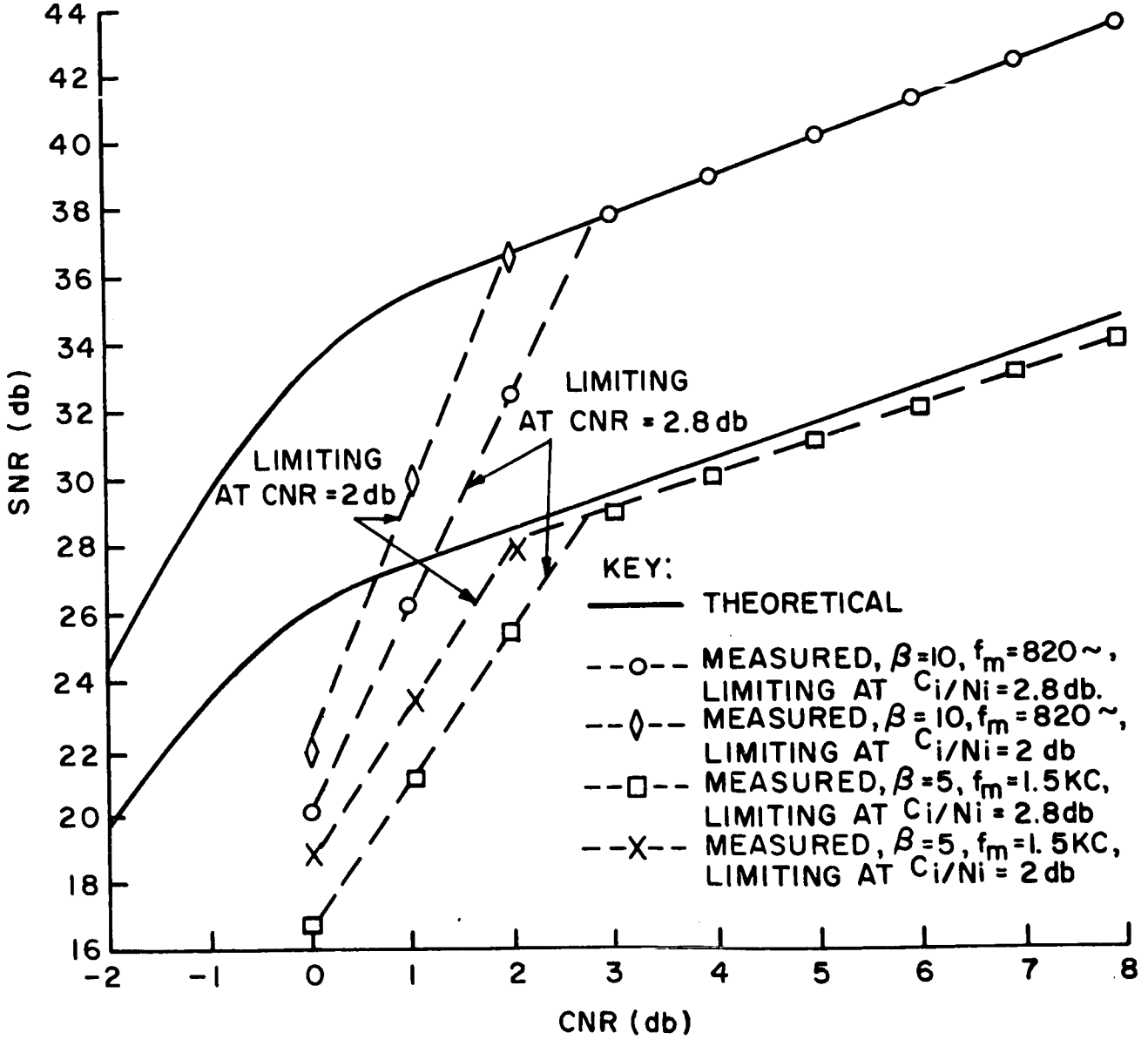

$$SNR = \frac{3\beta^2(\beta+1)(CNR)}{1+16\sqrt{3}\,(\beta+1)^2(CNR)\,e^{-\pi^2(CNR)}\,I_o\left(\frac{2\pi\beta f_m}{G_1 G_2 A}\cdot CNR\right)}$$

Fig. II-2 SNR Vs. CNR For Single Sine Wave Modulation Using Phase Locked Loop Demodulator

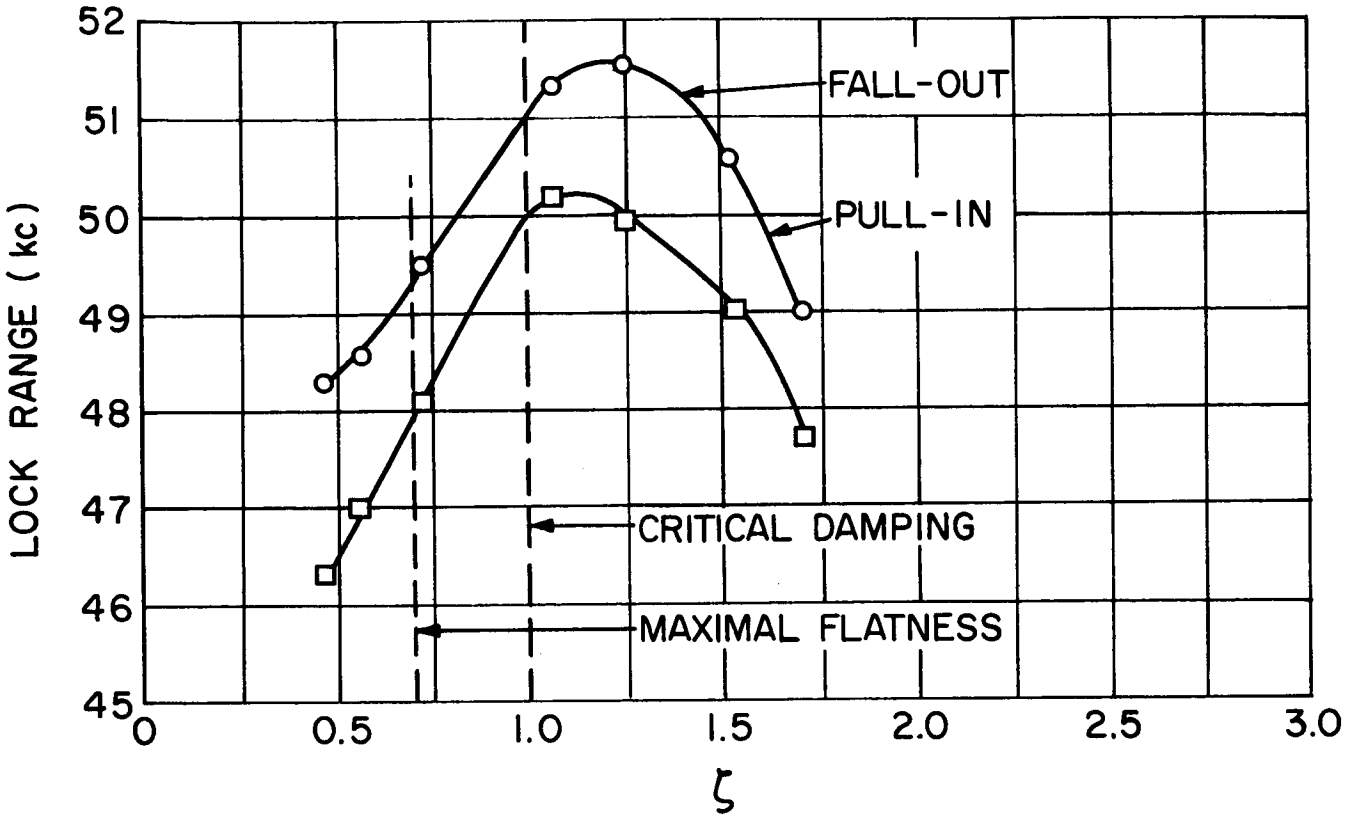

(a) – LOCK RANGE VS. DAMPING FACTOR

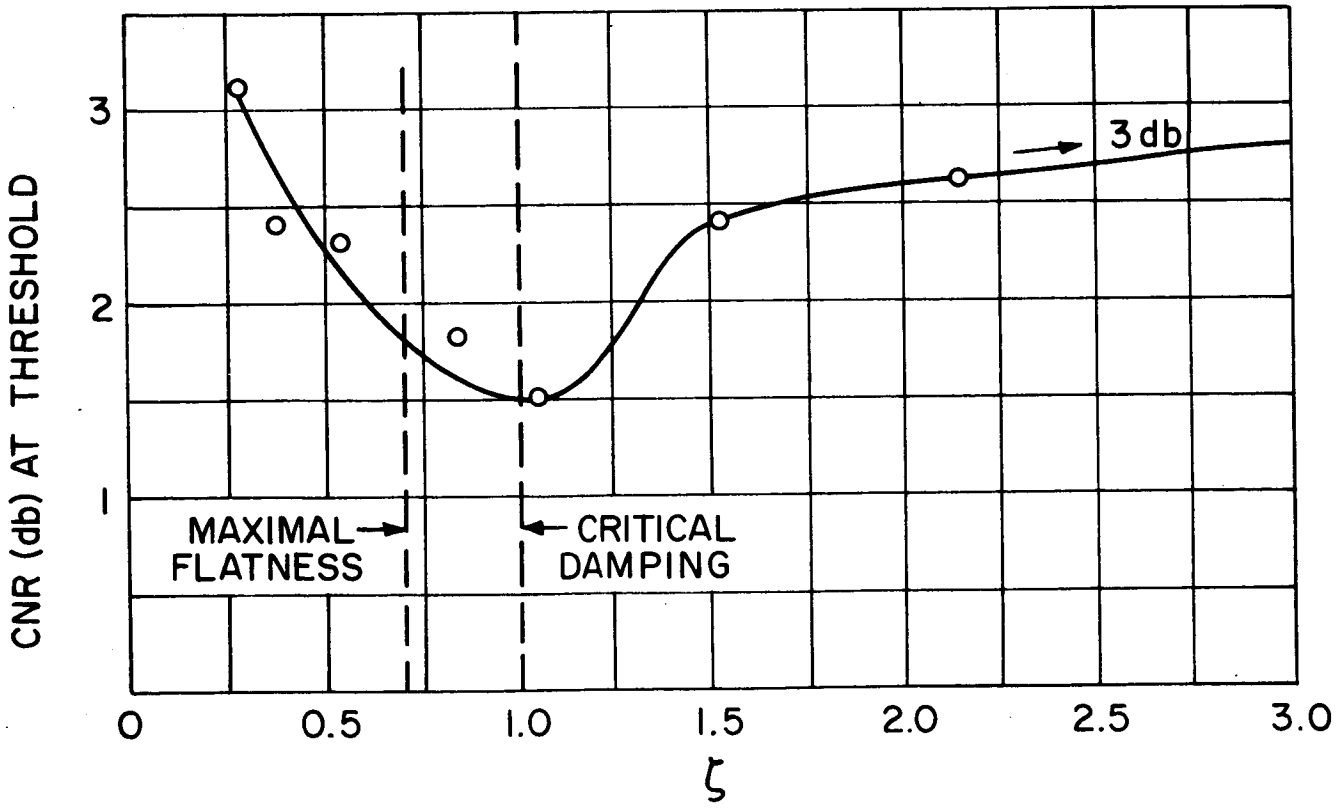

(b) – CNR at THRESHOLD VS. DAMPING FACTOR

Fig. II-3 Effect of Loop Damping on Lock Range and Threshold

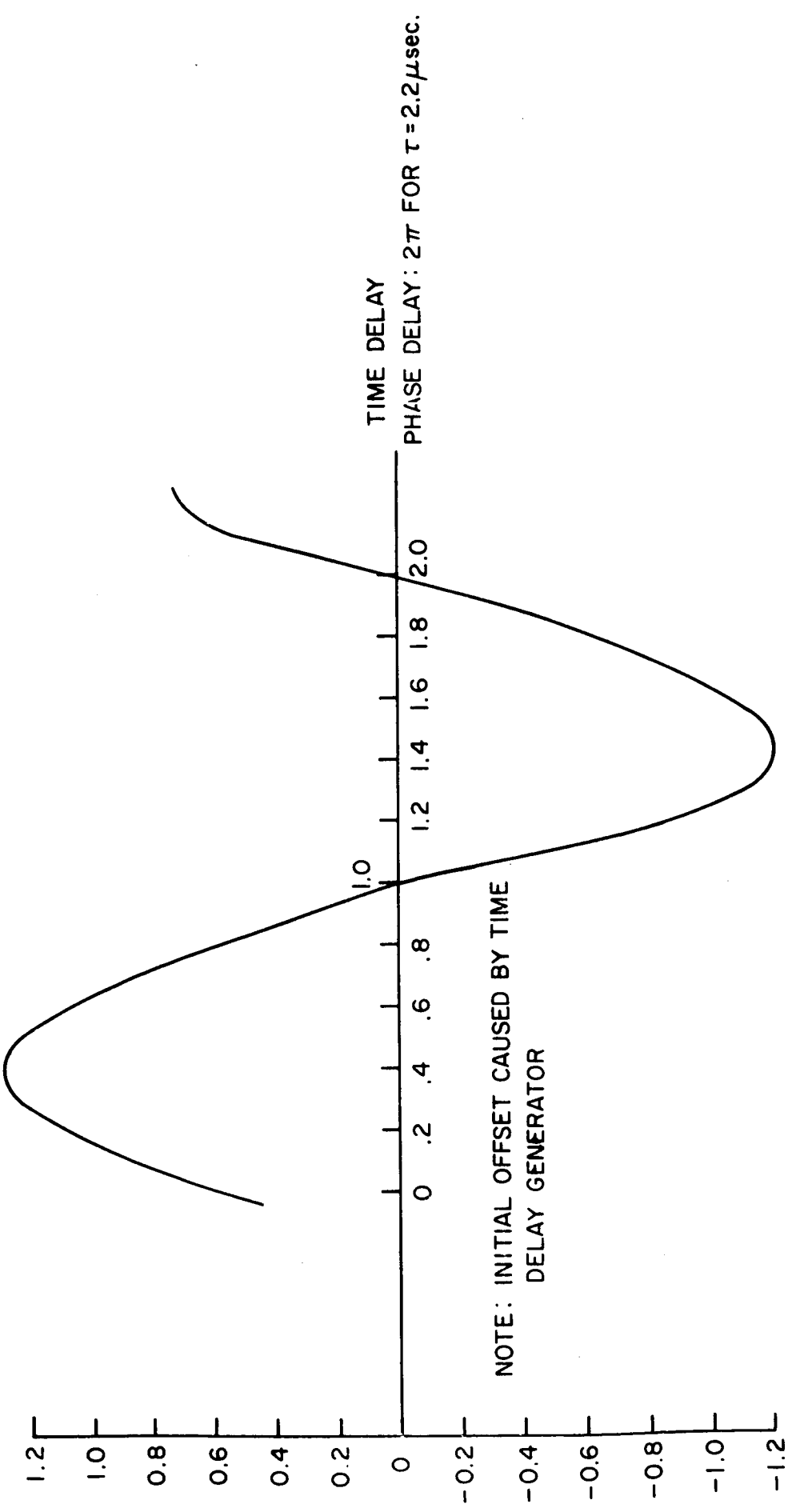

Fig. II-4 RESPONSE OF BALANCED BRIDGE MULTIPLIER Edc OUT VS. TIME DELAY

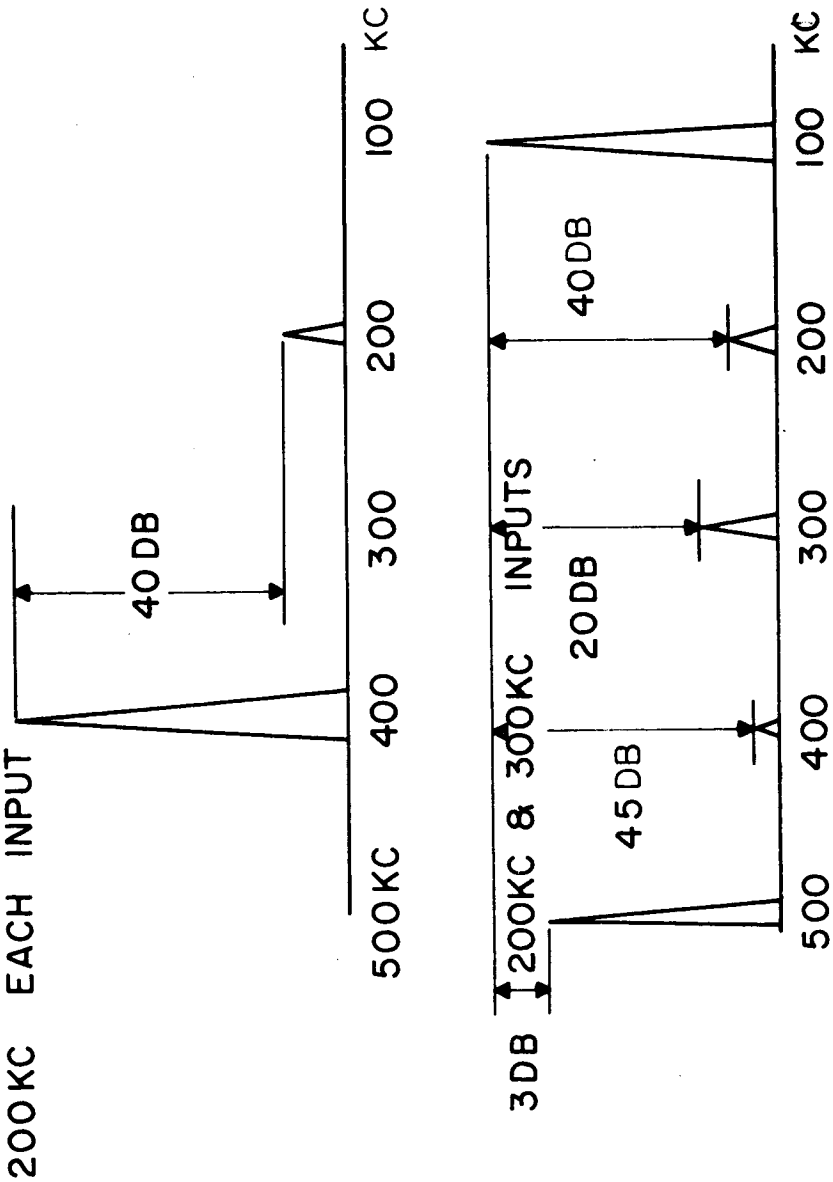

Fig. II-5 Spectral Characteristics of Balanced Bridged Multiplier

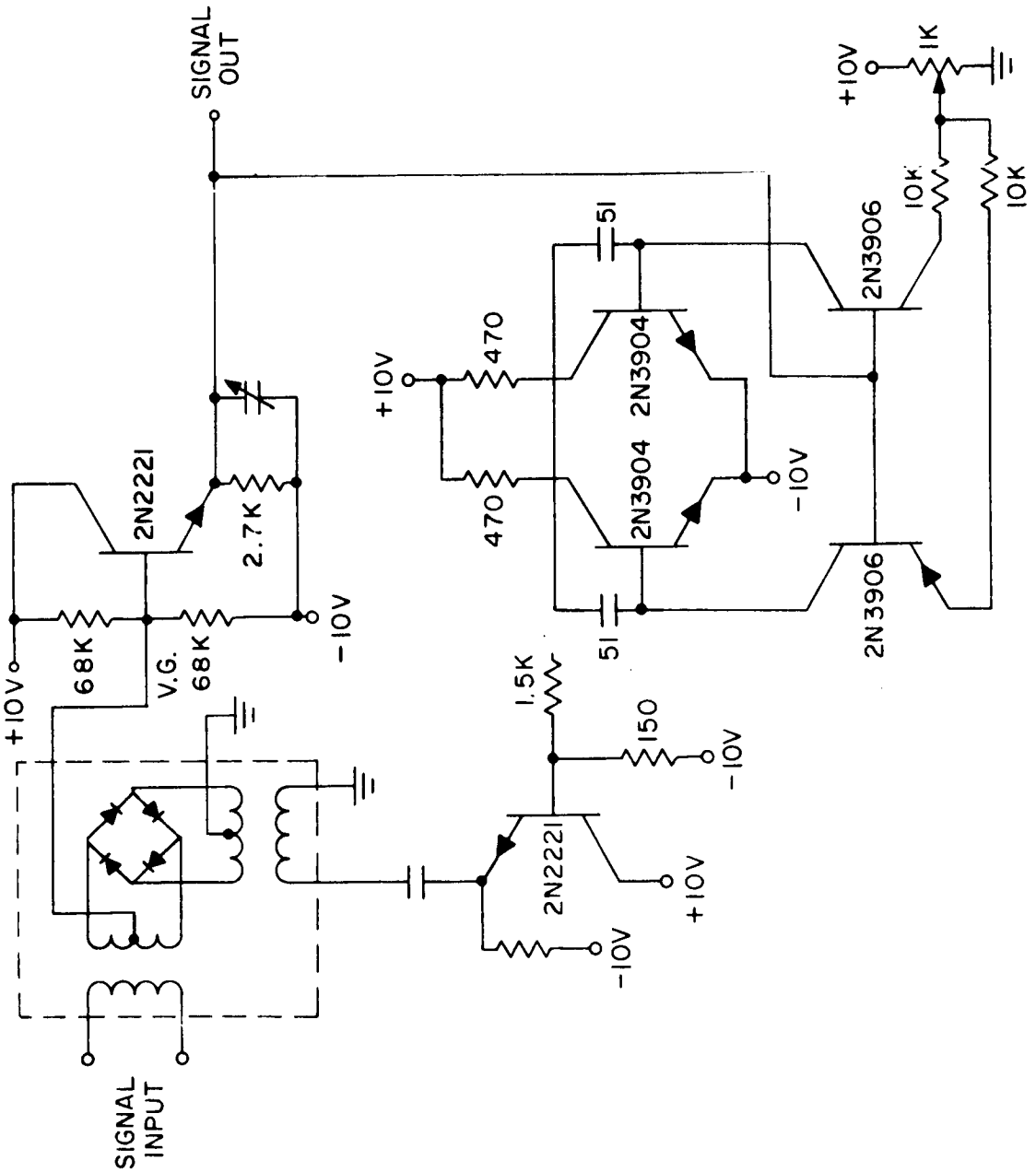

Fig. II-6 Phase Locked Loop (Schematic Diagram)

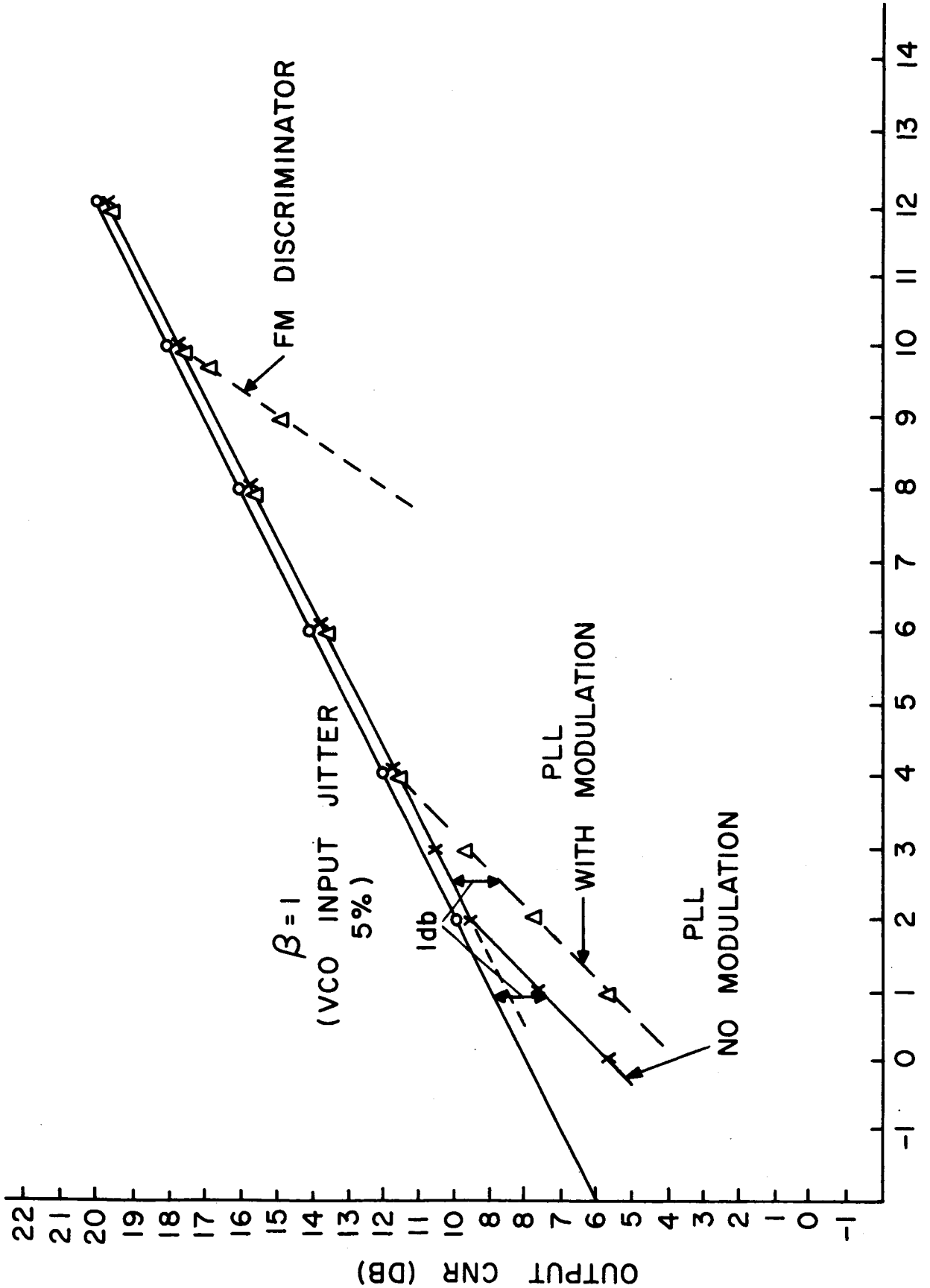

Fig. II-7 Output SNR Vs. Input CNR PLL and Discriminator

III. Frequency Modulation and Demodulation

Introduction

This section discusses several important topics in FM. Section A deals with the response of an FM discriminator to an analog, FM modulated signal in a fading enviroment, and the error rates present when detecting digital signal using a discriminator (fading and non-fading channels are considered).

Section B deals with a novel frequency demodulator constructed at the Polytechnic Institute of Brooklyn.

Section C discusses several novel FM circuits and the response of an FM wave to these networks.

III.A1. ANALYSIS OF AN F.M. DISCRIMINATOR WITH A FADING SIGNAL PLUS ADDITIVE GAUSSIAN NOISE

INTRODUCTION - Rayleigh Type Fade

A signal, characterized by non-selective fading, is added to white stationary Gaussian noise of zero mean and passed through a bandpass i.f. amplifier which is symmetric about the carrier frequency, f_o. The bandwidth, 2B, is assumed wide enough so that the signal passes undistorted. The i.f. output which is now in the form of signal plus bandlimited Gaussian noise is applied to an ideal limiter and then frequency demodulated. This is illustrated in Fig. 1.

It is desired to investigate both theoretically and experimentally the signal-to-noise ratio at the output of the FM discriminator to that at the input of the ideal limiter in order to determine the effects of fading on the threshold. To do this one must first compute the power spectrum at $\underset{\sim}{\dot{\phi}}$. Hence, one needs the correlation function $R_{\underset{\sim}{\dot{\phi}}}(t)$.

The modulation, $\underset{\sim}{D}(t)$, will be considered as $\beta \sin (2\pi f_m t + \underset{\sim}{\gamma})$ where $\underset{\sim}{\gamma}$ is uniformly distributed in $(0, 2\pi)$. In practice one never knows the phase of the signal exactly. The inclusion of $\underset{\sim}{\gamma}$ makes the process stationary.

With the modulation set equal to zero ($\beta = 0$), the fading signal is usually taken to be a complex stationary random process with its power spectrum assumed to be symmetric about f_o. Specifically, the onesided power spectrum $W_c(f)$ is:

$$W_c(f) = \frac{\sigma_c^2}{\sqrt{2\pi}\, f_{H_1}} \, e^{-\frac{(f-f_o)^2}{2f_{H_1}^2}} \tag{1}$$

where

σ_c^2 is defined as the carrier power, $\overline{c^2}$. (If the envelope $\underset{\sim}{r}(t)$ is Rayleigh distributed, the carrier power is

$$\overline{c^2} = \frac{\overline{r^2}}{2} = \sigma_c^2 \tag{2}$$

The statistics of $\underset{\sim}{r}$ agree approximately with the measured statistics, in some cases, for periods of the order to several minutes on tropospheric and ionospheric scatter systems as well as for an ionospheric reflection transmission),

and

f_{H_1} is a function of the fading rate. The fading rate, or average number of times per second that the envelope crosses its median value with positive slope is equal to $1.48\, f_{H_1}$, a quantity which experimentally varies from a few tenths to a few cycles per second depending on the carrier frequency.

Using the Rayleigh model one finds that the noise at $\dot{\phi}$ at high CNR is proportional to $\frac{1}{r}$. This result can be used even at low CNR. However, if we allow the resulting output noise power is infinite. Physically this is not true, for when the signal fades below a minimum level r_o, the discriminator is detecting only noise and $\dot{\phi}$ is not proportional to $\frac{1}{r}$. The CCIR[1] has assumed that it is permissible to truncate the Rayleigh distribution at some point since when the fade drops below a certain level, the circuit will be completely cut off, or switched to a better path. Rather than ignore this small percentage of time, Pearson[2] states that it is more realistic to assume the envelope $r(t)$ to fade to a minimum level r_o and that no switching occurs. It is this approach that we take so that the statistics of r now follow the form of a truncated Rayleigh density:

$$p(r) = \left(1 - e^{-r_o^2/2\sigma_c^2}\right) \delta(r-r_o) + \frac{r}{\sigma_c^2} e^{-\frac{r^2}{2\sigma_c^2}} u_{-1}(r-r_o) \qquad (3)$$

where $\delta(r-r_o)$ is an impulse function, and $u_{-1}(r-r_o)$ a unit step function. The ratio of $(r_o/\sigma_c)^2$ will be defined as the fading depth (e.g. $r_o/\sigma_c = .1$ corresponds to a 20db fade). Assuming $(r_o/\sigma_c)^2 << 1$, as is always the case, it has been shown that the carrier power is the same as indicated by equation 2. The fading rate, obtained from a knowledge of the joint statistics of the truncated envelope and its derivative has been shown to be approximately $1.48\, f_{H_1}$. These statistics are obtained from the true Rayleigh statistics by means of the nonlinear transformation

$$r = \begin{cases} r, & r \geq r_o \\ r_o, & r < r_o \end{cases} \qquad (4)$$

The statistics of the phase $\underset{\sim}{\theta}(t)$ for which there is no experimental evidence (that the author is aware of) would be uniformly distributed in $(0, 2\pi)$ if the signal were truly Gaussian. It is assumed that these statistics apply here, the joint statistics of $\underset{\sim}{r}$ and $\underset{\sim}{\theta}$ being obtained from the Rayleigh case by means of the above non-linear transformation on $\underset{\sim}{r}$ and the linear relation $\theta^* = \theta$.

2. Analysis Procedure

Following the procedure of Rice[3], the discriminator output, $\dot{\phi}$, is expressed as the sum of the modulating signal, $\dot{D}$, the phase jitter $\dot{\theta}$, a Gaussian type noise term with amplitude dependent on the fading statistics, and a spike noise term. The correlation function of $\dot{\underset{\sim}{\phi}}$ can be shown to be the sum of the correlation functions of the individual terms mentioned above.

The first step in the computation of the output signal-to-noise ratio is to obtain the power spectrum of the discriminator output, $\dot{\phi}$, by Fourier transforming the correlation function at $\dot{\phi}$. The details of the calculation using the statistics of equation 3 appear in reference 4. The output power is then found by applying the spectrum of $\dot{\phi}$ to an ideal low pass filter of cut off frequency f_m yielding

$$P_o = P_{\dot{D}} + P_{\substack{\text{phase} \\ \text{jitter} \\ \dot{\theta}}} + P_{\substack{\text{Gaussian} \\ \text{term}}} + P_{\text{spike}} \tag{5}$$

where the last three terms are noise and signal mixed with noise. The output signal-to-noise ratio is defined as

$$\frac{S_o}{N_o} = \frac{P_{\dot{D}}}{P_{\substack{\text{phase} \\ \text{jitter} \\ \dot{\theta}}} + P_{\substack{\text{Gaussian} \\ \text{term}}} + P_{\text{spike}}} \tag{6}$$

3. Theoretical Results

Figure 2 shows signal-to-noise ratio curves for 20 db and 40 db fades as well as the no fading curve. The solid curve includes the modulation interaction with the noise. The dashed curve neglects it (i.e., in finding $P_{\substack{\text{Gaussian} \\ \text{term}}}$ and P_{spike}, $D \equiv 0$). The modulation index,

β, is 5, and the ratio of f_m / f_{H_1} is 10^4. Since the i.f. bandwidth $B_{i.f.}$ $= 2\beta f_m$ and the fading rate, $N_r = 1.48 f_{H_1}$, the bandwidth $B_{i.f.}$ $= 6.75 \times 10^4 N_r$. (i.e. for an i.f. bandwidth of 100KHz, the fading rate is 1.48Hz) Inclusion of the modulation shifts the threshold occurs at about 32 db for a 20 db fade and at about 52 db for a 40 db fade, the no fade threshold being approximately 10 db. In contrast with the no fading case, there is an upper limit, 81 db, that the output signal-to-noise ratio can approach with infinite input signal-to-noise ratio

$$\left(\frac{S_o}{N_o} \rightarrow \frac{P_D}{P_{\substack{\text{phase} \\ \text{jitter} \\ \dot{\theta}}}} \right) .$$

The curves shown in Figure 3 are also plotted for $\beta = 5$, but now $f_m / f_{H_1} = 10^3$ (i.e. $B_{i.f.} = 6.75 \times 10^3 N_r$ and with $B_{i.f.} = 100$KHz, the fading rate, $N_r = 14.8$Hz). The effect of neglecting the modulation interaction is indicated by the dashed line. The experimental points (dot-dash) for the 20 db fade will be discussed later. The threshold for the 20 db fade is the same as in the previous case (32db), the effect of the phase jitter, 0(t), starting to occur at about 45 db. (Note $\frac{S_i}{N_i} \rightarrow \infty$, $10 \log 10 \frac{S_o}{N_o} \rightarrow 62$db.) In the case of the 40 db fade, the effect of the phase jitter now dominates.

4. Experimental System and Results

Experimental results were obtained for a 20 db fade with $\beta = 5$ and a fading rate of 14.8 Hz. The output noise power was measured by neglecting the modulation interaction. The fading signal was simulated as shown in Fig. 4. The signals ξ (t) and η (t) are two independent Gaussian low pass noise processes with identical spectra. These processes are obtained from a zener diode by filtering and amplifying. The measured power spectrum of the zener diode is flat above $\frac{1}{2}$ Hz. The amplifiers are a.c. coupled with low frequency breaks of .1 Hz. A double pole at

10 Hz is used for the filtering so that the spectrum in eq. 1 is

$$W_c(f) \simeq \frac{2\sigma_c^2}{\pi f_{H_1}} \left(\frac{1}{1 + \left(\frac{f-f_o}{f_{H_1}} \right)^2} \right)^2 \qquad (7)$$

The fading rate was therefore 1.48 f_{H_1} or 14.8 Hz. The carrier frequency, f_o, was 455 KHz.

A block diagram of the overall system is shown in Fig. 5. The operation is as follows:

The comparator produced a pulse having a width equal to the time that the envelope is below a level r_o. This pulse, when applied to the blanking circuit, removes the discriminator from the output circuit. The blanking circuit is a balanced switching arrangement which short circuits the discriminator output so that transients at the output are negligible.

The shaping amplifier for the Gaussian noise generator consists of two tuned circuits with 3 db points at 50 KHz from the carrier. (A stagger-tuned arrangement of 100KHz bandwidth was also used, yielding similar results.)

We now refer again to Fig. 3 where the experimental results are superimposed for the 20 db fade. The curve agree more closely with the no modulation case, as is expected from our measurement procedure. Measurements above 40 db could not be made due to the presence of system noise. The 34 db and 40 db points were obtained by subtracting out the system noise.

5. Diversity

We now consider a diversity scheme using two independent fading signals with true Rayleigh characteristics in a predection combiner.

Letting the two fading signals be

$$\begin{aligned} \underset{\sim}{c}_1(t) &= \underset{\sim}{r}_1(t) \cos \quad [w_o t + \underset{\sim}{\theta}_1(t) + \underset{\sim}{D}(t)] \\ \underset{\sim}{c}_2(t) &= \underset{\sim}{r}_2(t) \cos \quad [w_o t + \underset{\sim}{\theta}_2(t) + \underset{\sim}{D}(t)] \end{aligned} \qquad (8)$$

where, with the modulation set equal to zero, the signals $\underset{\sim}{c}_1(t)$ and $\underset{\sim}{c}_2(t)$ are two independent stationary Gaussian processes of zero mean. The

envelopes are then Rayleigh distributed and the phases are uniformly distributed in (0, 2π). Furthermore, equal carrier powers are assumed. That is:

$$\frac{\overline{r_1^2}}{2} = \frac{\overline{r_2^2}}{2} = \sigma_c^2 \tag{9}$$

The signals in eq. 9 are applied to a predetection combiner, such as the one described by Adams and Mindes[6], so that the resultant signal $\underset{\sim}{c}(t)$ in fig. 1 may be written as

$$\underset{\sim}{c}(t) = \underset{\sim}{r}(t) \cos [w_o t + \underset{\sim}{\theta}(t) + \underset{\sim}{D}(t)] \tag{10}$$

where

$$\begin{aligned} r &= r_1 + r_2 \\ \theta &= \theta_1 \end{aligned} \tag{11}$$

The details of the calculation of the output signal-to-noise ratio are given in ref. 4. We note, however, that the output noise power above threshold in this case is finite.

Refer to Fig. 6, where the output signal-to-noise ratio is shown for the fading and no fading cases. The effect of the modulation interaction has been neglected. The modulation index, β is 5, and the ratio of f_m / f_{H_1} is 10^4 for curve A and 10^3 for curve B. Observe that the threshold is not as sharp as in the previous cases (see figures 2 and 3) occurring at approximately 28db. (We take as the threshold, the value of input signal-to-noise ratio at which the output signal-to-noise ratio is one db below the linear extension.) The phase jitter, $\dot{\theta}$, is the dominant factor in curve B. If a predetection combiner such as described by Boyhan[7] is used, the phase jitter is eliminated so that in eq. 82, $\theta = 0$. Then curves A and B merge with the dashed line, resulting in a curve that is now parallel to the no fading case above the threshold of 28db.

Note that the threshold for a 20db fade is the truncated Rayleigh case is only 32db compared with the diversity value of 28db. With 14db fade, a threshold of approximately 27db is obtained with the truncated Rayleigh density. It appears that we are doing better than order two diversity case as the truncation level is raised. This is readily explained,

since as we raise the truncation level a no fading situation is approached. Furthermore, the statistics described by eq. 45 do not occur physically, but would have to be simulated by using at least two separate channels. (Recall the CCIR[1] discussion about switching to another channel when the signal fades below a minimum level.) Thus, the truncated Rayleigh case is itself a switching diversity system of at least order two. The raising of the truncation level implies an increase in the order of diversity.

References

1. Contribution to the Xth Plenary Assembly, CCIR, Geneva 1963 (ITU, Geneva 1963) Vol 4, Document 103

2. Pearson, K. W. "Method for the Prediction of the Fading Performance of a Multisection Microwave Link" Proc. I. E. E. E., Vol. 12, No. 7, July 1965. In a private communication Pearson has pointed out that more information on this subject is available in an article by J. Battesti and L. Boithias which appears in Annales des Telecommunications. Tome 18, No. 5-6, May-June 1963 (In this article the captions of figures 3 and 4 are interchanged.)

3. S. O. Rice "Noise in F. M. Receivers" Chapter 25 in Time Series Analysis edited by M. Rosenblatt, Wiley 1963

4. E. A. Nelson "The Response of an F. M. Discriminator to an F. M. Signal in Randomly Fading Channels" Doctoral Dissertation, Polytechnic Institute of Brooklyn, 1967. A summary of one part of this dissertation was presented at the 1966 IEEE International Communications Conference.

5. R. Krulee, "Design of a Fading Simulator" Proc. 9th National Communication Symposium, Utica, New York, 10-63.

6. R. J. Adams and B. M. Mindes, "Evaluation of IF and Baseband Diversity Combining Receivers" I. R. E. Transactions on Communications Systems (6-58)

7. J. W. Boyhan "New Forward Acting Predetection Combiner" Digest of Technical Papers, 1966 I. E. E. E. International Communications Conference 6-66 Session 17 (100)

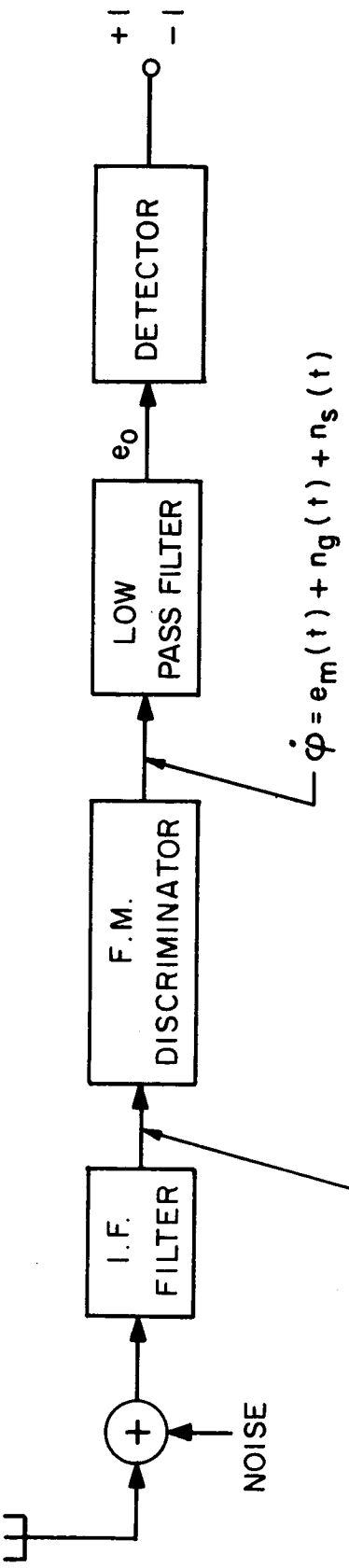
+1
-1
DETECTOR
LOW PASS FILTER
F.M. DISCRIMINATOR
I.F. FILTER
NOISE
e_o
$\dot{\varphi} = e_m(t) + n_g(t) + n_s(t)$
$A\cos\left(\omega_o t + \int^t e_m(\lambda)\, d\lambda\right) + N(t)$

Fig. III A. 1-1

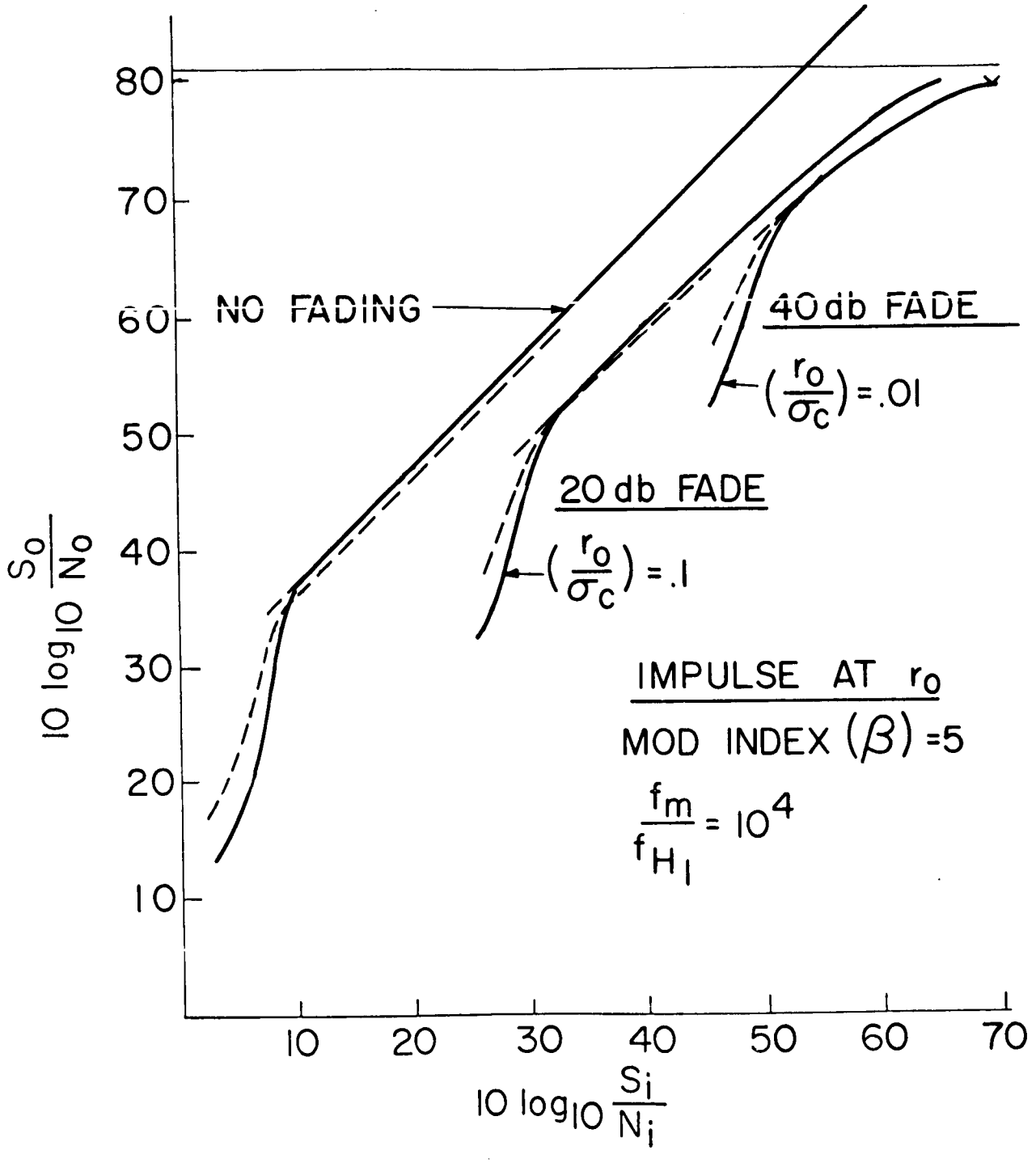
80
70
60
50
40
30
20
10
NO FADING
40db FADE
$(\frac{r_o}{\sigma_c}) = .01$
20 db FADE
$(\frac{r_o}{\sigma_c}) = .1$
IMPULSE AT r_o
MOD INDEX $(\beta) = 5$
$\frac{f_m}{f_{H_1}} = 10^4$
$10 \log_{10} \frac{S_o}{N_o}$
10
20
30
40
50
60
70
$10 \log_{10} \frac{S_i}{N_i}$

Fig. III A 1-2

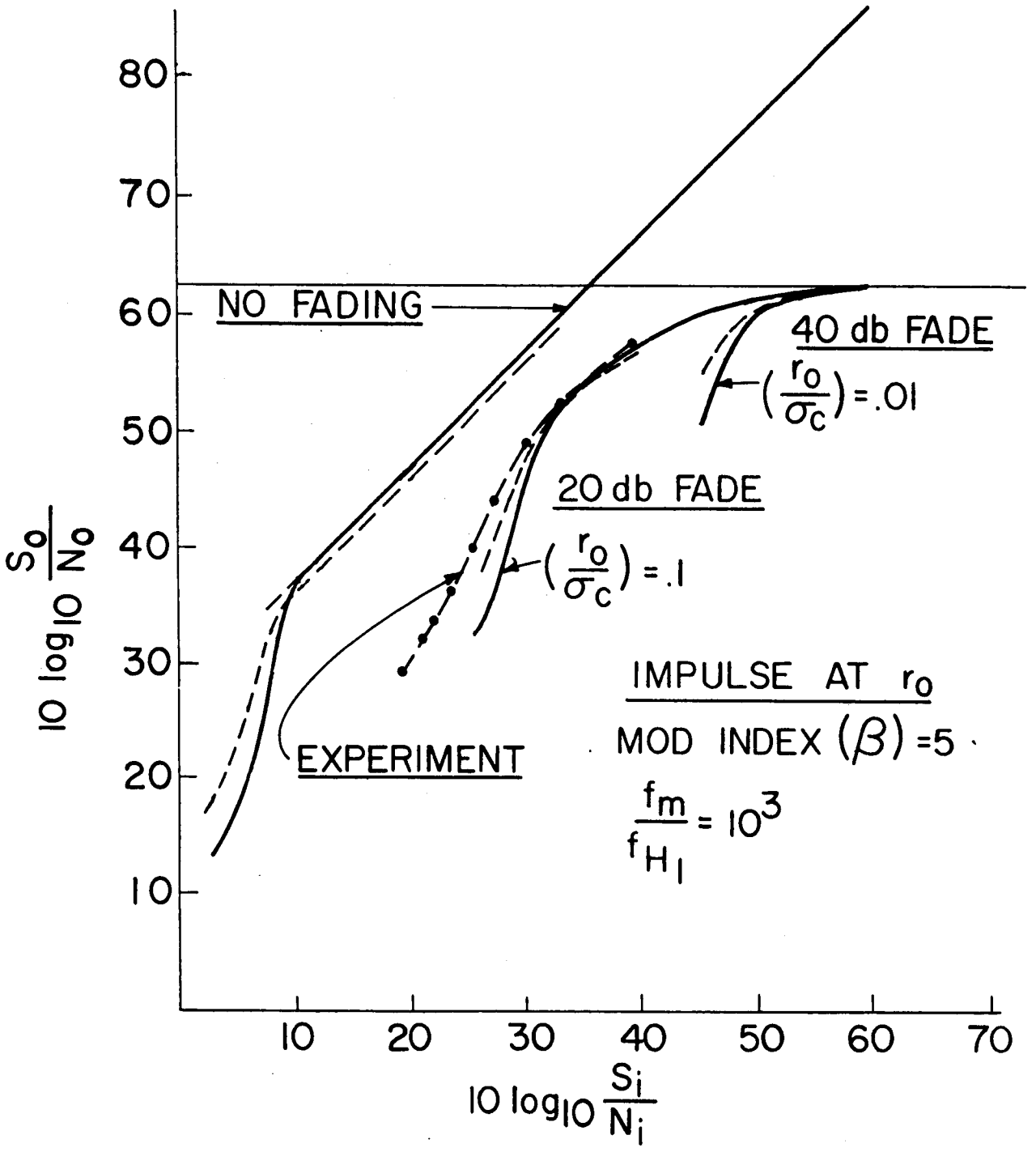
80
70
60
50
40
30
20
10
NO FADING
40 db FADE
$(\frac{r_o}{\sigma_c}) = .01$
20 db FADE
$(\frac{r_o}{\sigma_c}) = .1$
EXPERIMENT
IMPULSE AT r_o
MOD INDEX $(\beta) = 5$
$\frac{f_m}{f_{H_1}} = 10^3$
$10 \log_{10} \frac{S_o}{N_o}$
10
20
30
40
50
60
70
$10 \log_{10} \frac{S_i}{N_i}$

Fig. III A. 1-3

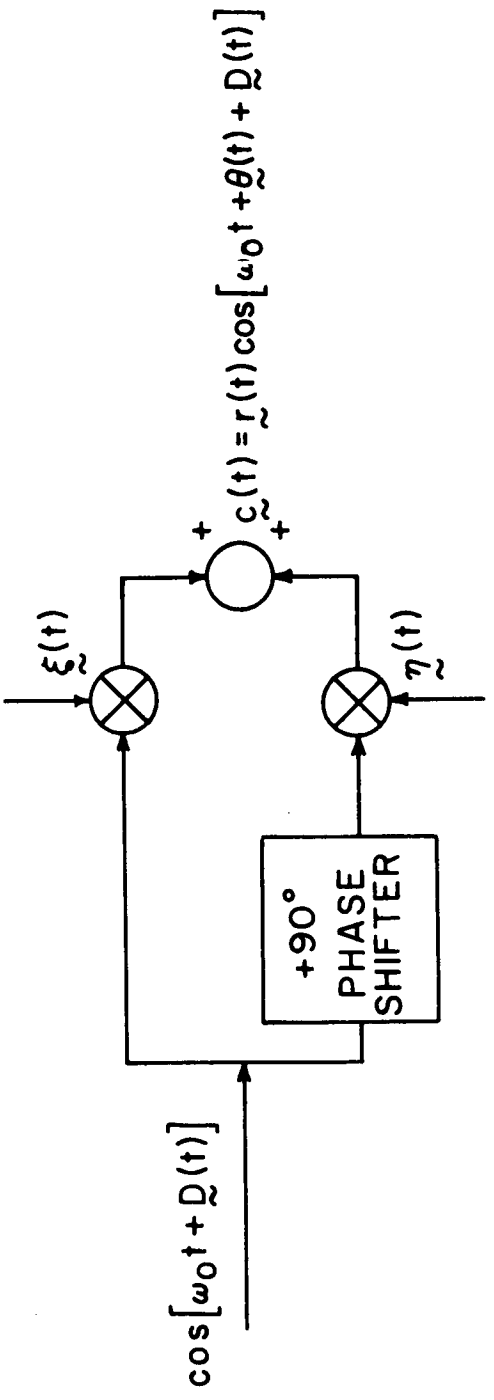
$\tilde{c}(t) = \tilde{r}(t)\cos[\omega_0 t + \tilde{\theta}(t) + \tilde{D}(t)]$
$\tilde{\xi}(t)$
$\tilde{\eta}(t)$
+90° PHASE SHIFTER
$\cos[\omega_0 t + \tilde{D}(t)]$

Fig. III A. 1-4

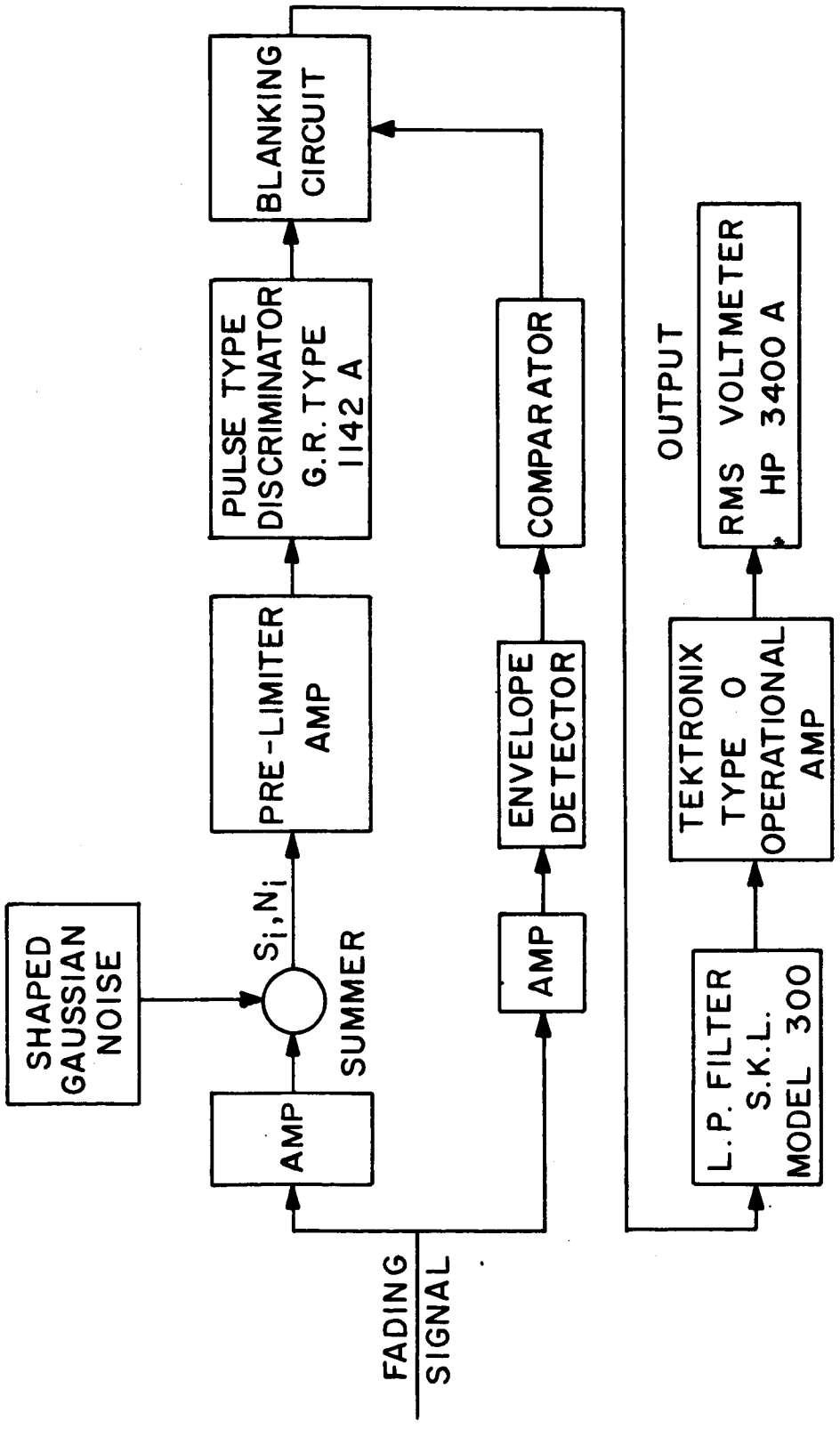
SHAPED GAUSSIAN NOISE
S_i, N_i
SUMMER
AMP
PRE-LIMITER AMP
PULSE TYPE DISCRIMINATOR G.R. TYPE 1142 A
BLANKING CIRCUIT
FADING SIGNAL
AMP
ENVELOPE DETECTOR
COMPARATOR
OUTPUT
L.P. FILTER S.K.L. MODEL 300
TEKTRONIX TYPE O OPERATIONAL AMP
RMS VOLTMETER HP 3400 A

Fig. III A.1-5

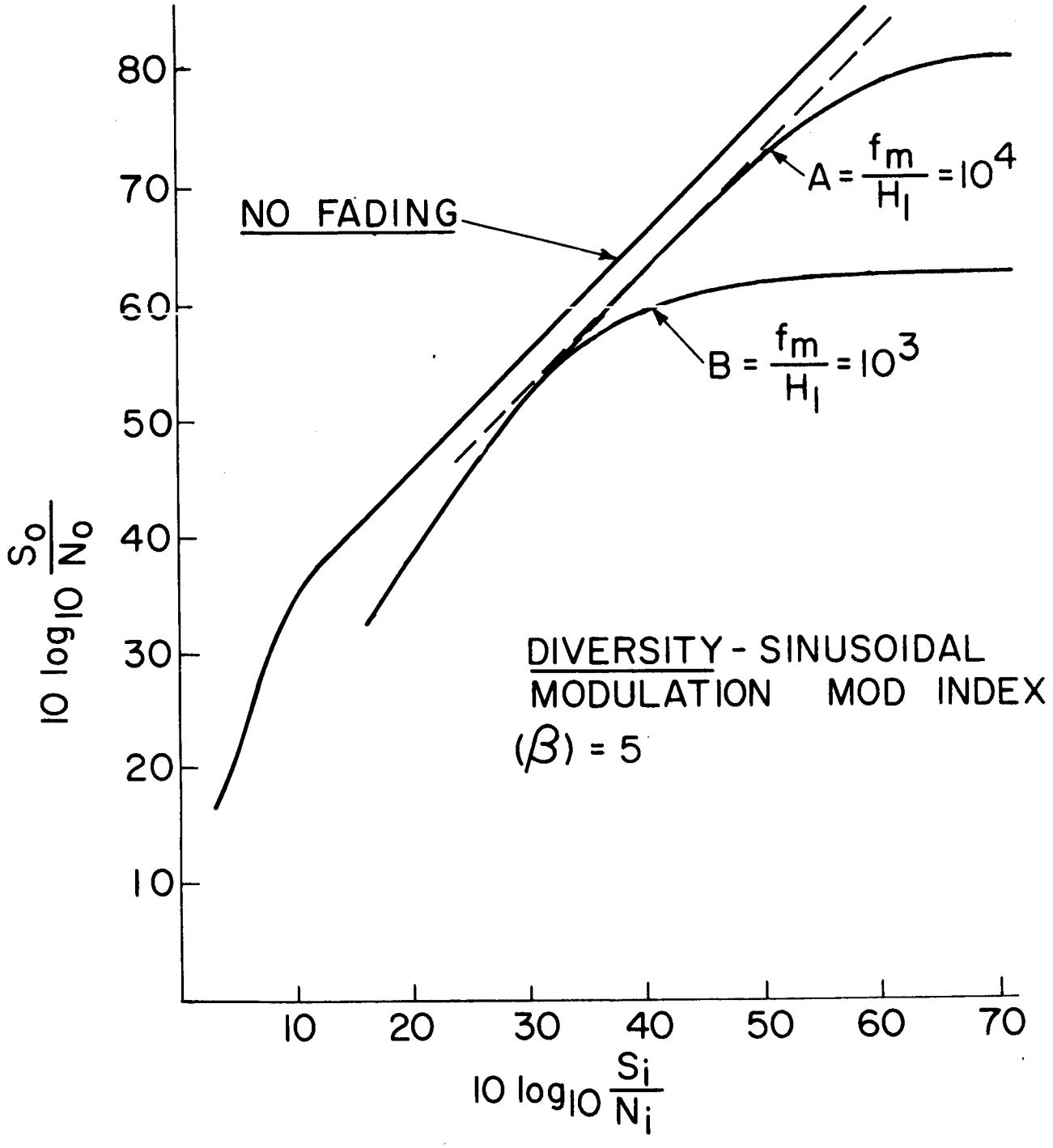
80
70
60
50
40
30
20
10
$\frac{S_o}{N_o}$ 10 log10
NO FADING
A = $\frac{f_m}{H_1}$ = 10^4
B = $\frac{f_m}{H_1}$ = 10^3
DIVERSITY - SINUSOIDAL
MODULATION MOD INDEX
(β) = 5
10
20
30
40
50
60
70
10 log10 $\frac{S_i}{N_i}$

Fig. III A. 1-6

III A2. DEMODULATION OF DIGITAL SIGNALS USING AN FM DISCRIMINATOR[1]

INTRODUCTION

Quite often it is convenient to demodulate a frequency shift keyed (FSK) signal using a discriminator and then detect the resultant baseband sequence using a suitable low pass filter and sample detector.

The introduction of the FM discriminator can degrade the system performance by increasing the errors observed per second. This is due to the discriminator's nonlinearity which even far above the threshold can generate a spike. Rice[2] has shown that the noise output of the discriminator consists of gaussian noise and spike noise. In the region of low error rate the errors caused by each type of noise can be computed separately and the total error rate then equals the sum of the individual error rates.

The calculation of the output gaussian noise and the expected number of spikes occurring per second was first made by Rice,[2] who applied his results to the calculation of signal to noise ratio. Rice assumed that the occurrence of the spikes are governed by a Poisson distribution. Schilling[3] verified this assumption above and below threshold.

In this study Rice's results are extended and the error rate calculated when demodulating an FSK signal consisting of an alternating 1010 sequence, a 11001100 sequence, and 111000111000 sequence calculated. Any other sequence can also be considered. It is shown below that there are three regions of interest in the problem. At very high Δ T products (Δ is proportional to the frequency deviation caused by a positive or a negative bit, and T is the duration of the bit) errors are due only to the gaussian noise. At an intermediate range of ΔT, the spikes produce the majority of the errors, and at low values of ΔT the gaussian noise produces most of the errors. The matched filter detector is shown to yield results similar to the discriminator detector at low and high values of ΔT.

A spike error correction device was developed which permits reversal of the decision based on the arrival and characteristics of the spike. The use of this device permits operation in the commonly used region of $1 \leq \beta \leq 4$ for digital signals, with error rates that more closely approximate those obtained theoretically with a matched filter. It is important to note that the "threshold" effect observed in signal to noise considerations is not observed in the same

sense in digital error rates. The effect of the spikes causes threshold when the signal to noise ratio is approximately 10db. On the other hand, gaussian errors predominate regardless of signal to noise ratio in the "gaussian" error region. In the spike region, "spike" type errors predominate in a corresponding manner. Thus, an increase in the error rate given by the guassian formulation alone, is obtained in certain regions of operations which are a function of modulation index β, which in turn is proportional to ΔT.[1]

I. Analysis

The FM signal and white gaussian noise

$$e_1(t) = A \cos\left(\omega_o t + \int^t e_m(\lambda)\, d\lambda\right) + \eta(t) \qquad (1)$$

(where $e_m(t)$ is a binary signal having values $\pm 2\pi\Delta$, each bit has a duration of T seconds) are passed through an IF filter and then demodulated using the FM discriminator of Fig. 1. The output signal is filtered by a low pass gaussian filter and sampled once per bit. The sampling rate is assumed fixed.

(a) Signal Characteristics

Three periodic sequences of signals are considered. The 1010, 11001100, and the 111000111000 sequences were chosen for simplicity of calculation. The analysis is, however, amenable to the consideration of any length sequence.

Before modulating the signal for transmission, the signal is filtered by an ideal low pass filter having a bandwidth, $\frac{1}{T}$ cps, as shown in Fig. 2. This restricts the bandwidth required for transmission and the bnadwidth of the IF filter in the receiver.

The filtered signal, $e_m(t)$ is then frequency modulated. The information is transmitted through a noisy channel where the noise is taken to be gaussian and additive. At the receiver the signal is demodulated through an ideal discriminator and passed through a low pass filter. (See Fig. 1)

The low pass filter has been assumed gaussian. This is a convenient assumuption since the integrations are easy to perform. It has been shown that commercially available 3 and 4 pole filters closely approach these characteristics. At the sampling instant the output signal has the amplitude shown in Fig. 3.

(b) The Output Gaussian Noise

The output gaussian noise is FM noise obtained by differentiating the phase jitter caused by the additive noise. The FM noise is filtered by the low pass filter. The output noise is a function of the modulation. An exact expression for the output gaussian noise power has been established. The equation indicates that the variation in output gaussian noise power including modulation and neglecting modulation is less than 1 db.

(c) Output Noise Due to Spikes

Rice[2] calculated the expected number of spikes occurring per second including modulation. One can show that when modulation is present, a spike has a much higher probability of occurrence than when no modulation exists. In addition, when a positive bit occurs, a negative spike has a significantly higher probability of occurence than a positive spike.

2. Calculation of Error Rates

(a) Error Rates due to Gaussian Noise

Assuming that the transmission of a positive or negative bit is equiprobable, the probability of an error, P_e, due to the gaussian noise can be found using the standard likelihood ratio technique.

The error rate due to gaussian noise for the various sequences are given by:

$$Pe(1010) = \frac{1}{2}\,\mathrm{erfc}\,\frac{5.66}{\sqrt{2N_o}} \qquad (2a)$$

$$Pe(1100) = \frac{1}{2}\,\mathrm{erfc}\,\frac{5.2}{\sqrt{2N_o}} \qquad (2b)$$

$$Pe(111000) = \frac{1}{2}\,\mathrm{erfc}\,\frac{6.16}{\sqrt{2N_o}} \qquad (2c)$$

where N_o is the output noise power due to the FM noise.

(b) Error Rates due to Spike Noise

One can show that an error caused by a spike is significant in a region of ΔT where the spike can cause only one error - an error in the bit occurring during the inception of the spike.

Figure 3 illustrates the procedure for calculating the error rate due to

spikes when an alternating 1010 pattern is transmitted. Figures 3a and 3b show the modulation and the spike after filtering by the gaussian filter. The width, D, of the spike is the time duration that the spike exceeds the filtered signal at its sampling point. Thus the probability of an error due to the spike is the probability of its arrival within the width D. The results of the calculations yield the following results:

$$Pe(1010) = 0.81\,\Delta T\,\left[\sin\frac{\pi}{2}, \frac{D}{T}\right]\, e^{-A^2/2Ni}$$

$$0.28 \leq \Delta T \leq 1.66 \qquad (3a)$$

$$= 0.81\,\Delta T\,, e^{-A^2/2Ni}$$

$$\Delta T \leq 0.28 \qquad (3b)$$

Similar results were obtained for the other sequences.

(c) Probability of Error Using an FM Discriminator

The total probability of error using an FM Discriminator is found combining equations 2 and 3. The probability of error using a 1010 sequence is shown in fig. 4.

If ΔT exceeds 1.66 in the 1010 case, errors are caused only by the output gaussian noise. If ΔT is below this value spikes predominate in causing errors. As ΔT decreases further, the gaussian noise again becomes the dominant term.

The region in which errors due to spikes predominate is

$$0.31 \leq (\Delta T)_{1010} \leq 1.66 \qquad (4)$$

The above calculations omit the possibility of an error being caused by a spike and gaussian noise in combination. This might occur when the signal strength at the sampling instant exceeds the spike height but the gaussian noise adds to the spike height causing an error to occur. These errors occur in a narrow region of ΔT just above 1.66 for the 1010 sequence.

3. Probability of Error of Matched Filter

The probability of error using a matched filter was computed and the results compared to the theoretical error rates of the FM Discriminator.

The matched filter error rate is given by:

$$Pe_{1010} = \tfrac{1}{2}\,\mathrm{erfc}\left[\frac{A^2}{2N_i}(\beta+1)(1-J_o[2\beta])\right]^{\frac{1}{2}} \qquad (5)$$

The results of eq. (5) are plotted in Fig. 5. It is readily seen that in the region of low ΔT the P_e of the FM discriminator closely approaches that of the matched filter. In the spike region, the matched filter has a substantially lower P_e. Note that due to the inherent nature of FSK which results in an argument under the error function of eq. (5) which consists of a Bessel function, the matched filter and the FM Discriminator display "bumps" as a function of ΔT or β. These bumps occur in the spike region ($0.7 \leq \beta \leq 5$) and represent the increase in error rate due to spikes.

4. Reduction of Errors by Spike Error Correction

The probability of a positive spike is much greater than that of a negative spike when the signal is negative and the reverse is true for a negative spike. Hence, the characteristics of an observed spike can be used to advantage in the correction of errors caused by these spikes. A system utilizing the spike characteristics for error correction has been developed. In this system a tentative decision is always made as to whether a positive or negative bit has been transmitted. The occurrence of a spike during the bit interval is also determined. Knowing the time of occurrence of the spike and the low pass filter characteristic, one can calculate whether or not the spike can cause an error; if it can the decision is reversed.

As expected a significant reduction in error rate only occurs in the "spike region". Fig. 6 shows the experimental results obtained with and without "spike error correction" for several values of CNR. The theoretical discriminator results are shown for comparison. Notice that the errors have been reduced by a factor of 3 using the experimental facility developed in our laboratory.

Conclusions

The results given above show that Rice's technique for analyzing the response of an FM discriminator to an analog signal can be extended to determine the probability of error of a frequency shift keyed digital signal. They also show that the errors are caused either by gaussian noise or spike noise. The optimum operating modulation index occurs at the junction of the spike and gaussian noise regions.

The matched filter and FM discriminator are seen to exhibit similar P_e in the gaussian region. In the spike region, the FM discriminator is significantly poorer. Improvement in P_e can be obtained by utilizing a spike correction device in conjunction with the FM discriminator. Further improvement toward obtaining the matched filter results are expected with the use of the FMFB or the PLL[4].

References

1. Schilling, D. L. and Hoffman, "Demodulation of Digital Signals Using an FM Discriminator, Presented at NEC - October 1966

2. Rice, S. O. "Noise in FM Recievers" Chapter 25 of Time Series Analysis edited by Rosenblatt, 1963

3. Schilling, D. L. and Ringdahl, I., "On the Distribution of Spikes Seen at the Output of an FM Discriminator Below Threshold" Proc. I. E. E. E. December 1964.

4. Schilling, D. L., Billig, J., and Kermisch, D., " Error Rates in FSK Using the Phase Locked Loop Demodulator", Proceedings of the 1st I. E. E. E. Annual Communications Convention, p. 75

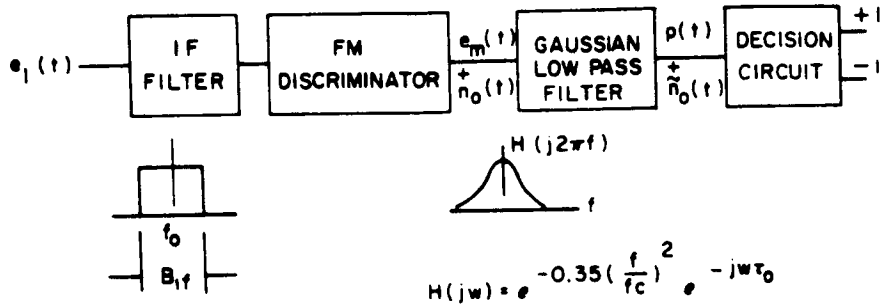

The FM Discriminator

Fig. III A 2-1

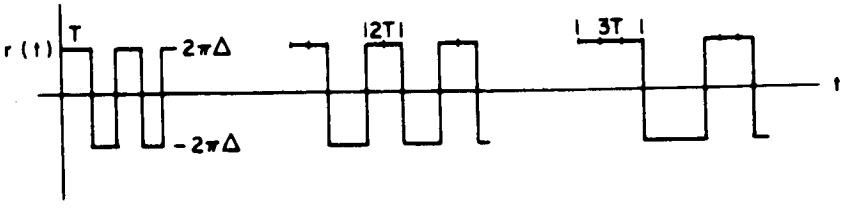

(a) The Three Sequences Transmitted

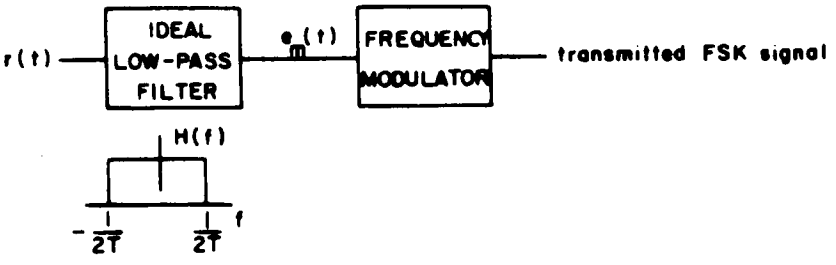

(b) The Filtering of the Data to be Transmitted

Fig. III A. 2-2

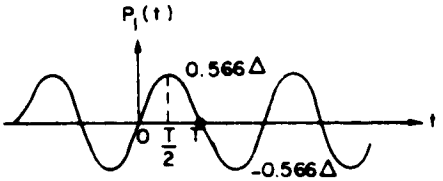

(a) Gaussian filtered 1010 sequence

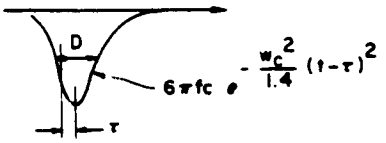

(b) Gaussian filtered Spike

Fig. III A. 2-3

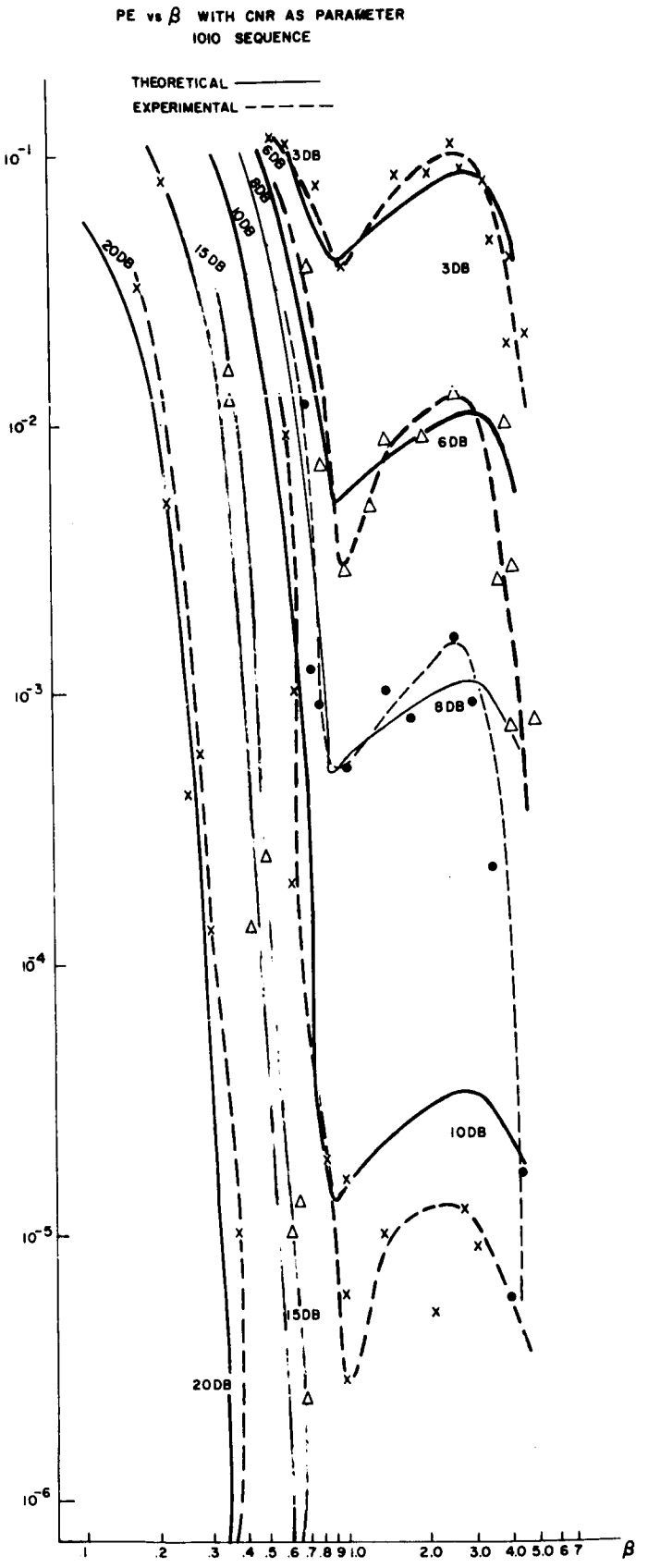
PE vs β WITH CNR AS PARAMETER
1010 SEQUENCE
THEORETICAL
EXPERIMENTAL
3DB
6DB
8DB
10DB
15DB
20DB
10^{-1}
10^{-2}
10^{-3}
10^{-4}
10^{-5}
10^{-6}
.1 .2 .3 .4 .5 .6 .7 .8 .9 1.0 2.0 3.0 4.0 5.0 6 7 β

Fig. III A 2.4

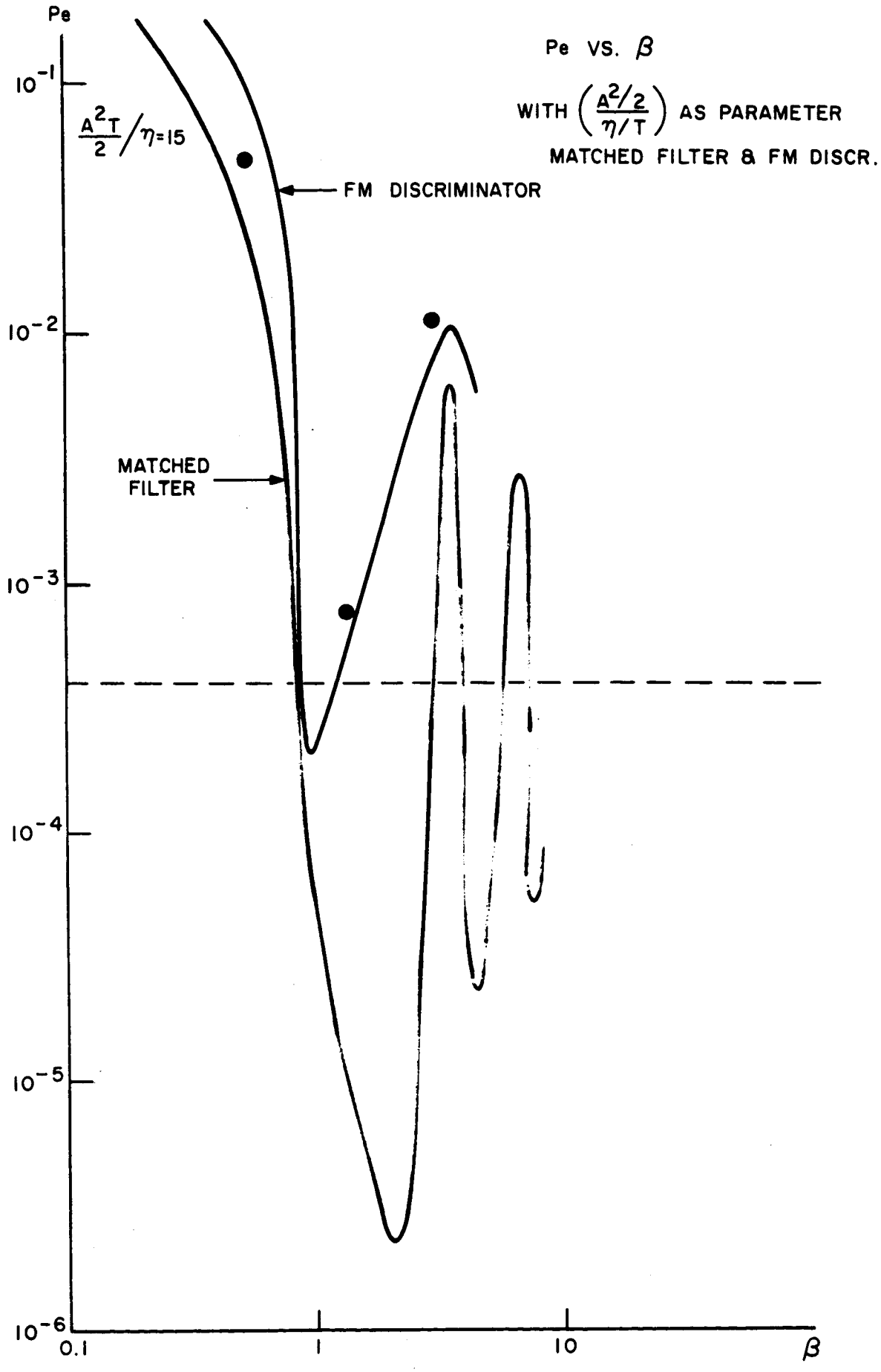
Pe
Pe VS. β
WITH (A²/2 / η/T) AS PARAMETER
MATCHED FILTER & FM DISCR.
10⁻¹
A²T/2 / η=15
FM DISCRIMINATOR
10⁻²
MATCHED FILTER
10⁻³
10⁻⁴
10⁻⁵
10⁻⁶
0.1
1
10
β

Fig. III A 2.5

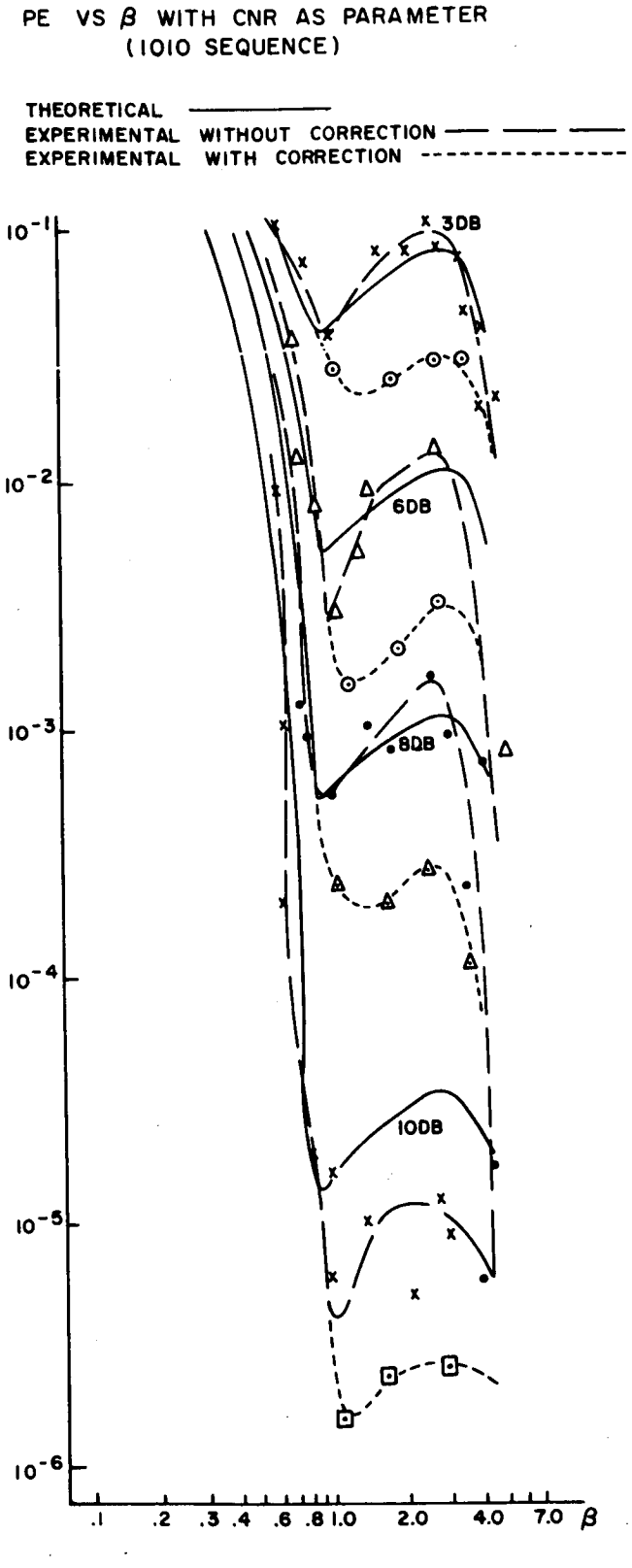
PE VS β WITH CNR AS PARAMETER
(1010 SEQUENCE)
THEORETICAL
EXPERIMENTAL WITHOUT CORRECTION
EXPERIMENTAL WITH CORRECTION
10^-1
10^-2
10^-3
10^-4
10^-5
10^-6
3DB
6DB
8DB
10DB
.1
.2
.3
.4
.6
.8
1.0
2.0
4.0
7.0
β

Fig. III A. 2-6

III. A3 FREQUENCY SHIFT KEYING THROUGH A FADING MEDIUM USING AN FM DISCRIMINATOR FOR DETECTION[1]

INTRODUCTION

A signal, characterized by non-selective fading, is added to white stationary Gaussian noise of zero mean and passed through a bandpass i.f. amplifier which is symmetric about the carrier frequency, f_o. The bandwidth, 2B, is assumed wide enough so that the signal passes undistorted. The i.f. output which is now in the form of signal plus bandlimited Gaussian noise is applied to an ideal limiter and then frequency demodulated. This is illustrated in Figure 1.

In this report we determine theoretically and experimentally the effect of fading on the error rate at the discriminator output using a suitable low pass filter and sample detector when the modulation is an alternating 1010 sequence of bit duration T seconds. Before modulating the signal for transmission, the binary sequence is passed through an ideal low pass filter of bandwidth $\frac{1}{T}$ (see figure 2), thus D(t) in Figure 1 appears sinusoidal in shape. This restricts the bandwidth required for transmission and the bandwidth of the I.F. amplifier in the receiver. The low pass filter is assumed to be of a Gaussian shape as shown in figure 3.

The characteristics of the fading channel have been discussed in section III. I. In that section it was noted that the CCIR[2] has assumed that it is permissible to truncate the Rayleigh distribution at some point since when the fade drops below a certain level, the circuit will be completely cut off, or switched to a better path.

An experimental system has been set up according to the CCIR recommendation. Thus, the approach taken is to determine the error rate by neglecting the time that the envelope is below r_o. The ratio of $(r_o/\sigma_c)^2$ is defined as the fading depth (e.g. $r_o/\sigma_c = .1$ corresponds to a 20db fade).

II. Analysis Procedure

To determine the output error rate one first considers the expression for $\dot{\phi}$ (see figure 1) in a bit interval T. We assume slow fading so that in any bit interval the fading variables r and θ may be regarded as constant. Using the model of Rice[3] and following the procedure of III. A2 the output of the discriminator, $\dot{\phi}$ can be expressed as the sum of the modulating signal, D, a

Gaussian noise type term with amplitude dependent on the fading statistics, and a spike noise term. Applying this signal to the low pass filter yields a filtered version of these terms.

The error rate computation is an extension of the work described in III.A2. An error occurs at the sampling instant if a positive bit was sent and a negative bit is recorded. The error mechanism can be due to the Gaussian noise term alone, a negative spike alone (positive spikes cause no errors), and a combination of the noise and spike term. (Schilling[4] has shown that it is highly unlikely for a positive spike to cancel a Gaussian noise error since when a positive bit is sent the negative spike has a much higher probability of occurrence. The error rate is assumed low enough so that each type of noise error can be calculated separately, the total error rate equaling the sum of the individual error rates. With this assumption, there is no more than one spike present in each bit interval. Thus,

$$P\left(\frac{\text{error}}{+}\right) = P\left(\frac{\text{error-Gaussian}}{+}\right) + P\left(\frac{\text{error-neg. spike}}{+}\right) + P\left(\frac{\text{error-Gaussian and neg. spike}}{+}\right) \quad (3)$$

Since the system is symmetrical, eq. 3 is also the error rate for a negative spike. Equation 3 is also the total error rate when the positive and negative bit transmitting probabilities are equal.

If the bit amplitude is made sufficiently large (increasing the modulation index) then a negative spike will cause no error. In the region where spikes can cause errors, the possibility of the Gaussian noise term and a spike jointly causing errors is neglected so that

$$P\left(\frac{\text{error}}{+}\right) - P\left(\frac{\text{error-Gaussian}}{+}\right) + P\left(\frac{\text{error-neg. spike}}{+}\right) \quad (4)$$

The calculations appear in reference 1.

III. Results

Figure 4 shows a plot of error rate for a 14db fade as a function of modulation index, β, for several input signal-to-noise ratios. The solid curve indicates the theoretical results and the circled points correspond to the experimental results. In the region below a modulation index of unity Gaussian noise errors dominate while for the region of modulation index between unity and four, spike errors are dominant. At higher modulation indices, the effect of joint errors is observed (the curve of SNR of 20db).

References

1. E.A. Nelson " The Response of an FM Discriminator to an FM Signal in Randomly Fading Channels" Ph.D. Dissertation Polytechnic Institute of Brooklyn 1967.

2. Contribution to the Xth Plenary Assembly, CCIR, Geneva 1963 (ITU, Geneva 1963) Vol. 4, Document 103

3. S.O. Rice "Noise in F.M. Recievers" Chapter 25 in Time Series Analysis edited by M. Rosenblatt, Wiley 1963

4. D.L. Schilling and E. Hoffman "Demodulation of Digital Signals Using an FM Discriminator" Proc NEC 10-66

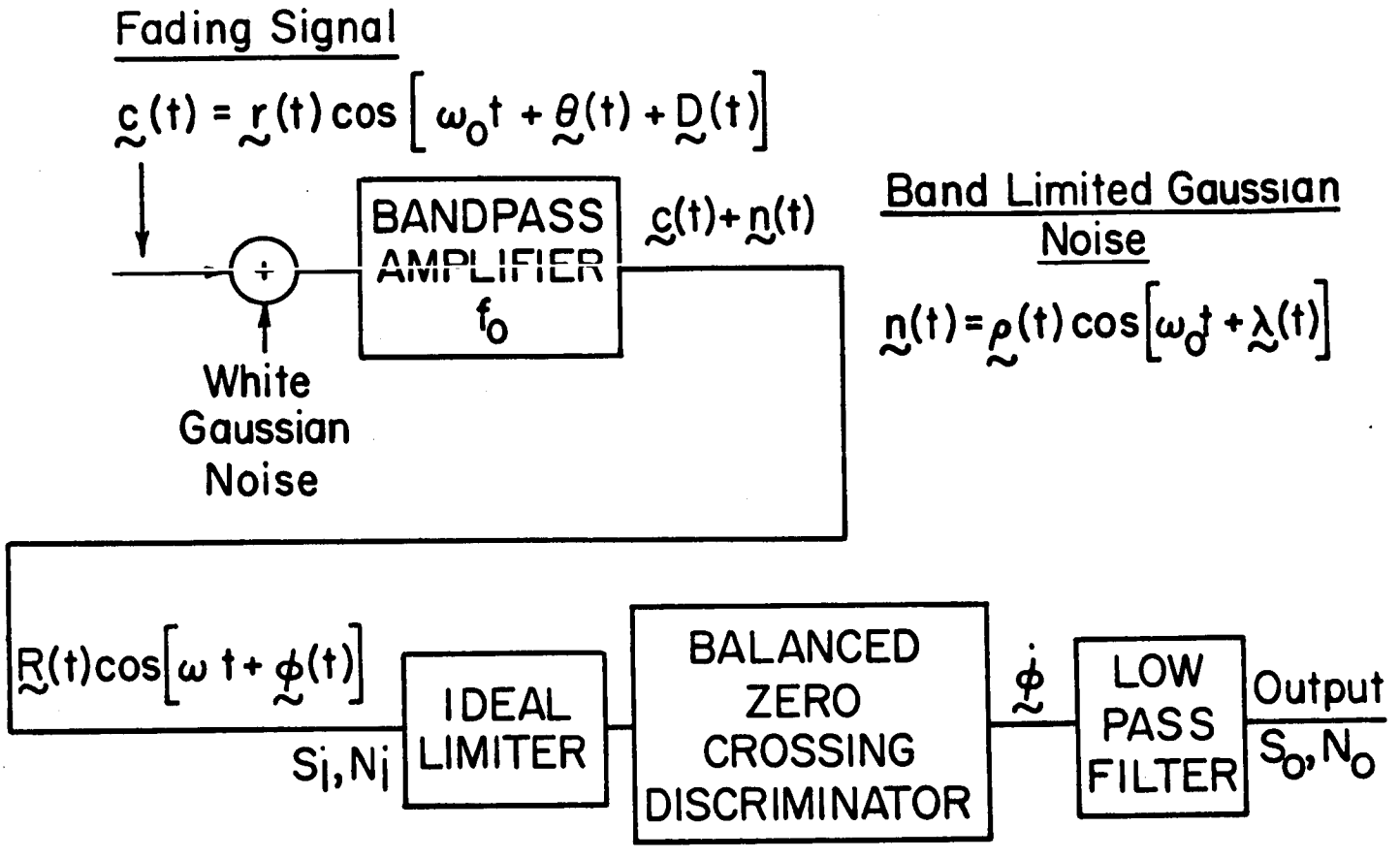

Fig. III A. 3-1 FM System

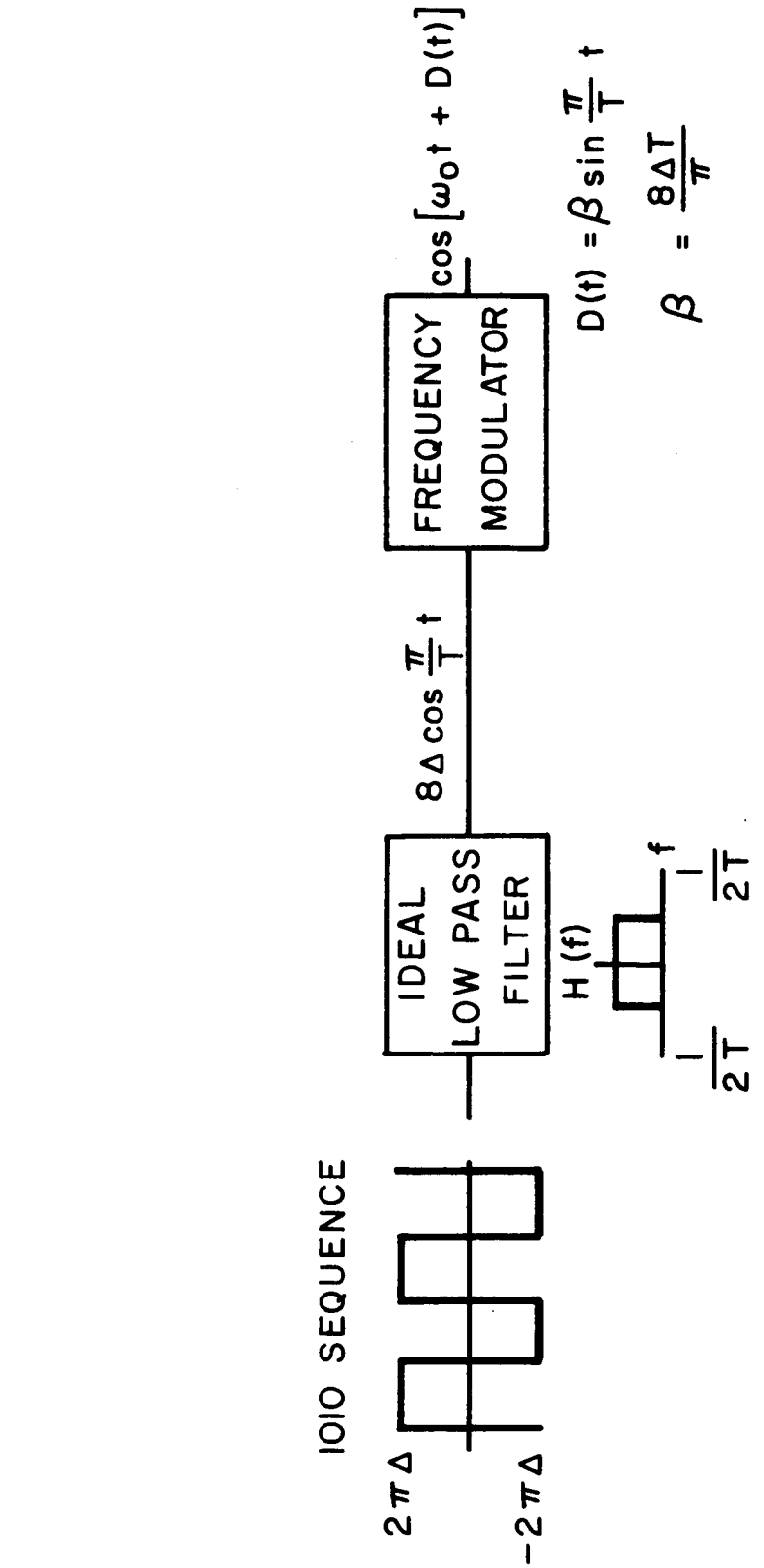
1010 SEQUENCE
2πΔ
-2πΔ
IDEAL LOW PASS FILTER
8Δ cos π/T t
FREQUENCY MODULATOR
cos [ω₀t + D(t)]
H(f)
f
1/2T
1/2T
D(t) = β sin π/T t
β = 8ΔT/π

Fig. III A 3-2

$$h(t) = \frac{\omega_m}{\sqrt{1.4\pi}} e^{-\frac{\omega_m^2 (t - t_o)^2}{1.4}}$$

$$H(\omega) = e^{-0.35 (f/f_m)} e^{-j\omega t_o}$$

$$f_m = \frac{1}{2T}$$

Fig. III A 3-3

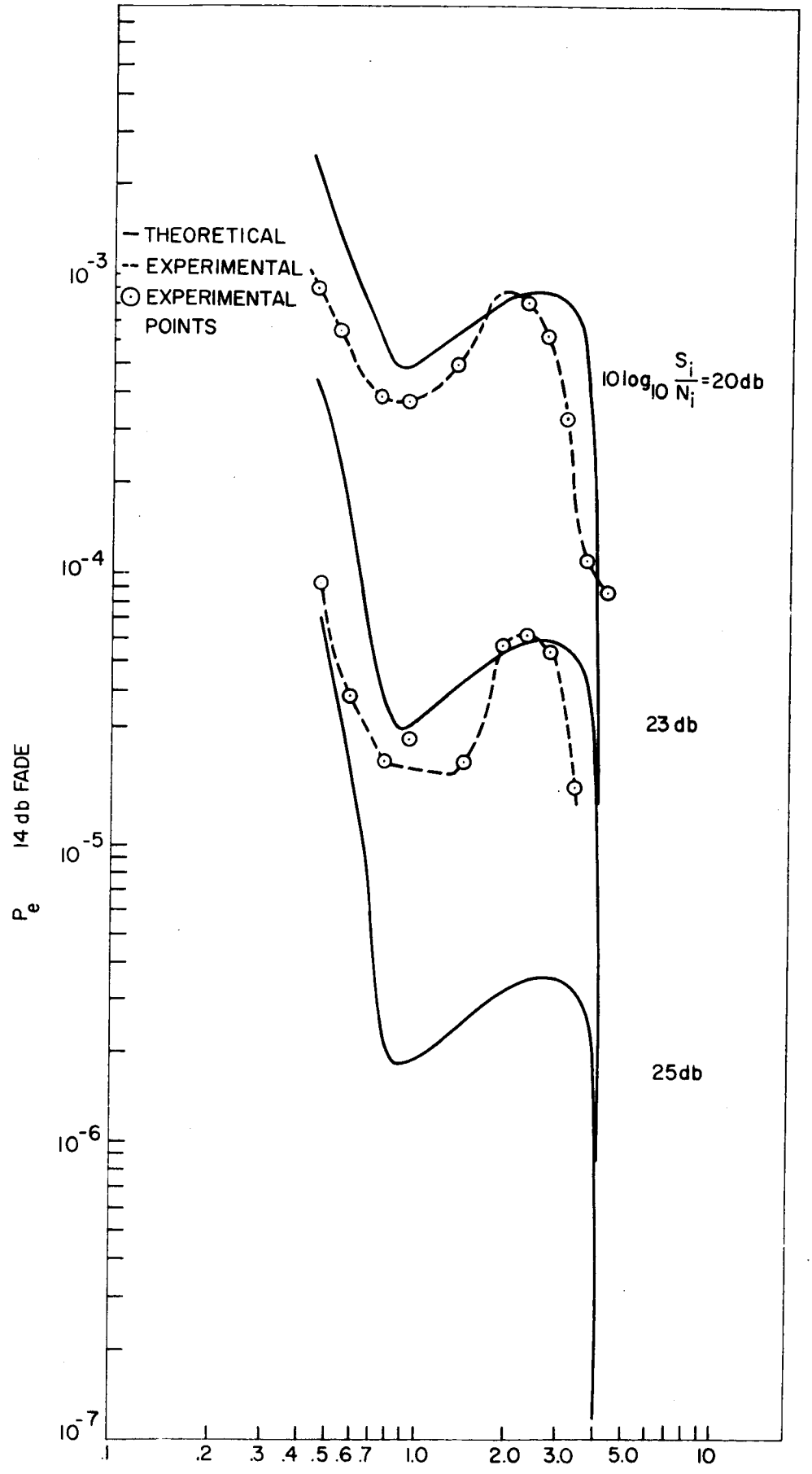

Fig. III A. 3-4 Error Rate for 14db Fade

III - B Frequency Feedback Demodulator

I. Introduction

In this section of the report a new Frequency Feedback Demodulator (FFD) is introduced which is capable (both theoretically and experimentally) of extending the noise threshold exhibited by the standard limiter and discriminator. This threshold extension is achieved by the FDD's ability to supress the noise "clicks" which occur at low input signal to noise ratios in the ordinary discriminator. In addition, because the FFD does not lock in phase or frequency, it exhibits no second threshold which is due to "loss-of-lock clicks" appearing at the output.

Two basic embodiments of the FFD are presented. One embodiment is a self contained device which directly processes the input FM signal which typically appears at the output of the IF strip of a receiver. The second embodiment of the FFD is a loop which processes the output of an ordinary limiter-discriminator at baseband. This operation at low frequencies has the advantage of making the device functional in any frequency range where a discriminator can be constructed, say up to the 100GHz band.

In the paragraphs to follow the two types of the FFD are presented in block diagram form and shown to be mathematically equivalent, and their ability to obtain the demodulated F.M. signal for the case of high input signal to noise is demonstrated. With the aid of a model for the input noise, the ability of the FFD to supress output noise "clicks" is then shown. Finally, employing a physical circuit realization of the FFD, experimental signal in noise data are taken. Simultaneous data are taken on a limiter and discriminator and compared to the FFD data to show that the FFD does indeed extend the noise threshold.

II. Basic Operation of FFD

The block diagrams of the R. F. and baseband versions of the FFD are shown in figure III-B-1 and figure III-B-2 respectively. The R. F. version of the FFD consists basically of a balanced demodulator (without a limiter) whose output is fed back to the input in such a way that demodulator center frequency tracks the instantaneous input frequency, thus providing an error signal and output signal which closely correspond to the instantaneous frequency. In addition, since the demodulator output is virtually insensitive to amplitude variations of the output signal at its center frequency, and since the feedback causes this type of operation, amplitude variations in the input are not transmitted to the output. Hence the R. F. version of the FFD acts as a limiter-discriminator without the incorporation of a physical limiter circuit · Such a limiter circuit would discard the amplitude information which is essential to threshold improvement.

To further understand the operation of the circuit shown in figure(III-B-1), consider the F. M. signal with amplitude variations $e_1(t)$ applied to the input of the system

$$e_1(t) = a(t) \cos [\omega_o t + \varphi(t)] \qquad \text{(III-B-1)}$$

where a(t) is the instantaneous amplitude, $\varphi(t)$ is the instantaneous phase and ω_o is the carrier frequency.

For this input the output of the differentiator $e_2(t)$ takes the form

$$e_2(t) = -\frac{a(t)}{\omega_a} \{\omega_o + \dot{\varphi}(t)\} \sin [\omega_o t + \varphi(t)] + \left(\frac{\dot{a}(t)}{\omega_a}\right) \cos [\omega_o t + \varphi(t)] \qquad \text{(III-B-2)}$$

where ω_a is an arbitrary constant. For the case where $\omega_o >> \dot{a}(t)$ (which is usually true in practice), equation (2) reduces to

$$e_2(t) = \frac{a(t)}{\omega_a} \{\omega_o + \dot{\varphi}(t)\} \sin [\omega_o t + \varphi(t)] \qquad \text{(III-B-3)}$$

Clearly with $e_2(t)$ given by equation (III-B-3) (3) the output of the FFD is given by

$$e_o(t) = A \{a(t) [\frac{\dot{\varphi}(t)}{\omega_a} - n e_o(t)]\} * h(t) \qquad \text{(III-B-4)}$$

where A is the gain of the loop amplifier, n is the multiplier constant and h(t) is the impulse response of the loop low pass filter(integrator).

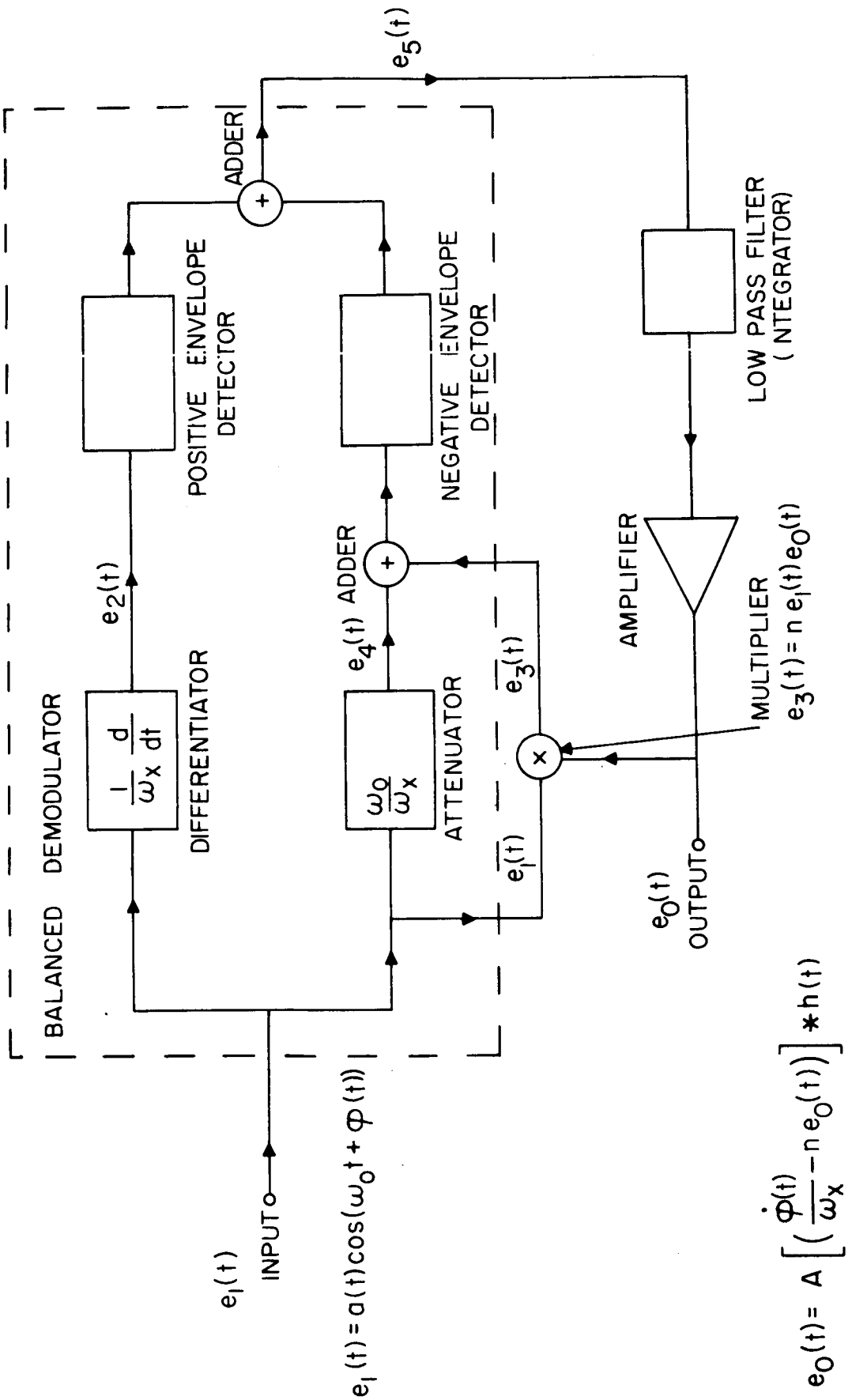

Fig. III-B-1 Block Diagram of the R.F. version of the FFD.

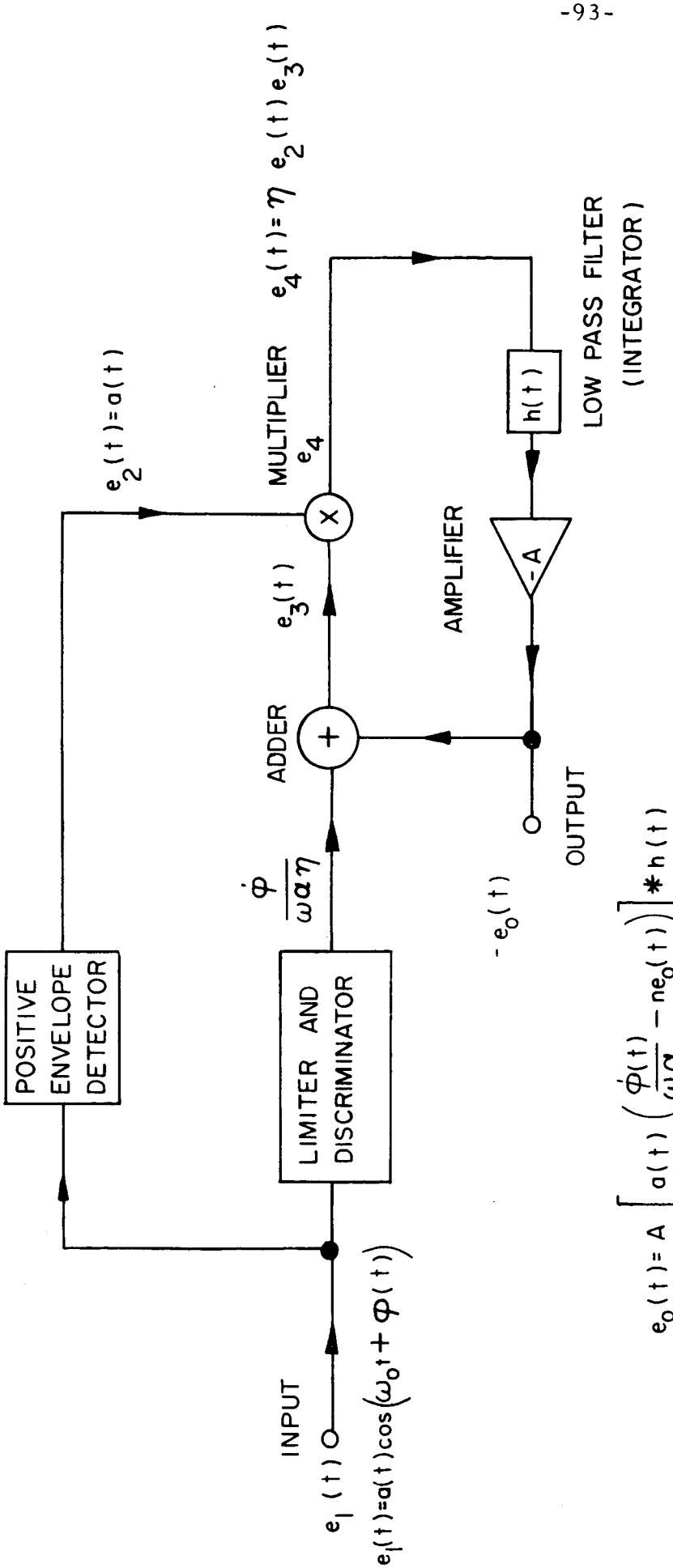

Fig. III-B-2 Block Diagram of the Baseband Version of the FFD

For the case where the low pass filter is indeed an integrator, as shown in figure III-B-3, equation III-B-4 takes the form

$$\frac{\dot{e}_o(t)}{\omega_\beta} + n A e_o(t)\, a(t) = \frac{A}{\omega_a}\, a(t)\, \dot{\varphi}(t) \qquad \text{(III-B-5)}$$

where ω_β is the integrator constant.

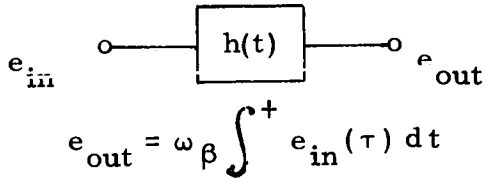

Figure III-B-3 Input-Output Relationship for an Integrator

It is now apparent from equation III-B-5 that if the loop is adjusted such that

$$[\dot{e}_o(t)/\omega_\beta] << n A e_o(t)\, a(t) \qquad \text{(III-B-6)}$$

then

$$e_o(t) = \frac{\dot{\varphi}(t)}{n\omega_a} \qquad \text{(III-B-7)}$$

which is the desired output of the FFD and is clearly independent of the input amplitude variations. Obviously the inequality III-B-6 can be met only if a(t) does not become zero; hence the FFD output is identical to the output of a limiter discriminator only when the input signal is not heavily corrupted by a deterministic signal or noise, i.e. the input signal to noise ratio is high.

Inequality III-B-6 which is necessary to make the FFD act as a limiter discriminator tor small amplitude disturbances or high input signal to noise may be interpreted physically as choosing the loop gain sufficiently high such that $\dot{\varphi}(t)$ passes through the closed loop bandwidth. Clearly for the case where an uncorrupted FM signal of the form

$$e_1(t) = A_o \cos[\omega_o t + \varphi(t)]$$

is applied to the F. F. D. equation III-B-5, for the system output, takes the form

$$\frac{\dot{e}_o(t)}{\omega_\beta} + n A e_o(t) A_o = \frac{A}{\omega_a} A_o \dot{\varphi}(t) \qquad \text{(III-B-8)}$$

which is the equation of a first order, linear, time-invarient system of band-

width $nA\,A_o\,\omega_\beta$ driven by $\frac{AA_o}{\omega_a}\,\dot{\phi}\,(t)$; hence the closed loop bandwidth is $nA\,A_o\,\omega_\beta$. Choosing this bandwidth wide enough to pass $\dot{\phi}\,(t)$ insures that the first term on the left of equation (III-B-8) is negligible, and since for small amplitude variations (high input signal to noise) $a(t) = A_o$ the inequality III-B-6 is also insured.

It is now quite clear that the RF version of the FFD yields an output identical with that of a limiter-discriminator provided the amplitude variations of the input signal are small and the closed loop system bandwidth* is adjusted to pass $\dot{\varphi}(t)$. Since $\dot{\phi}\,(t)$ in general consists of signal plus noise, and the noise occupies a bandwidth equal to that of the IF bandwidth, the closed loop bandwidth must be equal to or greater than the IF bandwidth. It is shown later that to reduce noise "clicks" one wishes to choose the closed loop bandwidth to be as small as possible; hence an optimum choice is obtained by choosing it equal to the IF bandwidth.

The baseband version of the FFD shown in Figure III-B-2 consists of the output of an FM limiter-discriminator driving a feedback loop whose loop gain is directly proportional to the amplitude of the input FM signal $e_1(t)$. This amplitude dependence is achieved by envelope detecting the input signal and multiplying the closed loop signal by the envelope $a(t)$. It is easy to see that the output of this baseband FFD has exactly the same differential equation as the RF version if the input has the form $e_1(t) = a(t)\,\cos\,[\omega_o t + \varphi\,(t)]$; consequently the theoretical performance of the two systems is identical. The baseband FFD also performs as an ideal limiter-discriminator for small variations in $a(t)$ and with the closed loop bandwidth adjusted to be large enough to pass $\dot{\phi}\,(t)$ undistorted. A look at figure III-B-2 indicates, however, that for small variations in $a\,(t)$ about a level A_o, $[\dot{\phi}\,(t)/n\omega_a]$ just passes through a linear, baseband feedback loop with sufficient bandwidth to transmit it to the out put to yield

$$e_o\,(t) = \dot{\phi}\,(t)/n\omega_a \,.$$

*Although $h\,(t)$ is chosen in this development to be an integrator, the same results are readily shown to be true for any low pass $h(t)$ which does not result in instability.

Figure III-B-2 also indicates why the two versions of the FFD supress noise "clicks" when the input signal to noise level becomes low. As is well known, when a "click" occurs in $\dot{\varphi}$ due to noise, a(t) usually becomes small. The reduction in a(t) reduces the loop bandwidth which causes the loop output to remain essentially constant until a(t) again increases, thereby suppressing "clicks" from the loop output.

In the section below a noise model is postulated with which a mathematical analysis of "click" supression is made. Experimental data is then presented to substantiate the analysis.

III "Click" Supression by the FFD

In order to determine how the FFD supresses the "clicks" that appear in the output of a limiter discriminator as the input signal to noise ratio becomes low, one must first consider the mechanism which causes a click. If noise and an FM carrier are present at the input to the FFD the input signal $e_1(t)$ takes the form

$$\begin{aligned} e_1(t) &= A_o \cos \omega_o t + n(t) \\ &= A_o \cos \omega_o t + \rho(t) \cos [\omega_o t + \theta(t)] \\ &= R_e \left\{ e^{j\omega_o t} [A_o + \rho(t)\, e^{j\theta(t)}] \right\} \end{aligned} \qquad \text{(III-B-9)}$$

where A_o is the FM carrier amplitude and n(t) is the input noise which may be written as $\rho(t) \cos [\omega_o t + \theta(t)]$. Figure III-B-4 shows a phasor diagram which corresponds to the low frequency portion of equation III-B-9. On the figure the resultant a(t) and $\varphi(t)$ of $e_\rho(t)$ are shown. Clearly

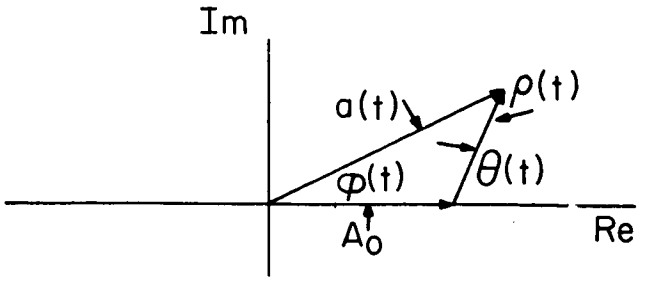

Figure III-B-4 Phasor Representation of a Carrier Plus Noise.

as $\rho(t)$ and $\theta(t)$ vary randomly, random variations in a(t) and $\varphi(t)$ occur. If $\rho(t)$ remains small so too do the variations in a(t) and $\varphi(t)$. As the input noise increases, however, $\rho(t)$ occasionaly becomes larger than A_o, and if at the same time $\theta(t)$ crosses π, $\varphi(t)$ increases or decreases suddenly by 2π and a sharp pulse in $\varphi(t)$ of area 2π occurs. This pulse, shown in figure III-B-5, is a discriminator "click".

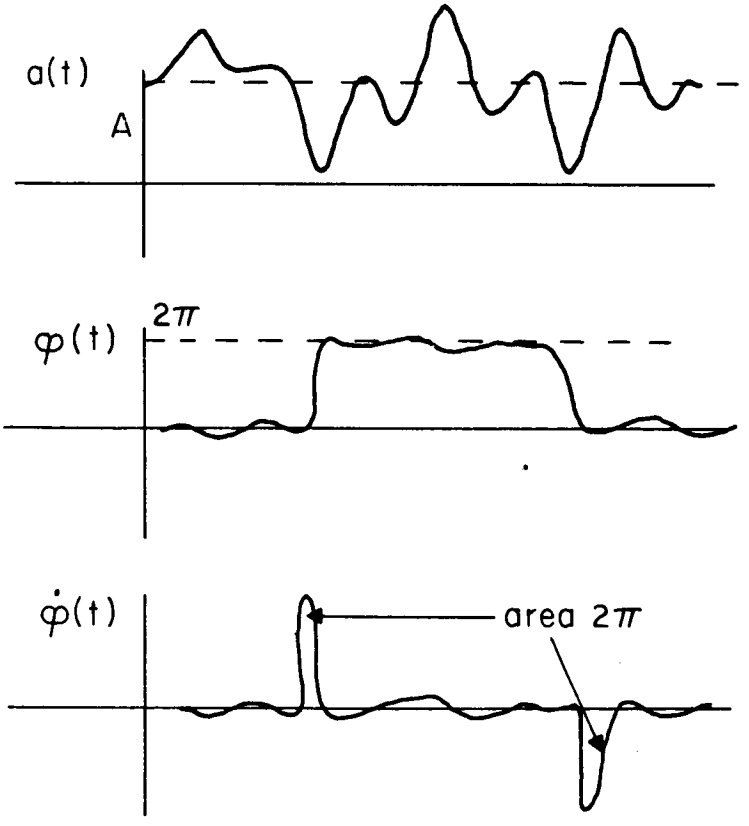

Figure III-B-5 "Click" Formation Process

At the onset of 'clicks' (the point where the input noise has become

large enough relative to the carrier to cause a few "clicks" per second) the probability that $\rho > A$ is small; hence most clicks occur with ρ just slightly larger than A or equivalently with $a(t) \approx 0$. As the input noise increases further, however, the average value of a(t) at the time a click occurs increases slightly. It is the fact that a(t) is small at the time of a "click" which permits its use to control the loop gain of the FFD and thus hold the output at a constant value during the click.

To understand this mechanism of click supression more clearly the model for a(t) and $\dot{\phi}(t)$ shown in figure III-B-6 is adopted and applied at the input of the FFD. By breaking the solution of equation III-B-5 into the three time regions, $t < 0$, $0 \leq t < t_o$, and $t_o < t$, and substituting in the model values of a(t) and $\dot{\phi}(t)$, three linear, time- invarient differential equations result whose solutions are found in the usual manner. In particular, for the limiting case of

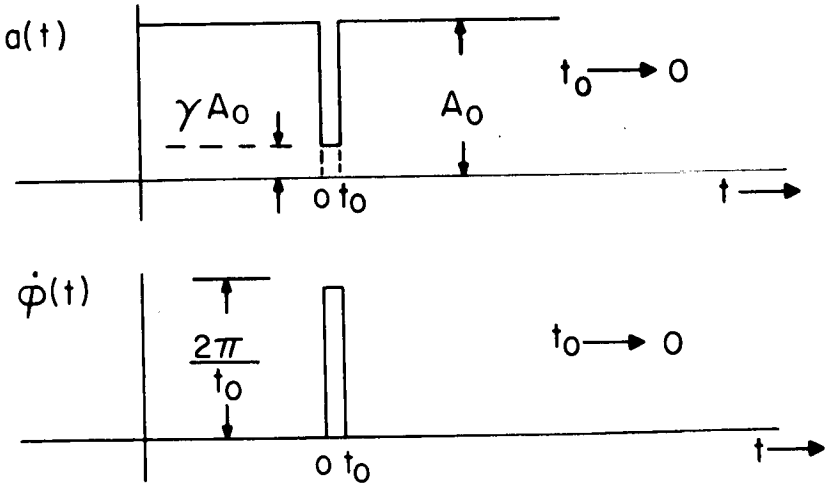

Fig. III-B-6 Model for a(t) and $\dot{\phi}(t)$ at the Time of a "Click".

$t_o \longrightarrow 0$ the system output $e_o(t)$ takes the form

$$e_o(t) = (\gamma)\left[2\pi \frac{\omega_\beta}{\omega_a} A A_o\right]\left[e^{-nA A_o \omega_\beta t}\right] U(t) \qquad \text{(III-B-10)}$$

where $U(t)$ is the unit step function.

It is apparent from equation (III -B-10) that for narrow pulses in $\dot{\varphi}(t)$, the output pulse amplitude is directly proportional to γ; hence if $a(t) \approx 0$ (i.e. $\gamma \approx 0$) when a "click" occurs, which is true at the onset of "clicks", the "click" is almost entirely removed from the output. Because of this phenomenon of "click" supression the output noise which causes the threshold in ordinary limiter-discriminators is greatly reduced and the FFD experiences an extension in threshold which is indeed measured experimentally.

It is of interest to note that equation III-B-10 is obtained as the "click" duration t_o approaches zero. If, on the other hand, t_o is increased relative to the reciprocal of the closed loop bandwidth, $e_o(t)$ approaches $\dot{\varphi}(t)/\omega_a \eta$ which is independent of γ thus affording no "click" supression. Since t_o in reality may not be varied but the closed loop bandwidth may, it is clear that for maximum click supression the closed loop bandwidth be chosen as small as possible. To be consistent with inequality III-B-6, the closed loop bandwidth should be chosen equal to the IF bandwidth through which the input FM signal is passed.

Although the above results are obtained with the loop low-pass filter chosen as an integrator, similar, although not identical, results are obtained with other low pass filter configurations. An optimum filter for "click" supression has not yet been found and work is continuing in this area.

IV Experimental Results

A circuit has been constructed to realize the baseband version of the FFD shown in figure III -B-2. The circuit operates at a carrier frequency of 50KHz and has a closed loop bandwidth of 1420Hz. To compare the FFD with a limiter-discriminator, both the FFD and General Radio - Frequency Meter and Discriminator are driven by a 50kHz FM signal with variable additive noise which has been passed through a 50kHz tripple pole IF band-

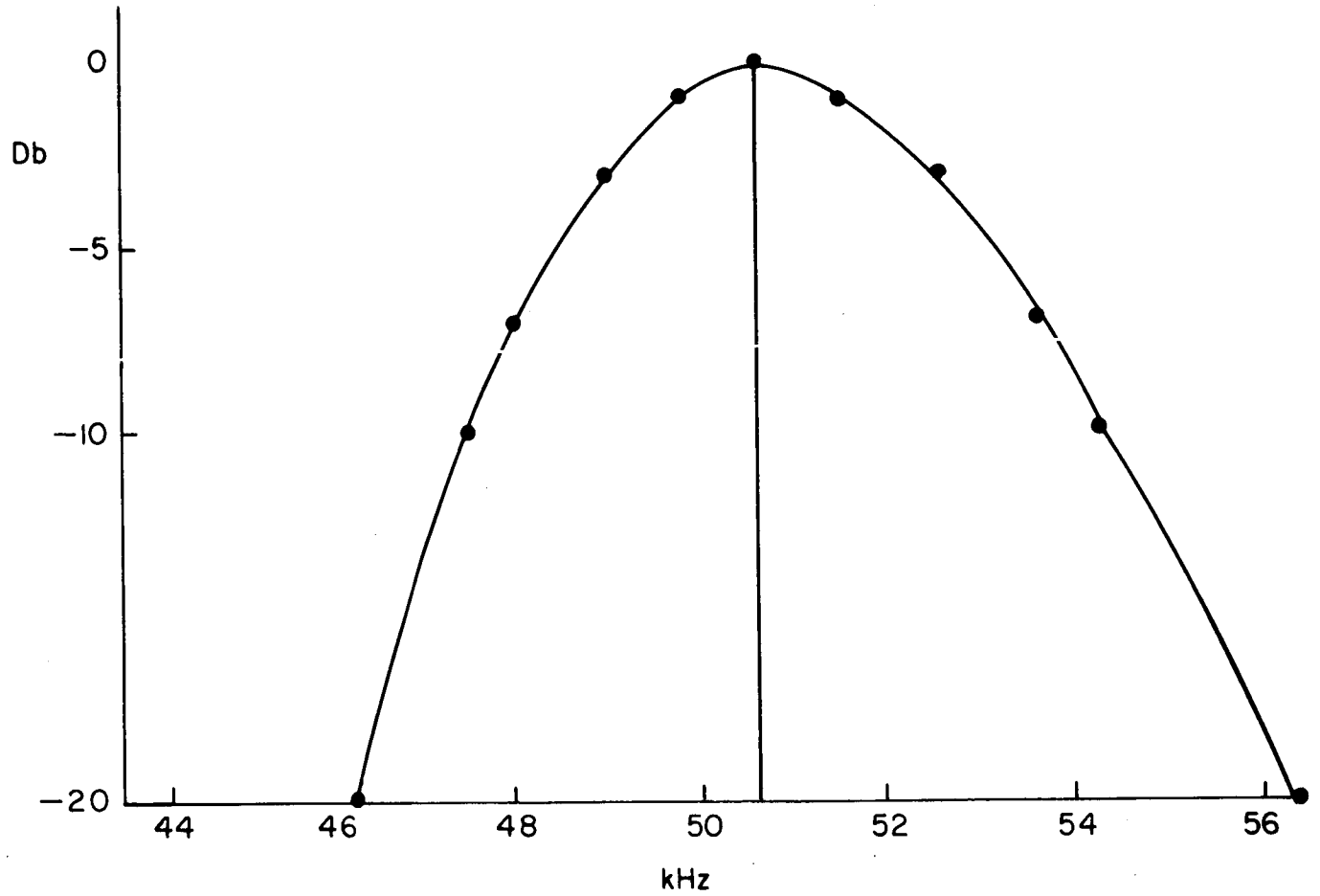

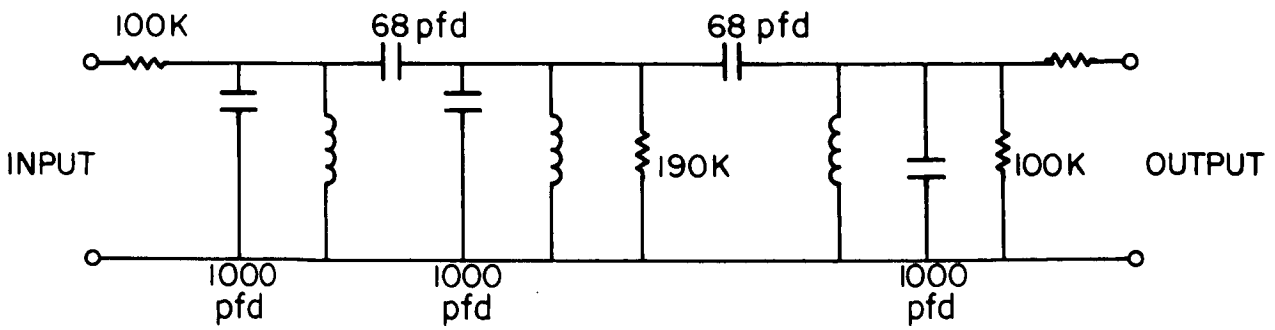

Fig. III-B-7 IF Filter and Filter Response

pass filter having a 3db bandwidth of 3.6kHz. The filter characteristic is shown in figure III-B-7. Both the FFD and the GR Frequency Meter have a Krohnhite model 310AB low pass filter at their outputs to provide the baseband filtering. Clearly with a fixed IF filter different modulation indicies may be realized by varying the bandwidth of the base band filters. Figure III-B-8 shows the complete experimental configuration for com - paring the FFD with the limiter discriminator. It should be noted that the

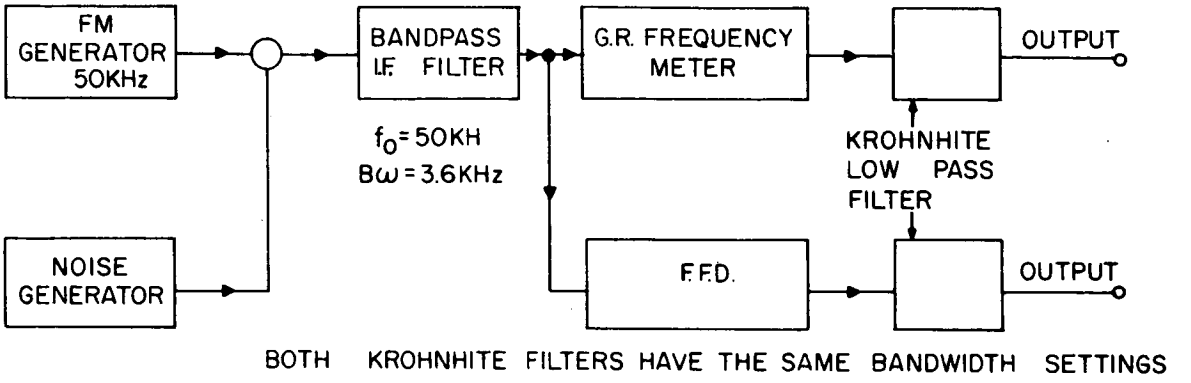

Figure III-B-8 Experimental Configuration for Comparing the FFD with the Limiter Discriminator

scale factor of the FFD is adjusted such that when a modulated FM signal is applied, its output amplitude is identical with that of the limiter-discriminator.

To observe the "click" supression mechanism of the FFD, an unmodulated carrier plus noise were applied to the system of figure III-B-8. For various carrier to noise ratios measured at the output of the IF filter, simultaneous traces of the two system outputs were recorded on a storage scope and photgraphed. For this test the baseband filters were set at 600 Hz. Figures III-B-9, 10, 11 compare the two system outputs with input carrier noise ratios of 6db, 4db, and 2db respectively. Figure III-B-12 shows the fine structure of "click" supression by expanding the time scale with an input carrier to noise ratio of 4db.

Although the photographs are dramatic evidence of "click" supression, they are only qualitative. To obtain a quantitative comparison of the two

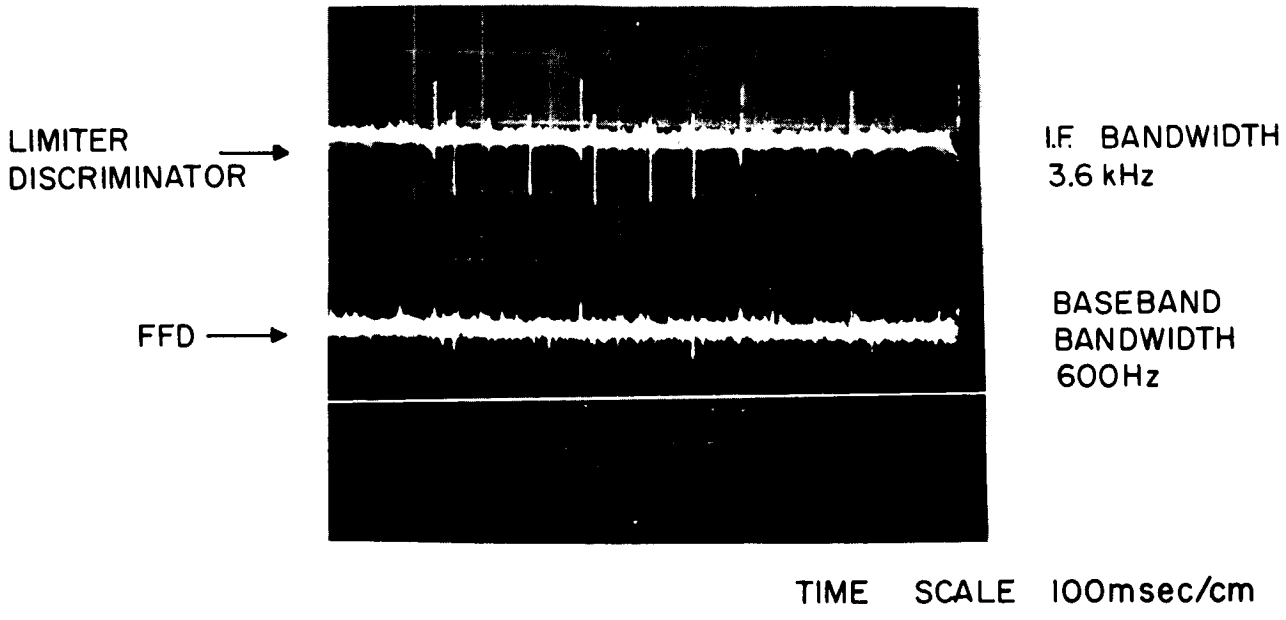

Fig. III-B-9 Comparison of FFD and Limiter-Discriminator for Carrier to Noise Ratio of 6db

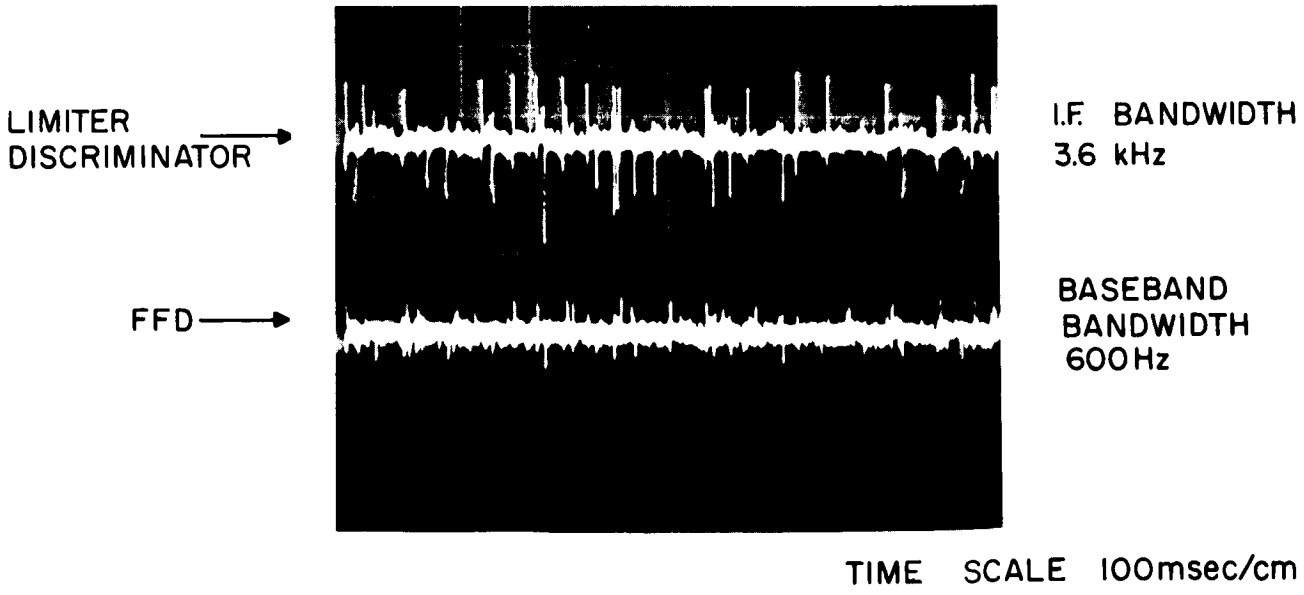

Fig. III-B-10 Comparison of FFD and Limiter-Discriminator for Carrier to Noise Ratio of 4db

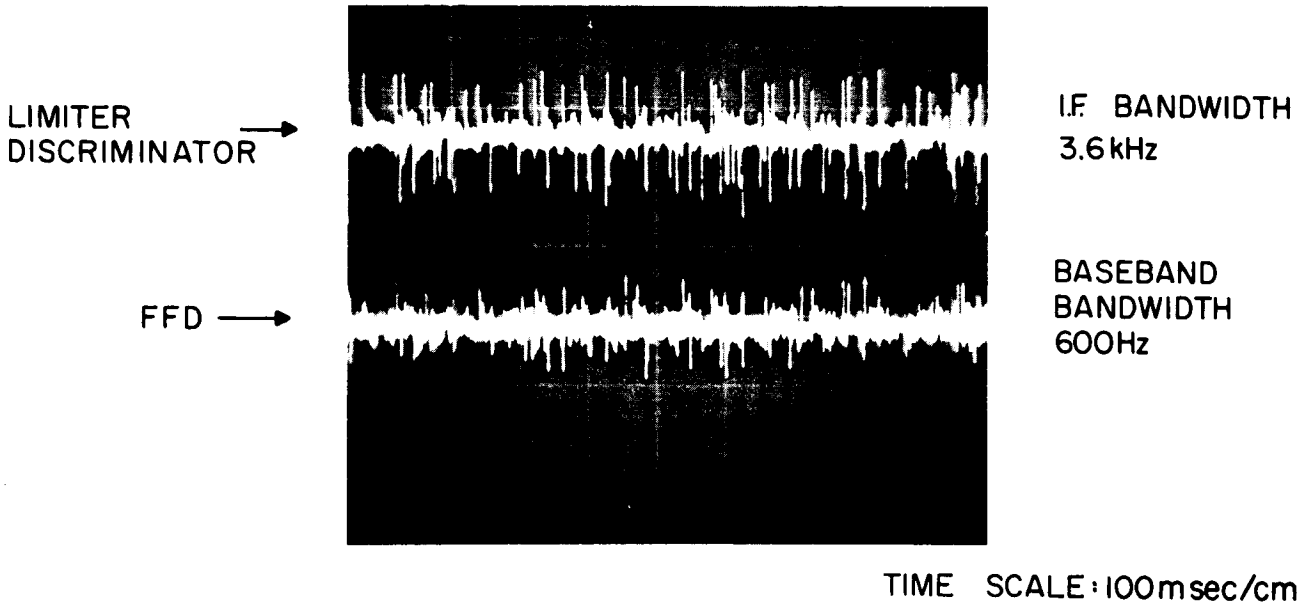

Fig. III-B-11 Comparison of FFD and Limiter-Discriminator for Carrier to Noise Ratio of 2db

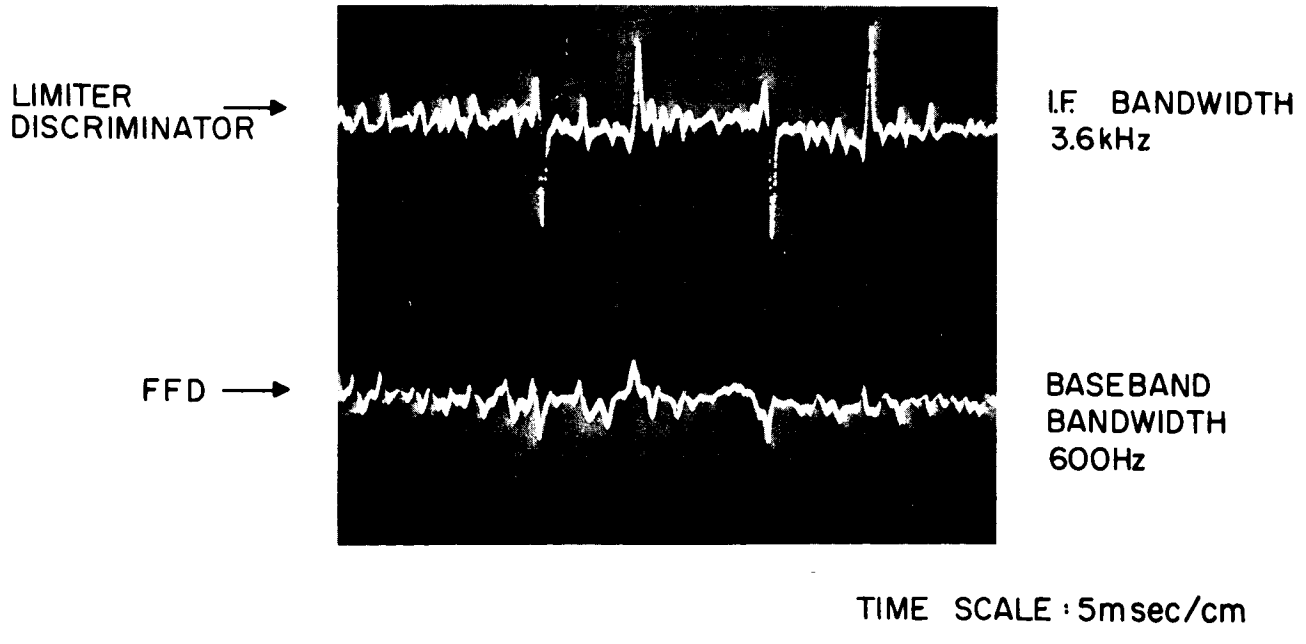

Fig. III-B-12 Comparison of FFD and Limiter-Discriminator for a Carrier to Noise Ratio of 4db

systems output signal to noise ratios are measured for the two systems. For these data the baseband bandwidth is set at 900Hz.

Figure III-B-13 is a plot of output signal to noise power vs input carrier to noise power for both systems where signal and noise are applied independently. With no noise, a carrier modulated with a 200Hz sinusoid to a 1.4kHz deviation is applied to both systems and the output signal level recorded. An unmodulated carrier of the same level, plus noise is then applied and the output noise of both systems is recorded for various carrier to noise ratios. The output signal to noise is then obtained by taking the ratio of the noise free signal power to the signal free noise power. It is clear from this plot that the supression of "clicks" does indeed increase the output signal to noise for a given input signal to noise.

Figure III-B-14 is a plot of output signal to noise power vs input carrier to noise power for both systems where modulation and noise are applied simultaneously. The carrier is modulated with a 5Hz signal to a 1.4kHz deviation. The signal power is obtained by placing the total output through a very low pass filter and the noise power is obtained by placing the output through a 20Hz high pass filter. Two sets of data are taken for baseband bandwidths of 900Hz and 600Hz and the curves are seen to be in general agreement with the previous curves. The signal in noise curves, however, lie below the curves of figure III-B-13 because of noise induced signal supression.

V. Conclusion

It is seen from the above data that the FFD does indeed suppress clicks thereby yielding an extension of the FM threshold. This "click" supression is particularly important in digital systems (FSK) where the "clicks" are almost exclusively responsible for the errors which occur in the vicinity of 6 to 10 db input carrier to noise ratios.

It is felt, that further improvement of the FFD can be obtained by choosing an optimum configuration for the low pass filtering within the loop.

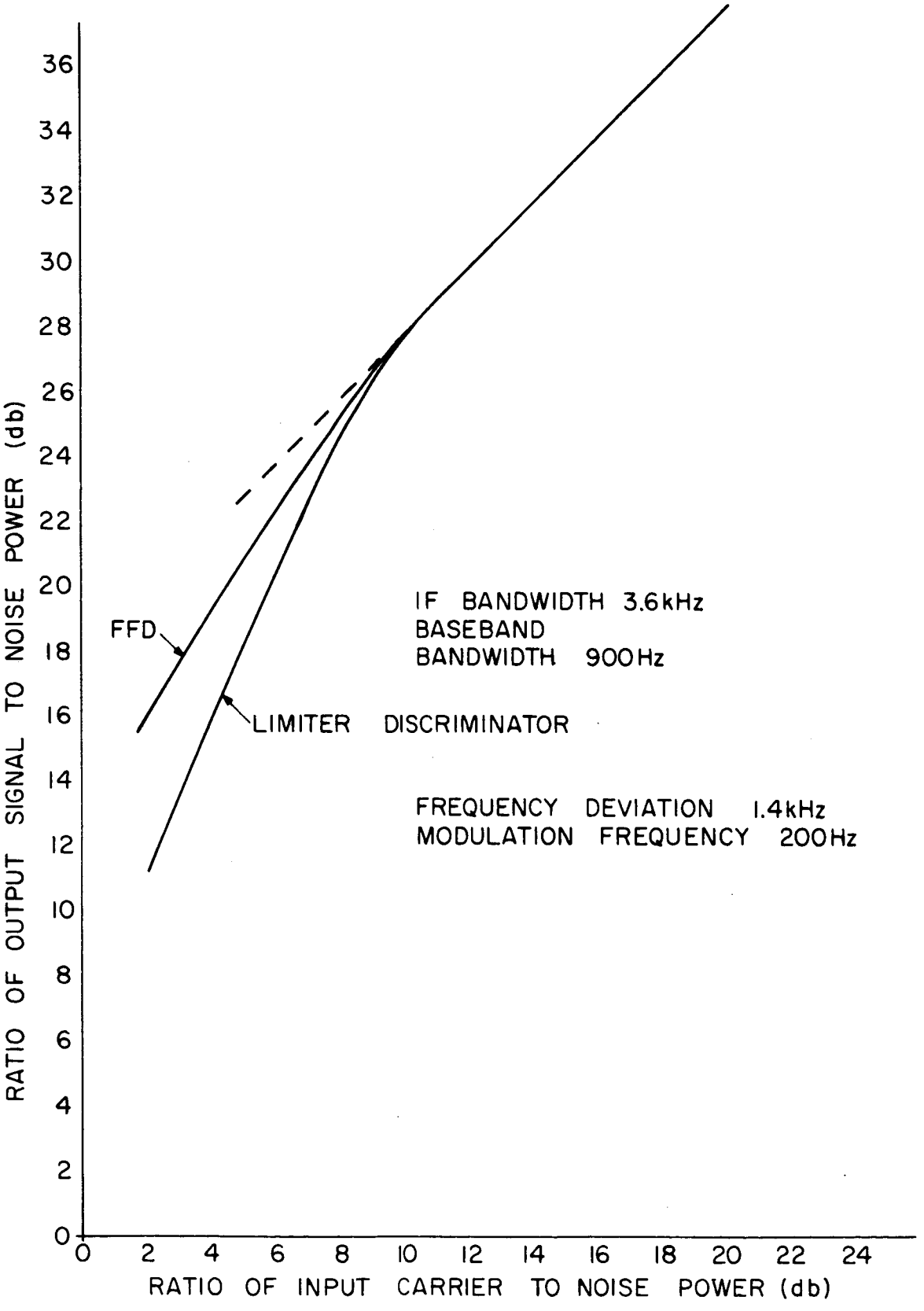

Fig. III-B-13 Plot of Output Signal to Noise Power vs. Input Carrier to Noise Power for the Case where Modulation and Noise are Applied Independently

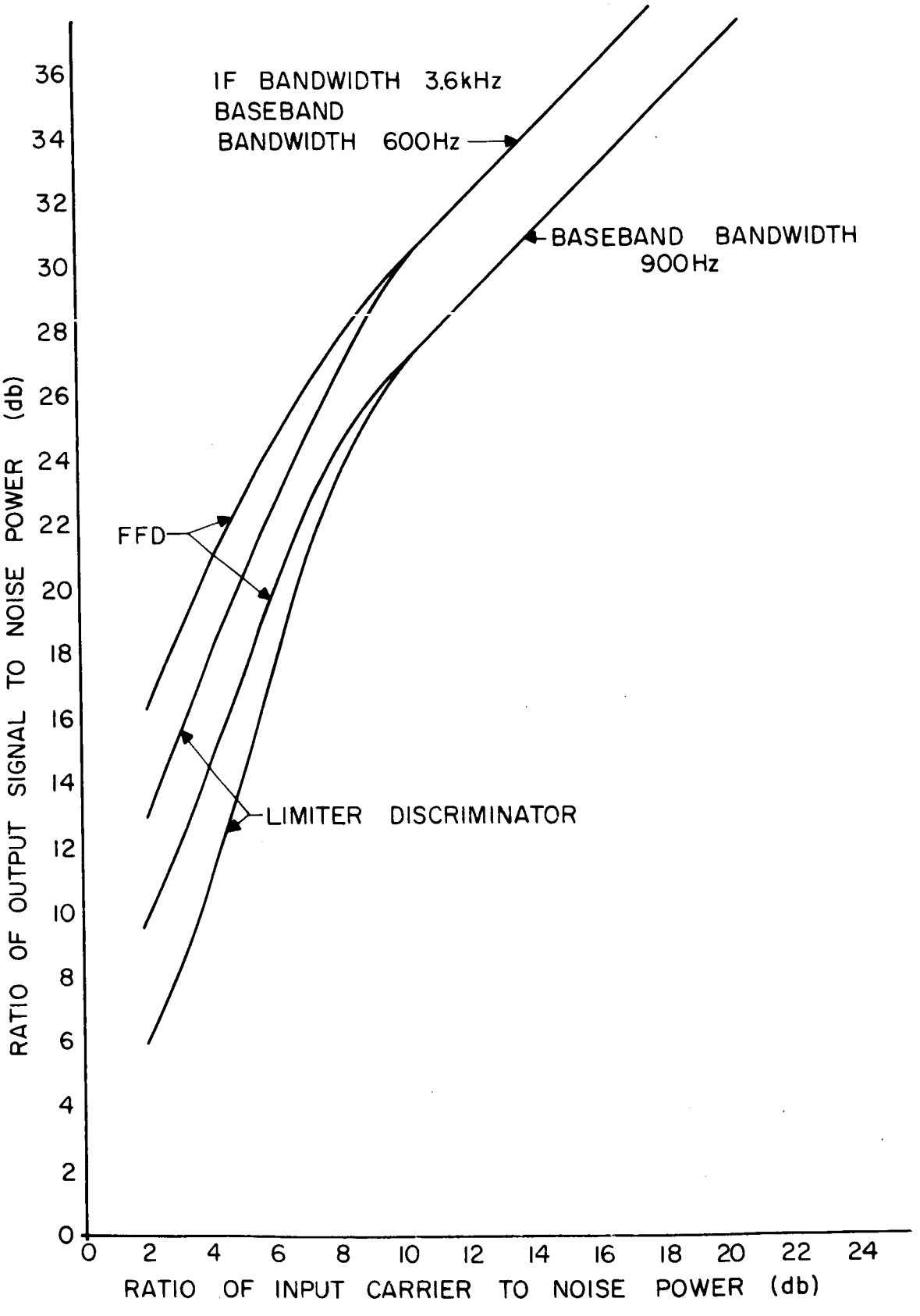

Fig. III-B-14 Plot of Ouput Signal to Noise Power for the Case where Modulation and Noise are Applied Simultaneously

III-C-1 Universal Tuned Circuit Distortion Curve for FM (Fig. III-C-1)

A universal curve has been developed experimentally that yields third harmonic distortion introduced by the passage at a sinusoidally modulated FM signal through a single tuned circuit ($Q \geq 5$). The parameters of the curve are $\Delta f/BW$ and f_m/BW where Δf is the modulating frequency, and BW is the total - 3db bandwidth of the tuned circuit. For low values of f_m/BW the curves have been shown to approach asymptotically to a theoretical quasi-static approximation for the distortion caused by a tuned circuit. For large values of f_m/BW the curves fall off as $\beta^2 = (\Delta f/f_m)^2$ as would be predicted for the small β case by a combination of sidebands approach.

As an example of the usage of these curves one sees that with a bandwidth of 50hHz then as long as $\Delta f \leq 15kHz$ then the precent 3rd harmonic distortion introduced by a tuned circuit will always be less than 1.5%

For smaller values of $\Delta f/BW$ than those shown in the curves the 3rd harmonic distortion may cease to predominate. Distortion then becomes very low and measurements become uncertain. For $\Delta f/BW \leq 0.2$ the total rms distortion should be less than 1% for any f_m. [Since the fundamental output is down approximately 3db when $(f_m/BW) \geq 0.5$ - for any $\Delta f/BW$ - one would not normally be interested in values of f_m exceeding half the bandwidth.]

References

Polytechnic Institute of Brooklyn Report Projects:

W. Hollis - June 1966 - Advisor D. T. Hess

M. Yang - June 1967 - Advisor K. K. Clarke

---

*This curve is shown as Figure III-C-1.

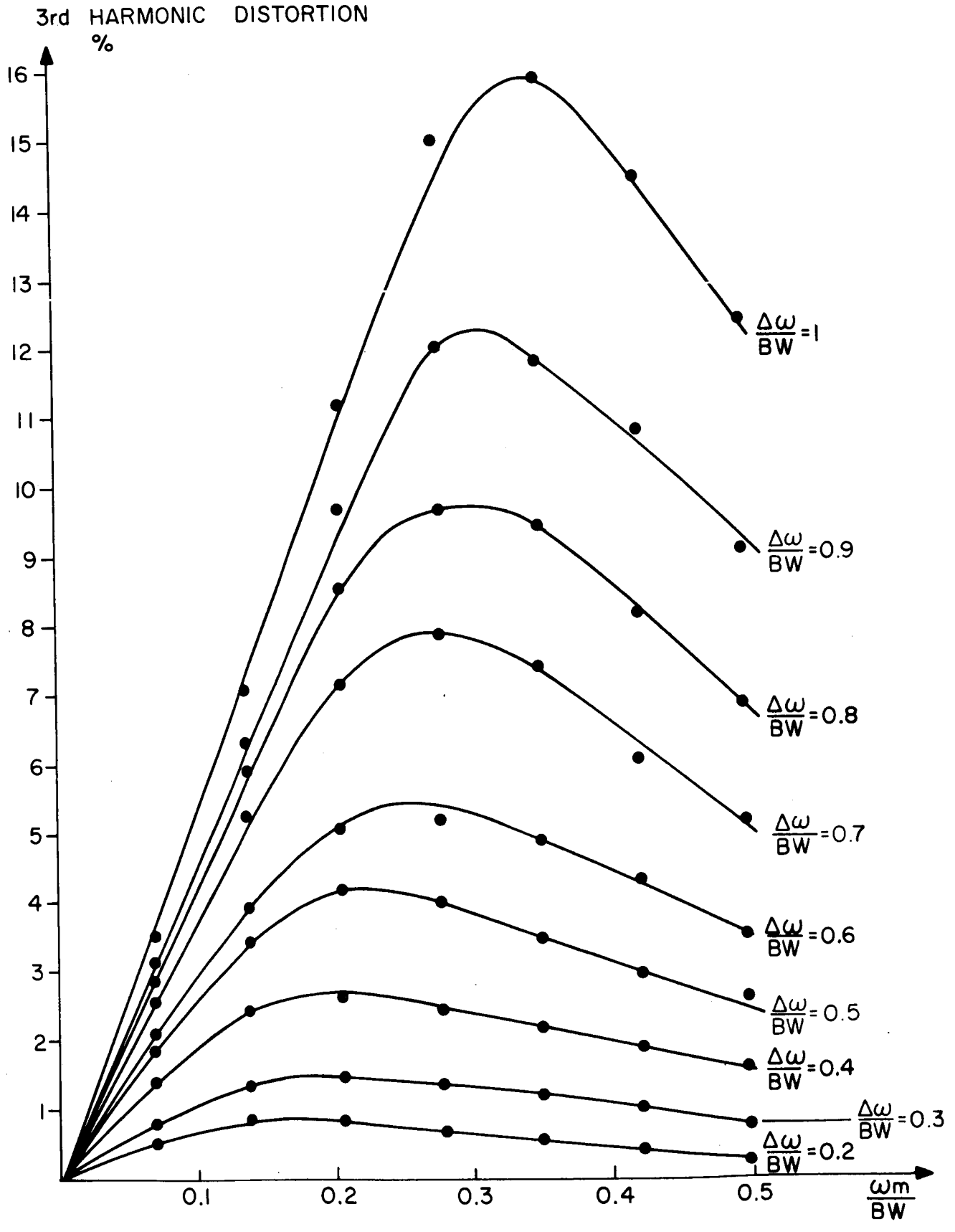

Fig. III-C-1 Universal Distortion Curve FM via a Single Tuned Circuit

III C-2 FM Spectra for Any Periodic Modulating Signal

A computer program that can be used to evaluate the spectrum of an FM wave modulated by any periodic signal is given. Results that have been obtained with this program, for four complex modulating waves are also presented.

The general FM signal

$$v(t) = \begin{matrix}\sin \\ \text{or} \\ \cos\end{matrix} \left\{ \omega_o t + \theta_o + \lambda \int_{-\infty}^{t} f(t)\, dt \right\} \qquad (1)$$

ω_o: carrier frequency

θ_o: orbitrary phase angle

λ : deviation

f(t): modulating signal

may also be written as,

$$v(t) = \sin \omega_o t \cos \left[\lambda \int_{-\infty}^{t} f(t)\, d\, t\right] + \cos \omega_o t \sin\left[\lambda \int_{-\infty}^{t} f(t)\, dt\right] \qquad (2)$$

or

$$v(t) = \cos \omega_o t \cos \left[\lambda \int_{-\infty}^{t} f(t)\, dt\right] - \sin \omega_o t \sin \left[\lambda \int_{-\infty}^{t} f(t)\, dt\right] \qquad (3)$$

where θ_o has been taken zero without loss of generality.

When f(t) is a periodic function, with a fundamental period T,

$f(t) = f(t + kT)$

$\cos \left[\lambda \int_{-\infty}^{t} f(\tau)\, d\tau\right]$ and $\sin \left[\lambda \int_{-\infty}^{t} f(\tau)\, d(\tau)\right]$ are also periodic functions with a period T and as such may be expanded into a fourier series.

let $\lambda \int_{-\infty}^{t} f(\tau)\, d\tau = g(t)$

then,

$$\cos g(t) = \sum_{n=0}^{\infty} A_n \cos n\omega_m t + B_n \sin n\omega_m t \qquad (4)$$

$$\sin g(t) = \sum_{n=0}^{\infty} C_n \cos n\omega_m t + D_n \sin n\omega_m t \qquad (5)$$

where $\omega_m = 2\pi / T$

$$A_o = \frac{1}{T} \int_o^T \cos g(t)\, dt \qquad C_o = \frac{1}{T} \int_o^T \sin g(t)\, dt$$

$$A_n = \frac{2}{T} \int_o^T \cos g(t) \cos n\, \omega_m t\, dt$$

etc. (6)

When the expansions (4), (5) are replaced into (2) and (3) we obtain

$$v(t) = \frac{1}{2} \sum_{n=0}^{\infty} \Big\{ (B_n + C_n) \cos (\omega_o t - n\omega_m t) - (B_n - C_n) \cos (\omega_o t + n\omega_m t) + (A_n - D_n) \sin (\omega_o t - n\omega_m t) + (A_n + D_n) \sin [\omega_o t + n\omega_m t) \Big\} \qquad (7)$$

or

$$v(t) = \frac{1}{2} \sum_{n=0}^{\infty} \Big\{ (A_n - D_n) \cos (\omega_o t - n\omega_m t) + (A_n + D_n) \cos (\omega_o t + n\omega_m t) - (B_n + C_n) \sin (\omega_o t - n\omega_m t) + (B_n - C_n) \sin (\omega_o t + n\omega_m t) \Big\} \qquad (8)$$

The problem now is the determination of the coefficients A_n, B_n, C_n, D_n.

Integrations (6) can not, in general, be performed analytically except for simple modulating signals. However, numerical integrations may be performed with a computer, to evaluate these integrals.

A computer program in FORTAN IV, that will evaluate the fourier coefficients in the expansions (4), (5) for any periodic modulating signal whose integral has been obtained, has been prepared. The expansion for cos g(t) is given in the appendix for the use of triangular wave modulation. A similar program obtains the expansion for the sin g(t) term. The integral of the modulating signal for

is inserted in between the comment statements FOFT IN and FOFT OUT. The increment involved in the integrations and the number of harmonies to be evaluated are fed as data together with the deviation, so that a binary object deck may be obtained for a given signal and those parameters changed at will without need for recompilation, thus saving computer-time.

This program has been used to evaluate the spectra for four non-sinusoidal modulating signals. Signals whose half cycles are,

1. Exponentials $e^{-a|t|}$ $a = 10/\pi$ $|t| \leq \pi/2$

2. Gaussian $e^{-2(t/T)^2}$ $|t/T| \leq \pi/2$

3. Triangular

4. Trapezoidal

these and cosine and square waves which may be treated analytically are shown in fig. III C-2a.

Figs. III C-2b and III C-2c show the envelope of the amplitude spectra for there six waves for a modulating index (= deviation since $\omega_m = 1$) of 2.0 and 5.0, respectively.

More extensive results and discussion may be found in "FM Spectra" Report Project for the degree of Master of Sc. June 1967, DAVRAS YAVUZ, prepared under the supervision of Prof. Donald Hess. The usefulness of the simple computation of spectra information for any periodic modulating signal will be readily appreciated by those engaged in FM system design. By extending the concept of period the same program may be utilized to determine spectra for binary signals that have periodic block structures rather than simple one-zero alternations.

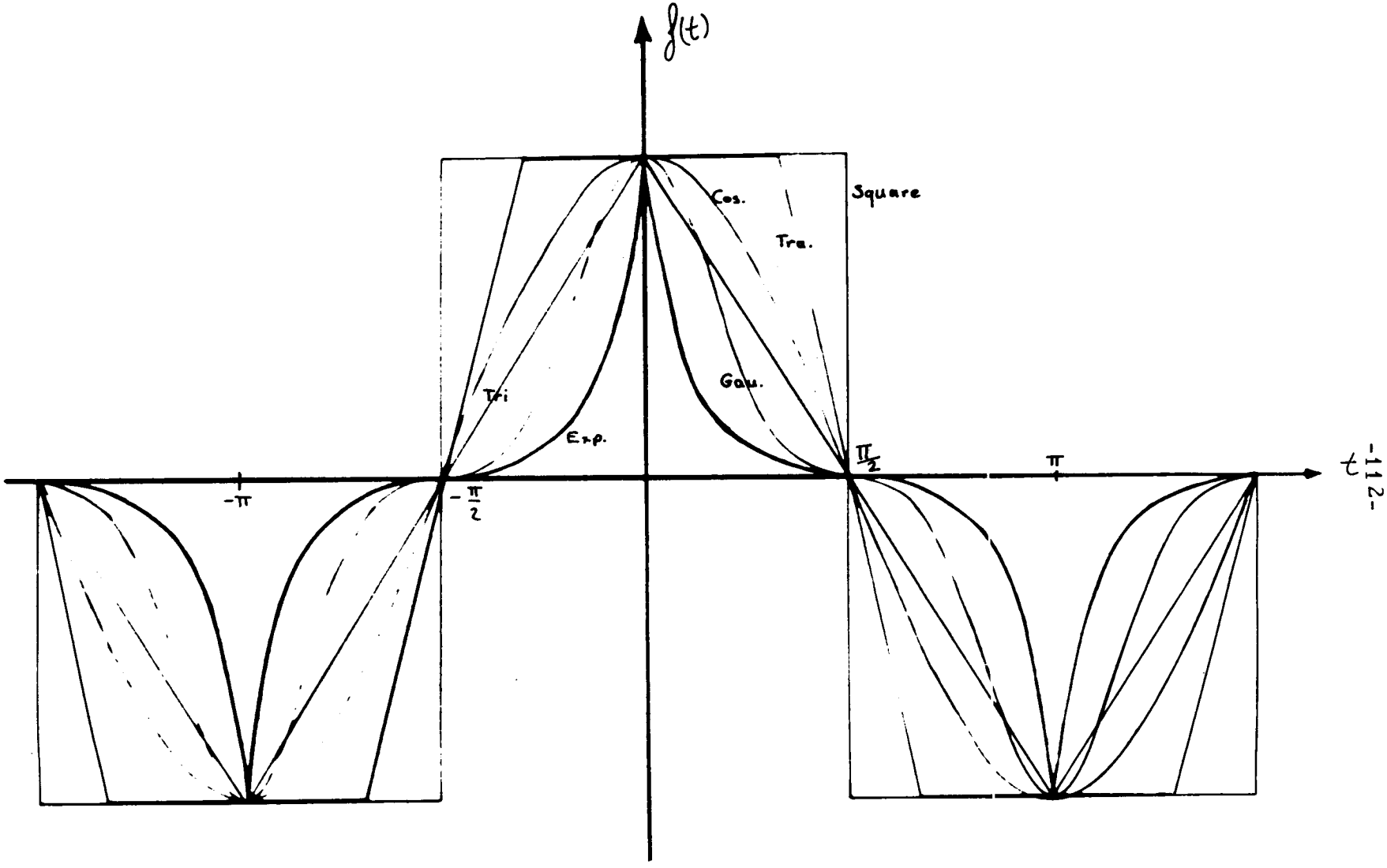

Fig. III-C-2(a) Modulating Waveforms for which Spectra have been obtained

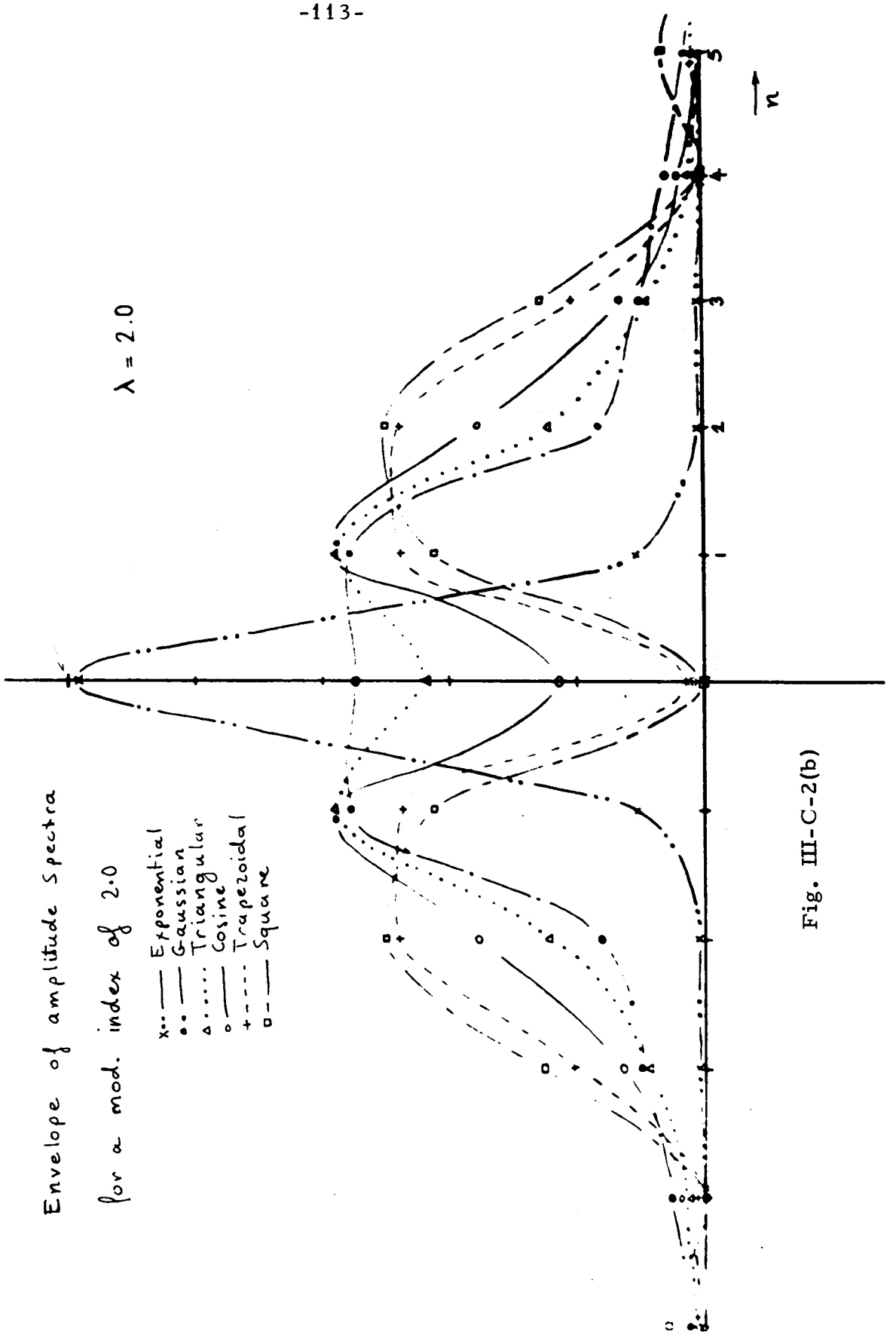
Envelope of amplitude Spectra
for a mod. index of 2.0
λ = 2.0
Exponential
Gaussian
Triangular
Cosine
Trapezoidal
Square
n
0
1
2
3
4
5

Fig. III-C-2(b)

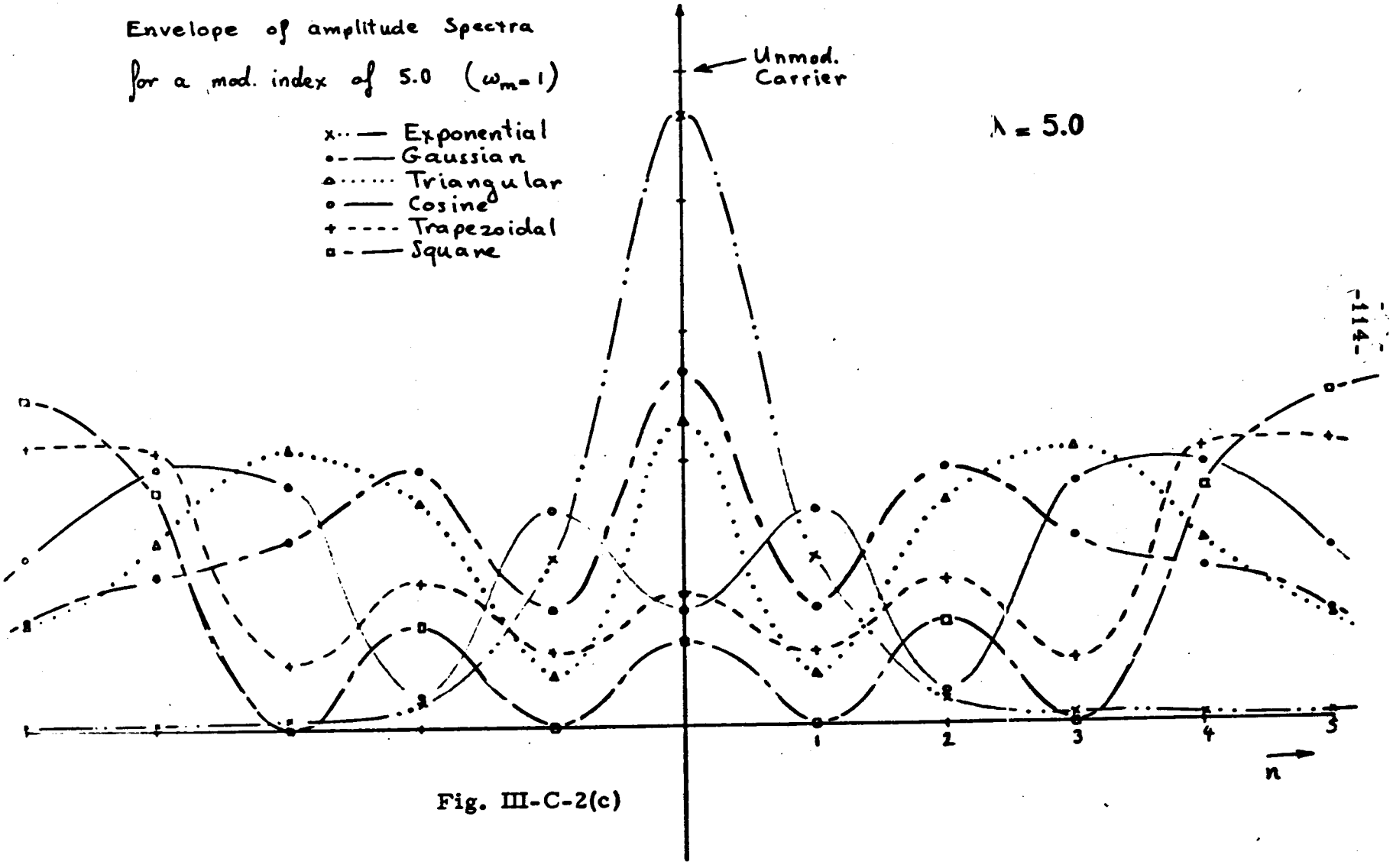
Envelope of amplitude Spectra
for a mod. index of 5.0 ($\omega_m = 1$)
Exponential
Gaussian
Triangular
Cosine
Trapezoidal
Square
Unmod. Carrier
$\lambda = 5.0$
1
2
3
4
5
n

Fig. III-C-2(c)

III-C-3 Wideband FM Generator

A solid state circuit realization of Hess's FM equation[1] has been achieved and tested.

The basic equation for FM, as derived by Hess is Eq. III-B-3-1

$$\omega_i(t) \int_o^t \omega_i(\tau)\, X(\tau)\, d\tau + \frac{dx(t)}{dt} = 0 \qquad \text{(C-3-1)}$$

It has a solution of the form

$$x(t) = K \cos \omega_i t$$

where

$$\omega_i = \omega_o + \Delta\omega \int f_m(t)$$

Figure III-B-3-1 shows a circuit in which both $V_1(t)$ and $V_2(t)$ have the form of x(t) in Eq B-3-1. This circuit requires linear gain controlled amplifiers for its realization. Several types of such amplifiers have been developed with the PIB laboratories and were available for this circuit synthesis.

If one assumes

$$i_1(t) = A(t)\, v_2(t) \qquad i_1^*(t) = Bv_1(t)$$
$$i_2(t) = A(t)\, v_1(t) \qquad i_2^*(t) = Bv_2(t) \qquad \text{(C-3-2)}$$

Then the two node equations follow

$$-i_1(t) - i_1^*(t) + Gv_1(t) + \frac{dv_1(t)}{dt} = 0$$
$$i_2(t) - i_2^*(t) + Gv_2(t) + \frac{dv_2(t)}{dt} = 0 \qquad \text{(C-3-3)}$$

These equations may be rearranged to yield

$$-A(t)\, v_2(t) + (G-B)\, v_1(t) + C\, dv_1(t)/dt = 0$$

$$A(t)\, v_1(t) + (G-B)\, v_2(t) + C\, dv_2(t)/dt = 0 \qquad \text{(C-3-4)}$$

(1) Donald T. Hess "FM Differential Equation" Proc IEEE (Correspondence) Vol 54, pp. 1089, August 1966.

when B = G then the equations combine to yield

$$\frac{A(t)}{C} \int^{t} \frac{A(\tau)}{C} v(\tau)\, d\tau + \frac{d\,v(t)}{dt} = 0 \qquad (C\text{-}3\text{-}5)$$

If $\omega_i(t) = A(t)/C$ then $v(t)$ has the form of $x(t)$ in Equation B-3-5.

One should note that this circuit utilizes no inductances. One should note also that it is exact and requires no particular restrictions upon either peak deviation [$\Delta f < (f_o - 2f_m)$ is required to prevent baseband and sideband overlaps] or upon modulating frequency.

As constructed DC coupling is utilized throughout the circuit hence the Q point is highly stabilized via a large amount of DC feedback.

Test results are shown in Figures III-C-3-1 through III-C-3-6. The first of these figures indicates the center frequency versus capacitance characteristic, the second indicates the deviation linearity all the way up to $\Delta f = f_o$, Figure III-B-3-4 indicates deviation vs modulating frequency for single tone modulation. Figure B-3-5 indicates the non-linear distortion generated by the particular circuit constructed. Note that for the present version one has less than 0.6% total rms distortion with a deviation of 50% of the carrier for all center frequencies below 1000hHz. There seems to be no theoretical reason why this limit can not be extended considerably.

The last figure shows center frequency temperature stability of the initial model. Note that no effort was made to provide temperature compensating resistors or capacitors in this initial version of the circuit. Presumably by properly choosing the temperature coefficients for the capacitors and for certain bias resistors one could reduce this temperature dependence to less than 1% for a 50°C change in temperature.

Reference:

Marko Jagodic, "Wideband Frequency Modulated Generator" PIB, M Sc. Report Project, 1967

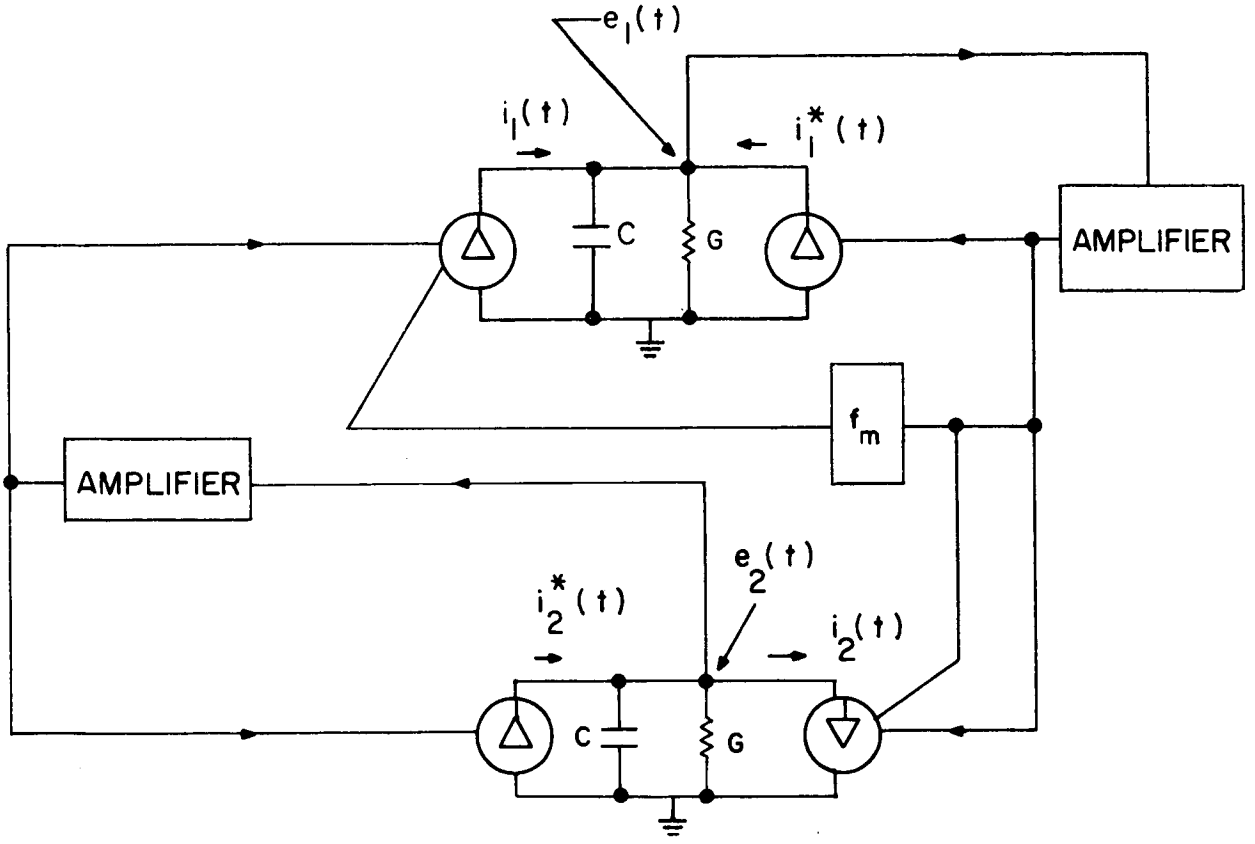

Fig. III -C-3-1 Block Diagram of circuit to be synthesized.

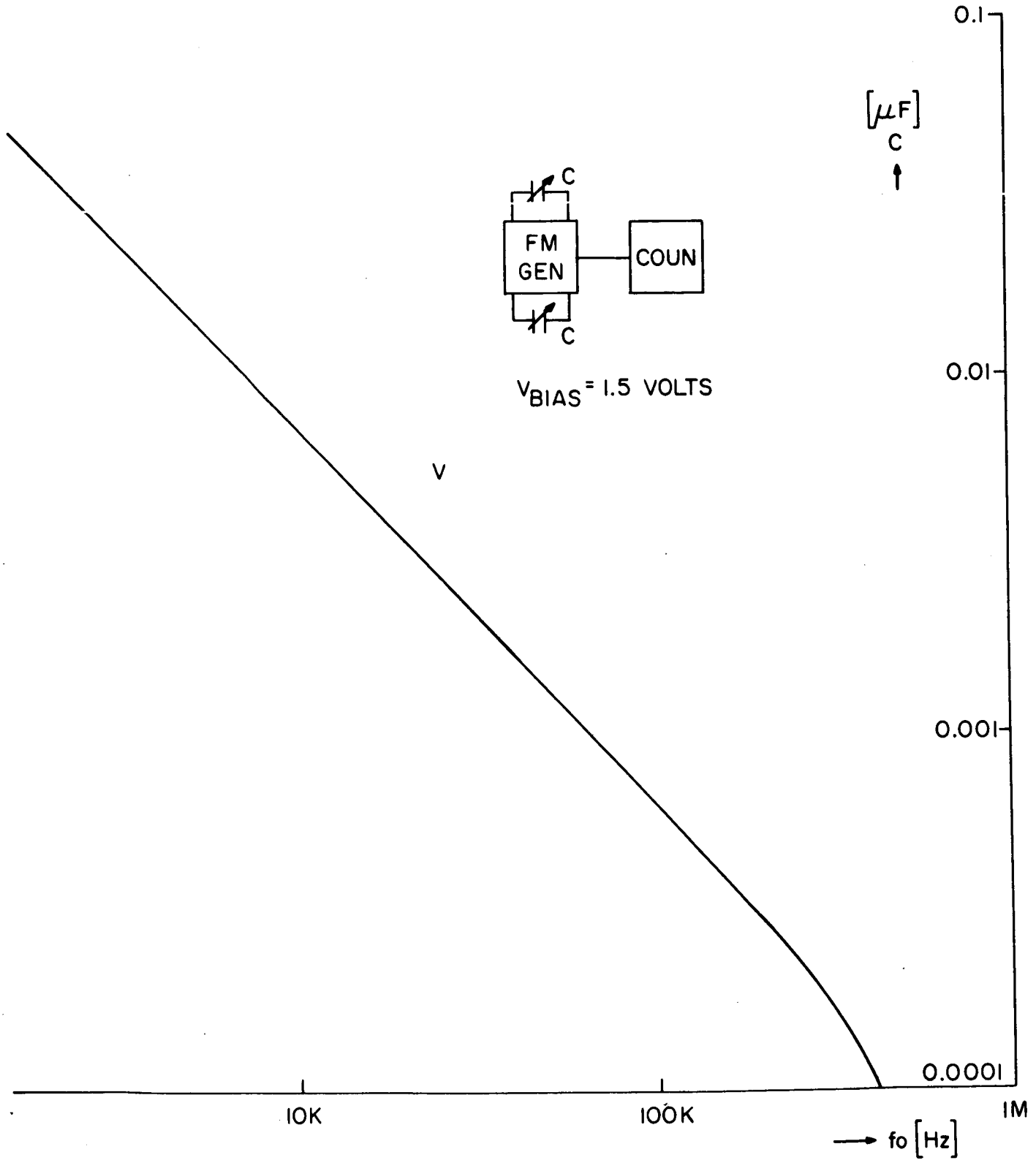

Fig. III-C-3-2 Center Frequency vs. Tuning Capacitance

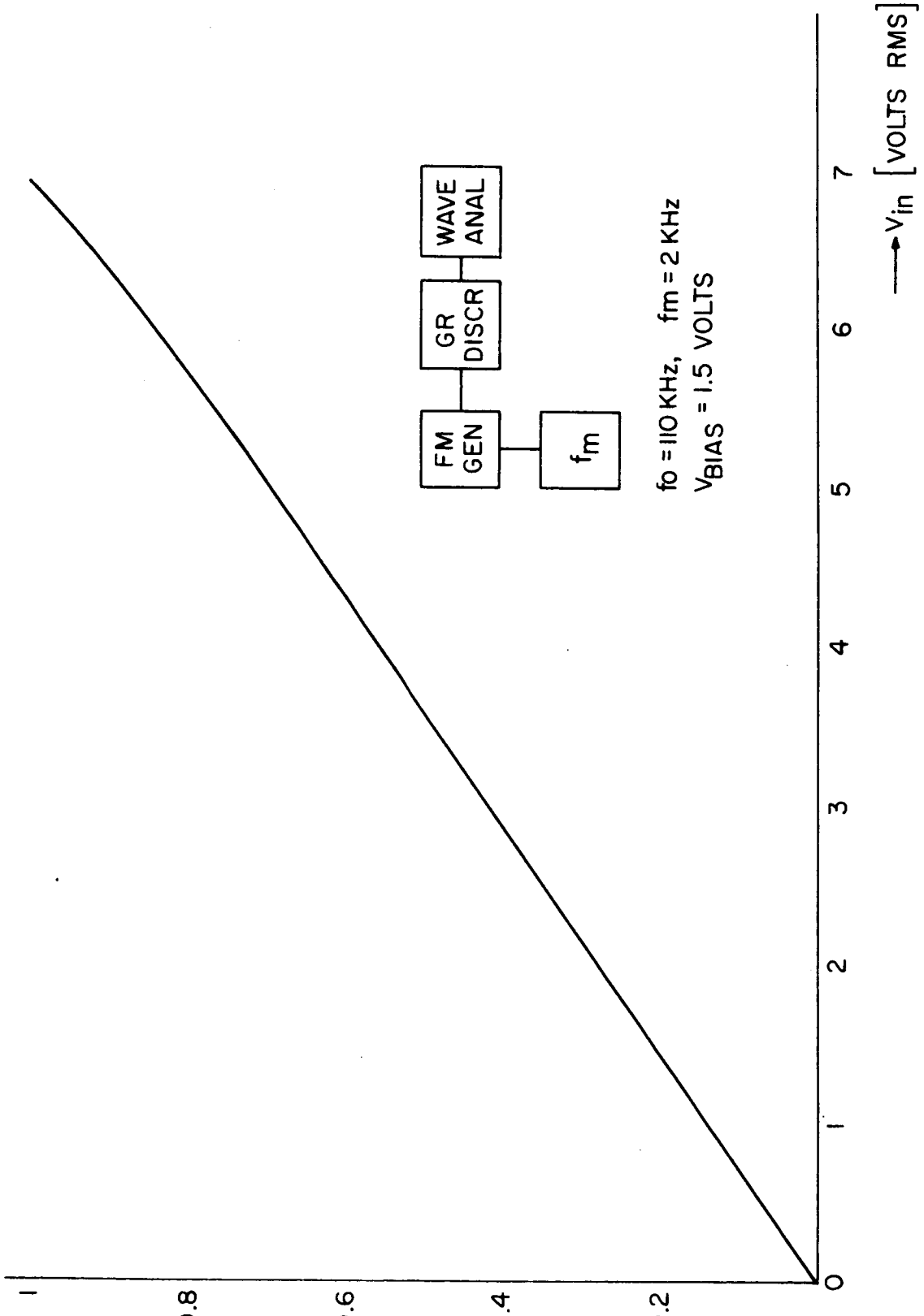

Fig. III-C-3-3 Deviation Linearity vs. Input Modulation Signal Amplitude

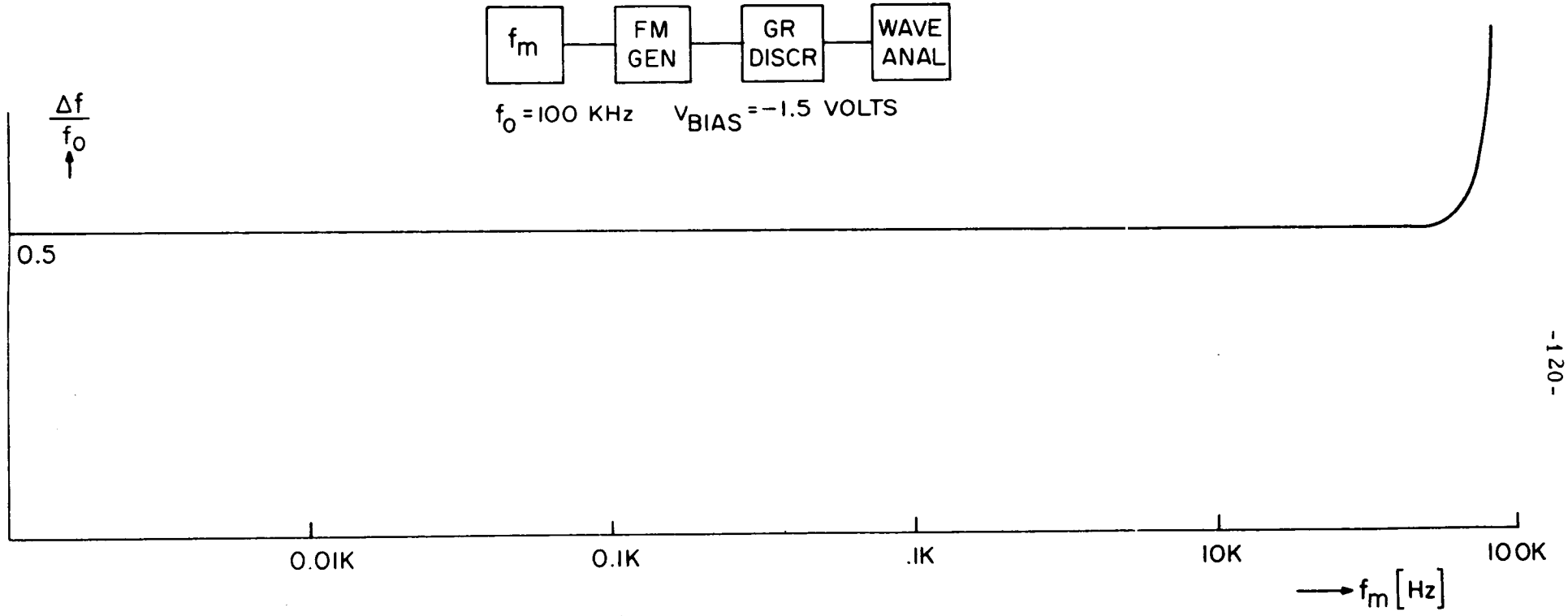
f_m
FM GEN
GR DISCR
WAVE ANAL
f_0 = 100 KHz
V_{BIAS} = −1.5 VOLTS
$\frac{\Delta f}{f_0}$
0.5
0.01K
0.1K
.1K
10K
100K
f_m [Hz]

Fig. III-C-3-4

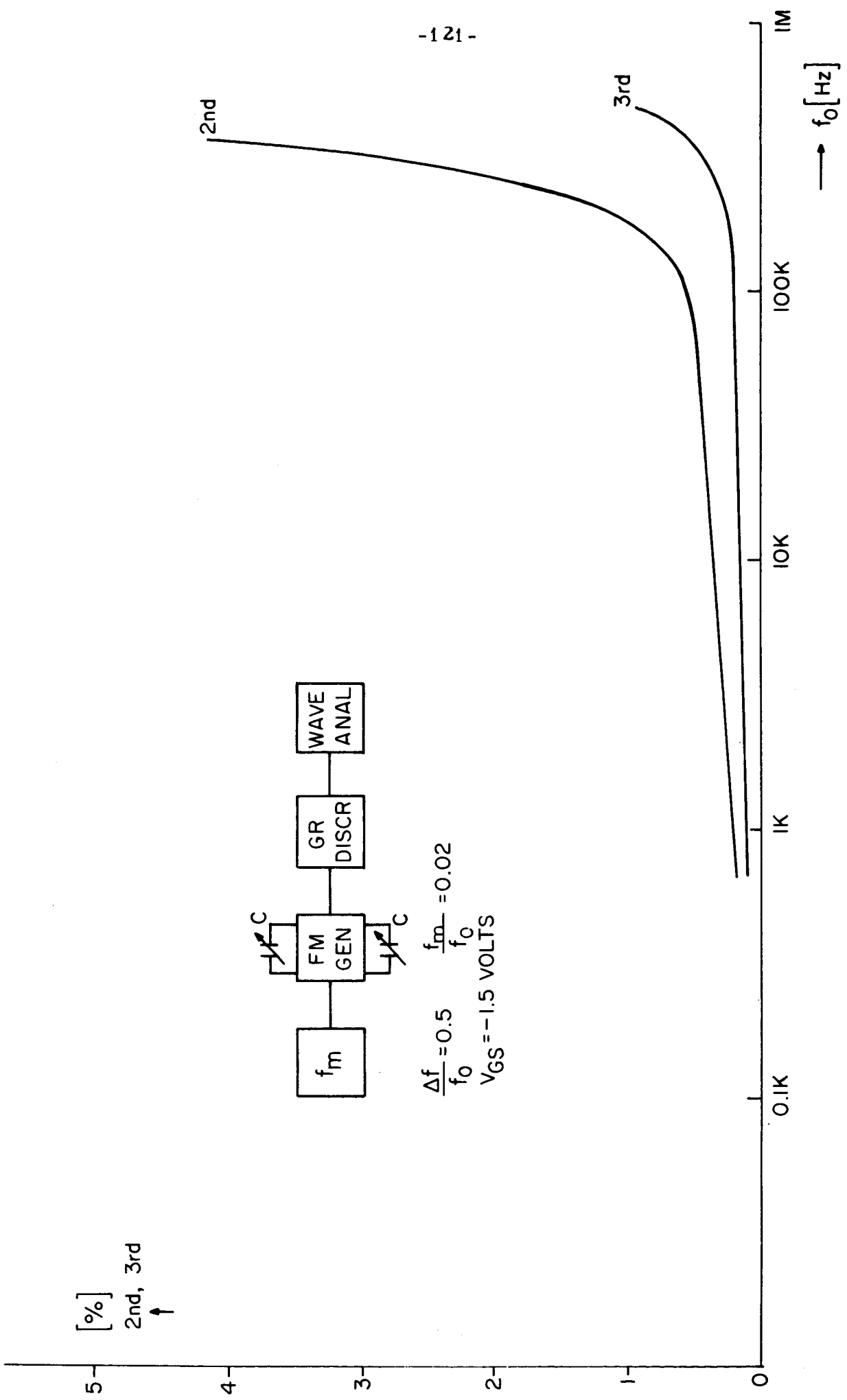

Fig. III-C-3-5 Harmonic Distortion in Detected FM Signal vs. Center Frequency

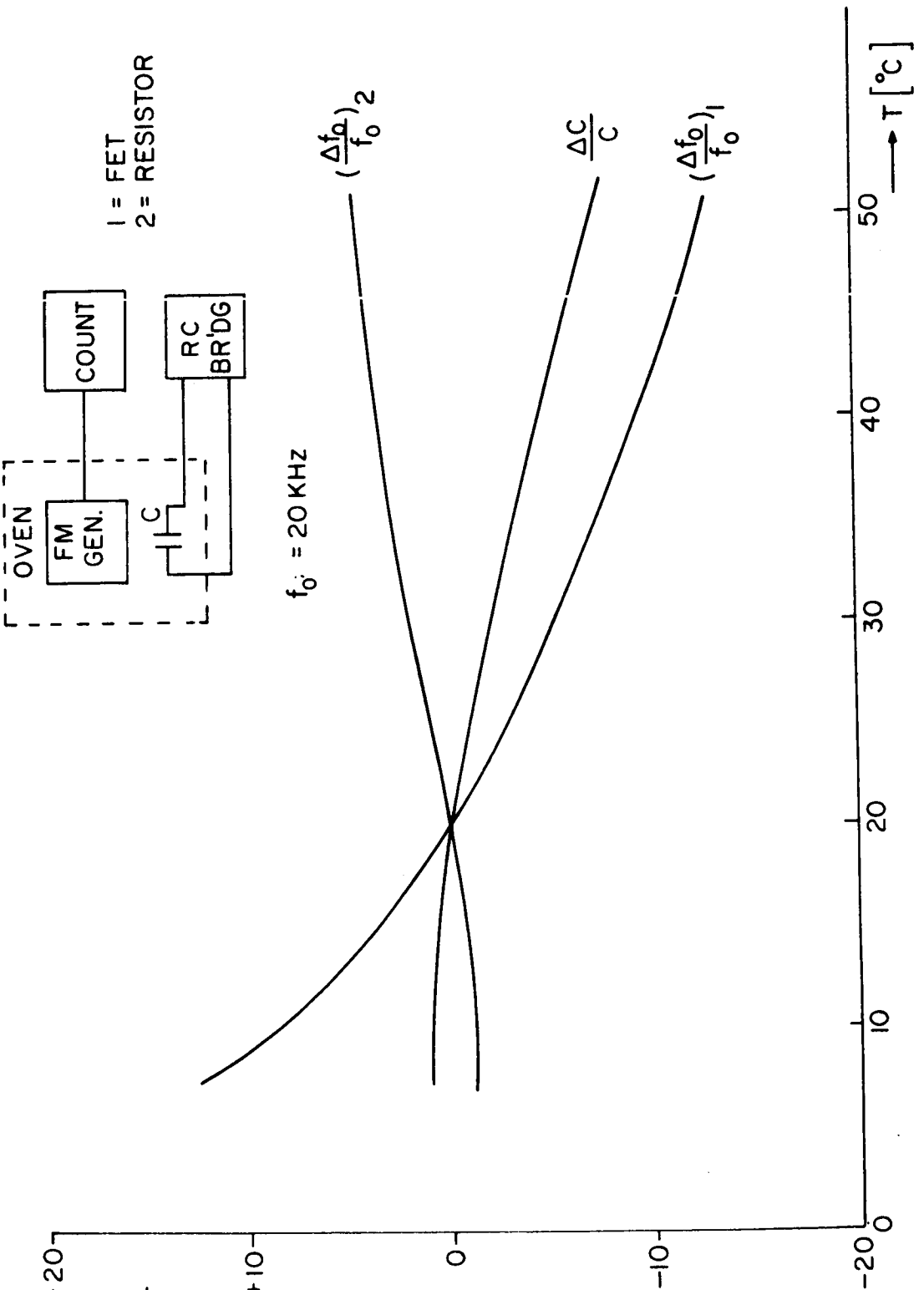

Fig. III-C-3-6 Temperature Stability of FM Circuit and of the Tuning Capacitors

IVa. Basic Results from the P.I.B. Water Tank Channel Simulator.

The water tank, channel simulator, together with its associated equipment, may be used to simulate a wide variety of fading channels normally encountered in practice. All of the fading conditions commonly encountered may be simulated except for polarization fading.

The simplest methods of producing a rapid fading simulation in the water tank is through the use of reflection fading. To produce reflection fading the ultrasonic beam is passed through a medium with time-variant scattering of the signal energy. This time-variant, inhomogeneous meidum is produced by passing a stream of air bubbles through the water in a region through which the ultrasonic beam passes. Since the bubbles, which are generated by a mechanism similar to a fish tank aerator, are essentially random in position, the scattering is also random and the fading parameters are controlled by the strength of the bubble field, size of bubbles, water temperature, etc. The scattering of the ultrasonic wave by air bubbles is due to the large difference in refractive index between the air and water. Besides the effects of this varying reflection and scattering, some of the energy of the ultrasonic beam is also randomly absorbed by the air bubbles, creating a second order absorption fading mechanism.

Figure IV - 1 (a) shows a schematic setup for the simulation of reflection fading in a line-of-sight path. To measure the characteristics of the fading one sends a CW, unmodulated carrier through the channel simulator and passes the output through a linear envelope detector. If one uses the system of Figure IV-2 and sets the output of the noise generator to zero, then the perturbations in the envelope of the fading signal may be analyzed on the probability density machine and the amplitude-frequency spectrum of the fading signal amplitude may be recorded on a spectrum analyzer. During such a test, the bubble field generator, i.e., the air nozzles, is supplied with reasonably constant air pressure

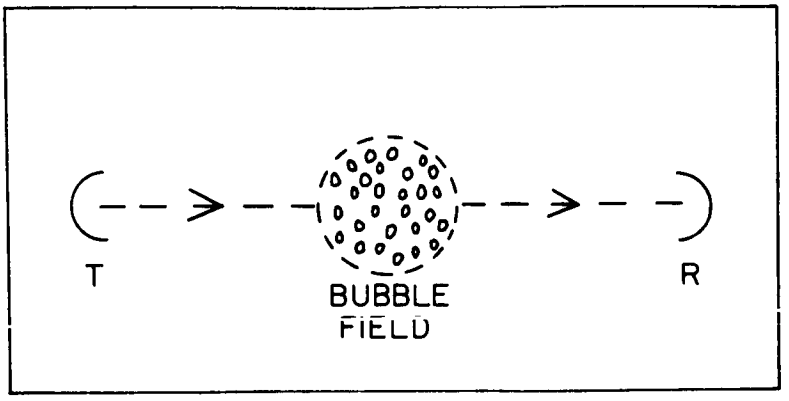

Fig. IV-1 (a) Line-of-sight Path

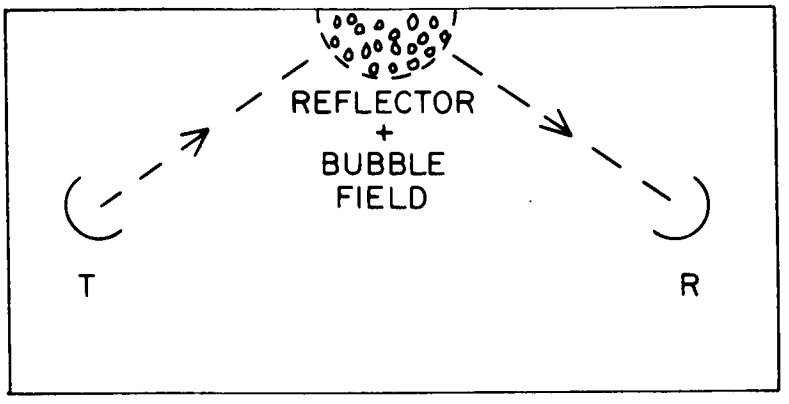

Fig. IV-1 (b) Reflection Path

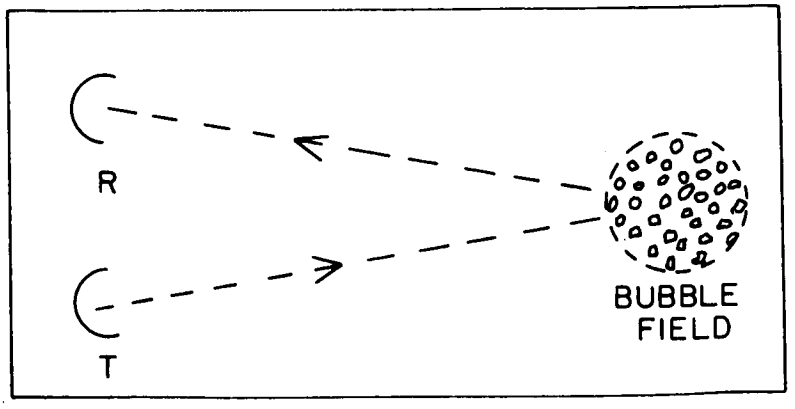

Fig. IV-1 (c) Scatter Path

(which is adjustable) and hence, the statistics of the bubble field perturbations remain constant over the testing interval (usually about one hour). If one wishes to maintain certain fading statistics over longer periods of time, due consideration must be given to such parameters as water temperature, degree of aeration of water, barometric pressure and tank water depth.

Using the channel simulator setup suggested in Figure IV-1(a) and the system of Figure IV-2, various voltage probability-density functions for the envelope of the fading carrier have been recorded as functions of the characteristics of the bubble field.

The most typical fading distribution encountered in practice is the Rayleigh distribution. Figure IV-5 shows the voltage probability density functions of several Rayleigh fading carriers. The system setup is as outlined previously. For this case a field of very large bubbles was employed. The effect of this bubble field is to produce Rayleigh fading and a slow fading rate.

From Figure IV-5 it is seen that the general shapes of the distribution functions, for various fading carrier levels at the input to the detector, all approximate the Rayleigh distribution. It is also seen that the locations of the peaks in the respective distributions coincide precisely with those which would be obtained from a theoretical Rayleigh distribution ; the theoretical and experimental comparison yields:

Input Level	Theoretical Peak	Experimental Peak
0.10 Vrms	+0.181 VDC	+0.18 VDC
0.20 Vrms	+0.362 VDC	+0.36 VDC
0.30 Vrms	+0.543 VDC	+0.54 VDC

From the same data one sees that the fading characteristics do not depend on the carrier level and hence that one may characterize the fading mechanism as a linear, multiplicative perturbation.

Figure IV-6 shows the amplitude-frequency spectrums of envelopes

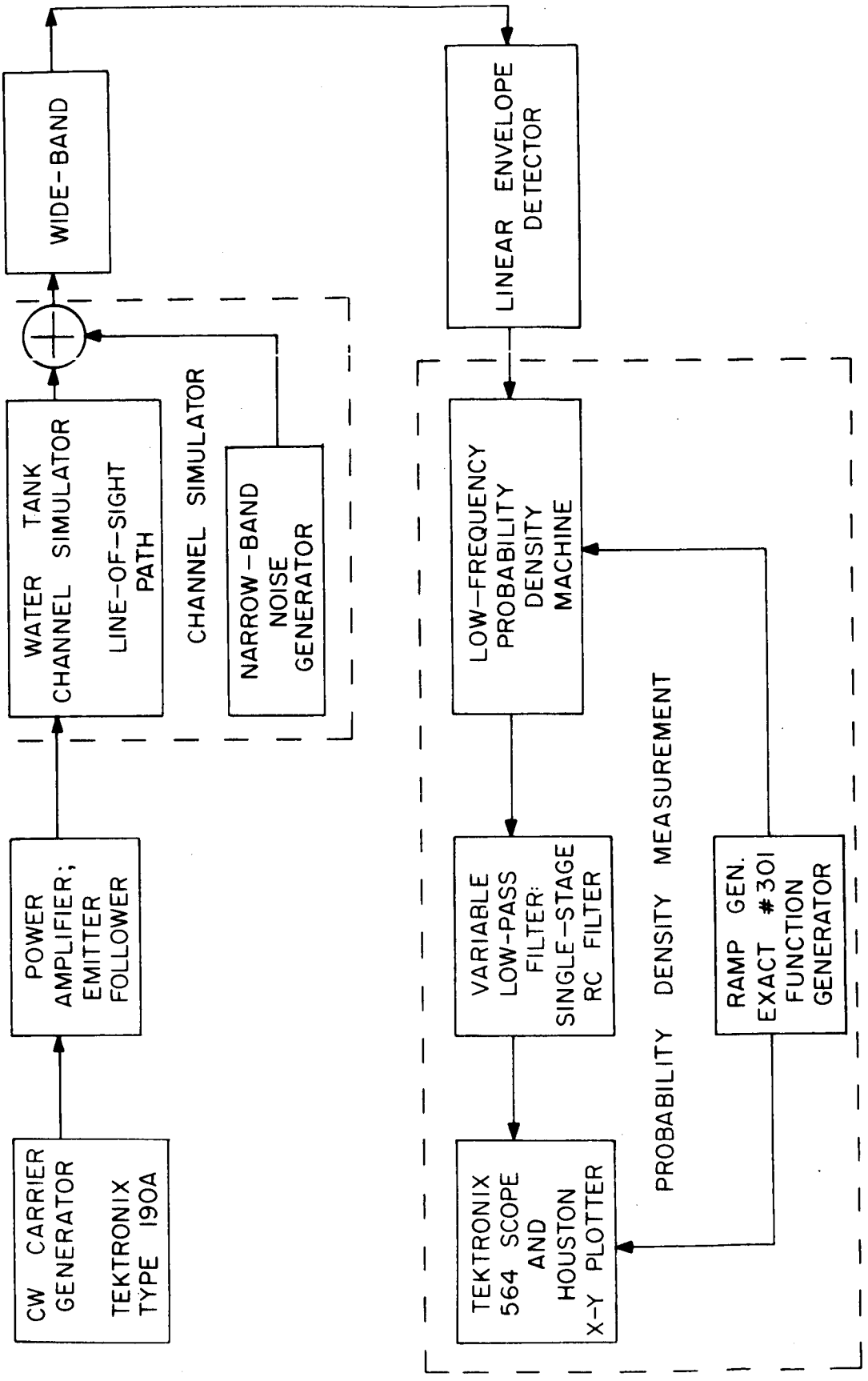

Fig. IV-2 System Diagram for Measurement of Probability Density Function of Received Waveform

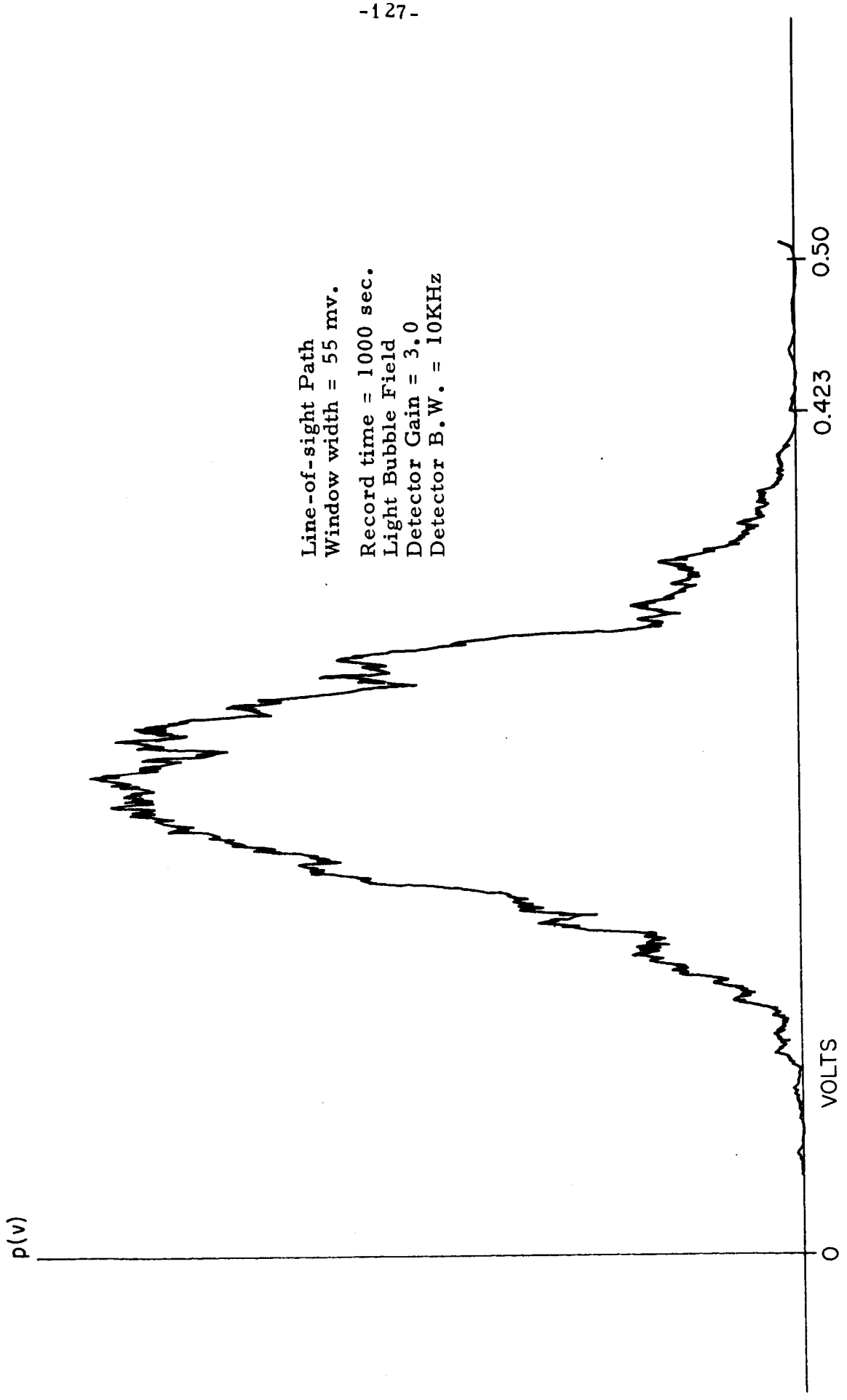

Fig. IV-3 Voltage Probability-Density Function of Fading CW Carrier

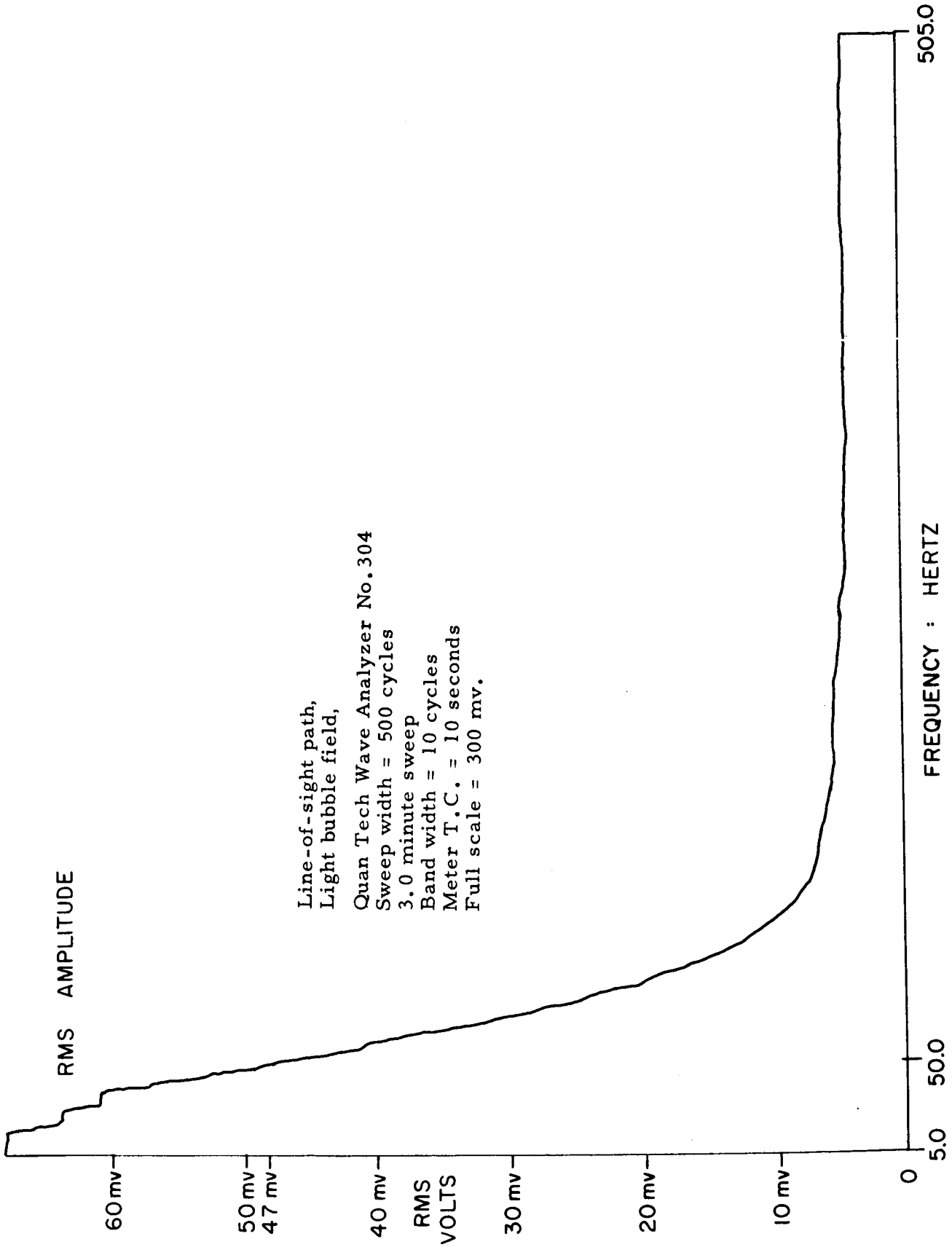

Fig. IV-4 Amplitude-Frequency Spectrum of Fading Carrier

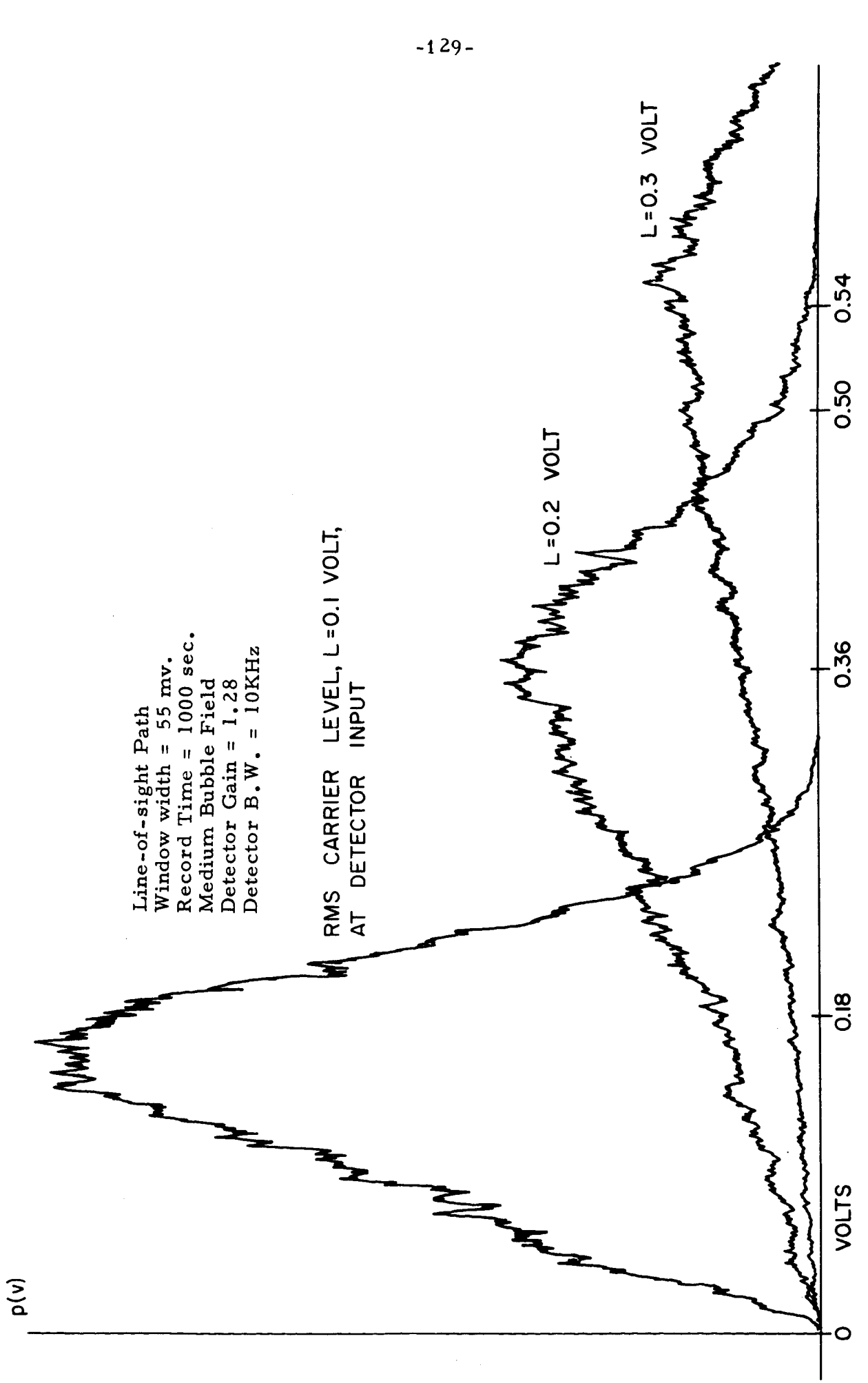

Fig. IV-5 Voltage Probability-Density Function of Fading CW Carrier

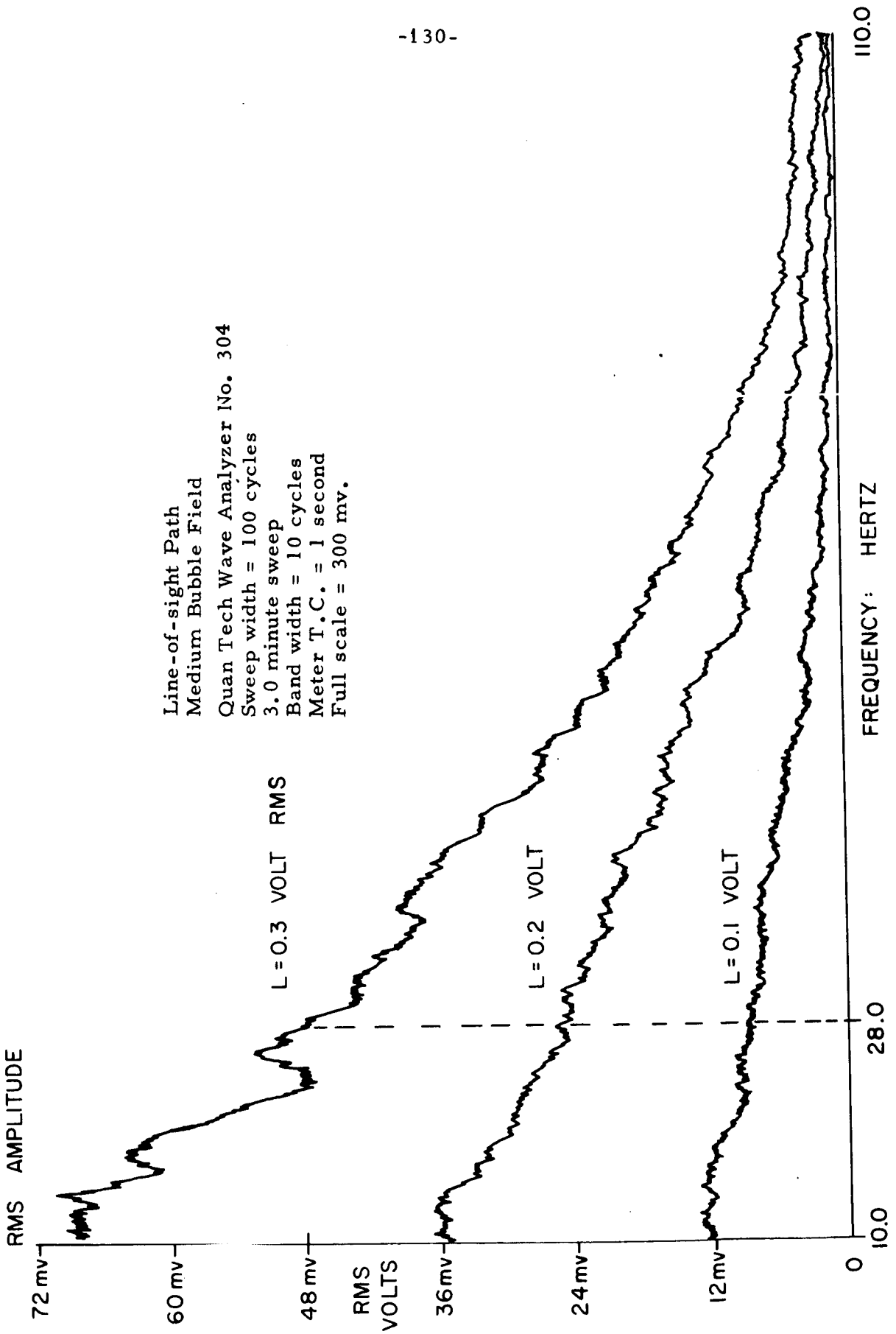

Fig. IV-6 Amplitude-Frequency Spectrum of Fading Carriers

of the above Rayleigh fading carriers. A Quantech 304 spectrum analyzer was used for these measurements. From Figure IV-6 one sees that the fading rates of the fading signals are precisely the same despite the unequal signal levels. This is further evidence to support the conclusion that the fading mechanism is a linear, multiplicative perturbation. It may also be seen that the fading rate for this case is 28 Hertz.

The amplitude-frequency spectrum of Figure IV-6 yields more information than the fading rates of the fading signals: It also yields their auto-correlation functions after some simple mathematical manipulations. If one takes the components of the amplitude-frequency spectrum and squares them, they will obtain the power spectral density. Once the power spectral density has been obtained, it is only necessary to take the inverse Fourier transform to obtain the fading signals auto-correlation function.

Figure IV-7(a) shows the approximate power spectral density for the fading carrier of Figure IV-6, L = 0.30 volts rms. One sees that this power spectral density function, $S(\omega)$, may be approximated by:

$$S(\omega) = \frac{2Kq}{q^2 + \omega^2} \qquad \text{(IV-1)}$$

where

K = 4.5 watts (normalized to 1 ohm resistor)

and

q = 180 seconds /radian

and

ω = radian frequency

Taking the Fourier transform of $S(\omega)$, the auto-correlation function, F(t) has the form:

$$F(T) = K \exp(-q|T|) \qquad \text{(IV-2)}$$

where (T) is the separation time between the function to be correlated and its delayed version. Thus the auto-correlation function of the Rayleigh distributed fading carrier (of Figure IV-5 for L = 0.3 volts rms) is shown in Figure IV-7(b).

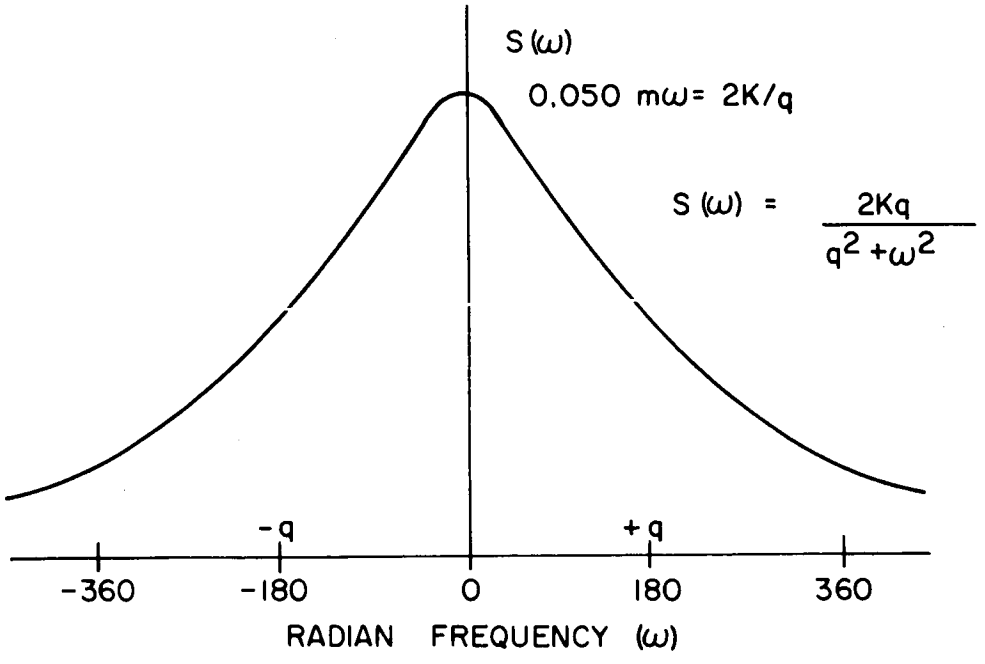

Fig. IV-7(a) Power Spectral-Density of Fading Carrier

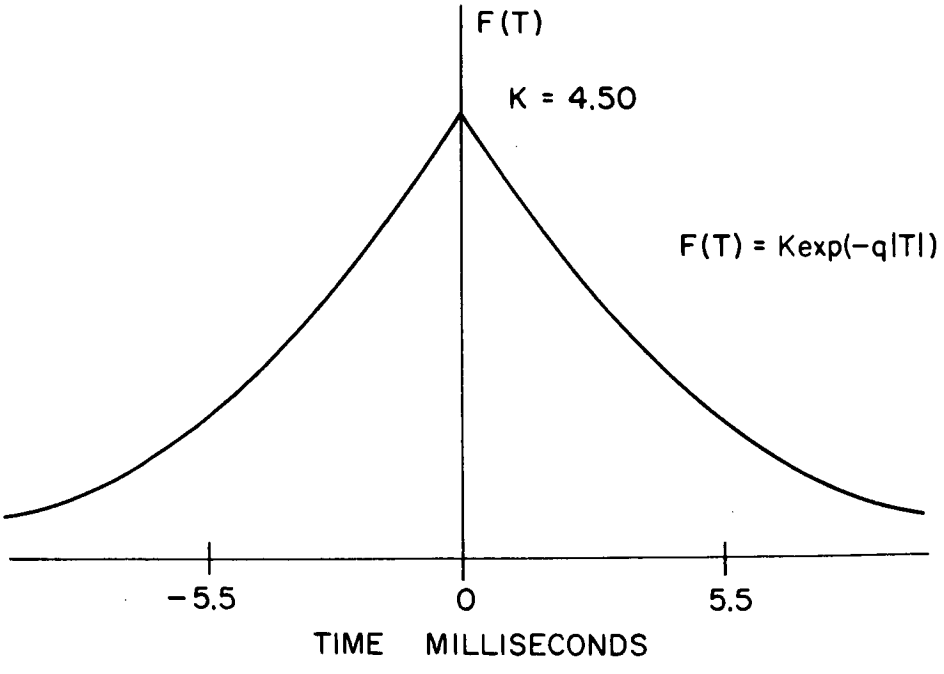

Fig. IV-7(b) Auto-correlation Function of Fading Carrier

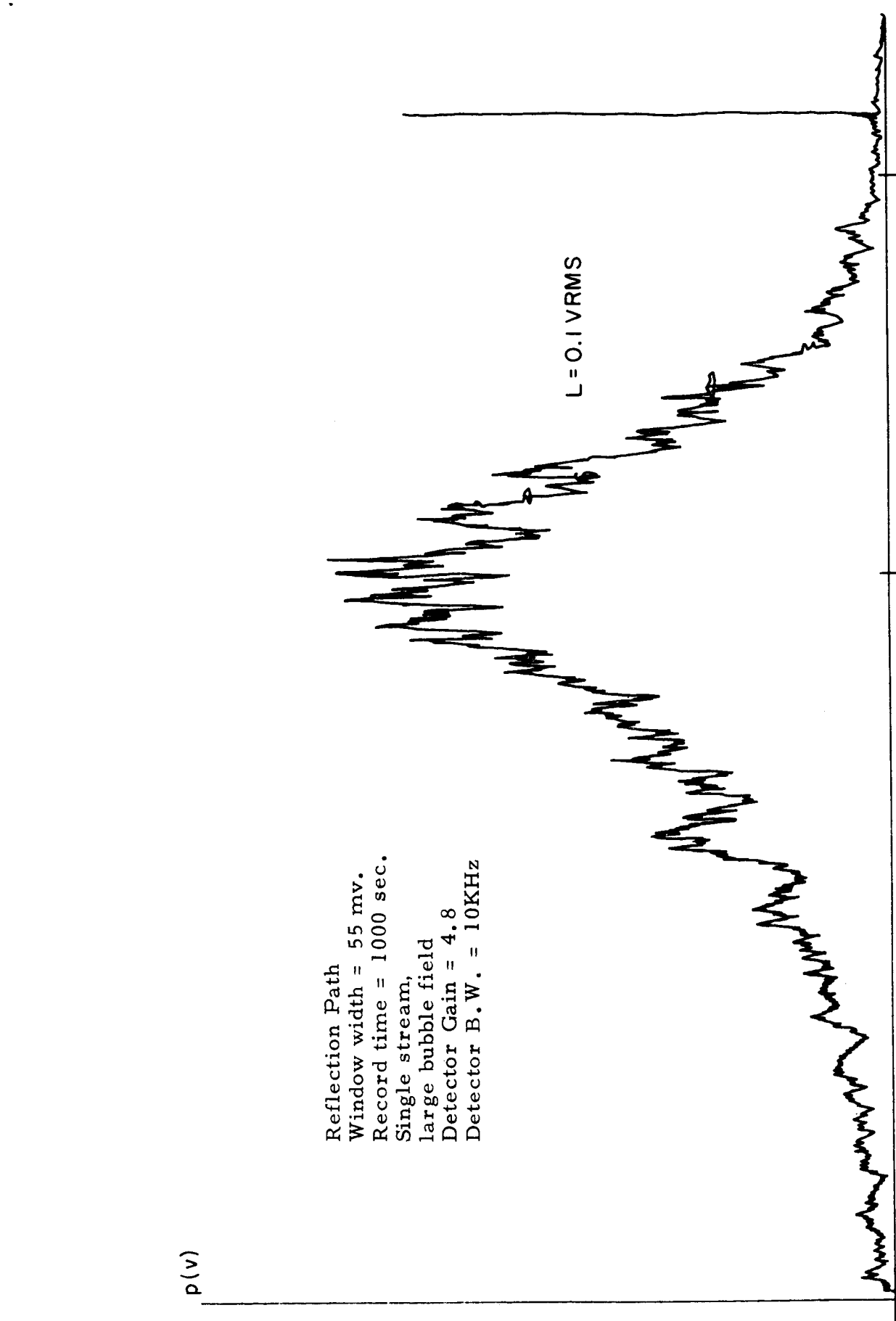

Fig. IV-8 Voltage Probability-Density Function of Fading CW Carrier

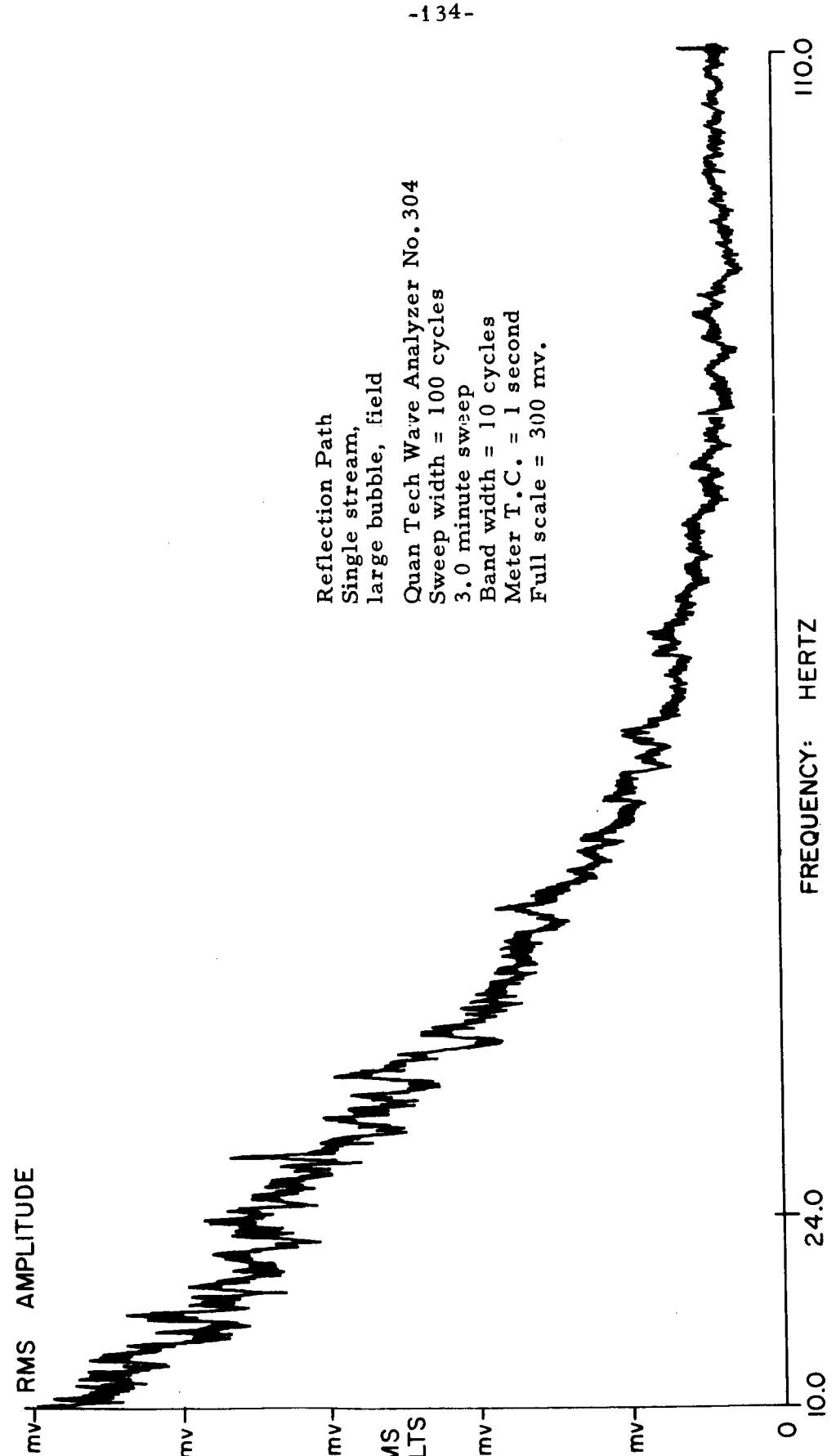

Fig. IV-9 Amplitude-Frequency Spectrum of Fading Carrier

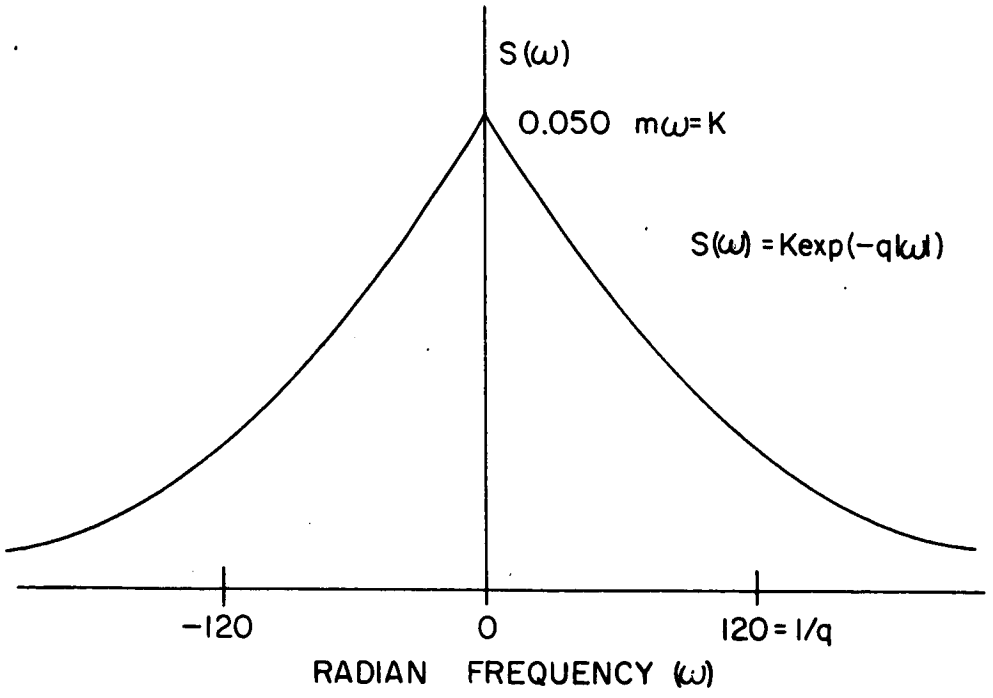

Fig. IV-10(a) Power Spectral-Density of Fading Carrier

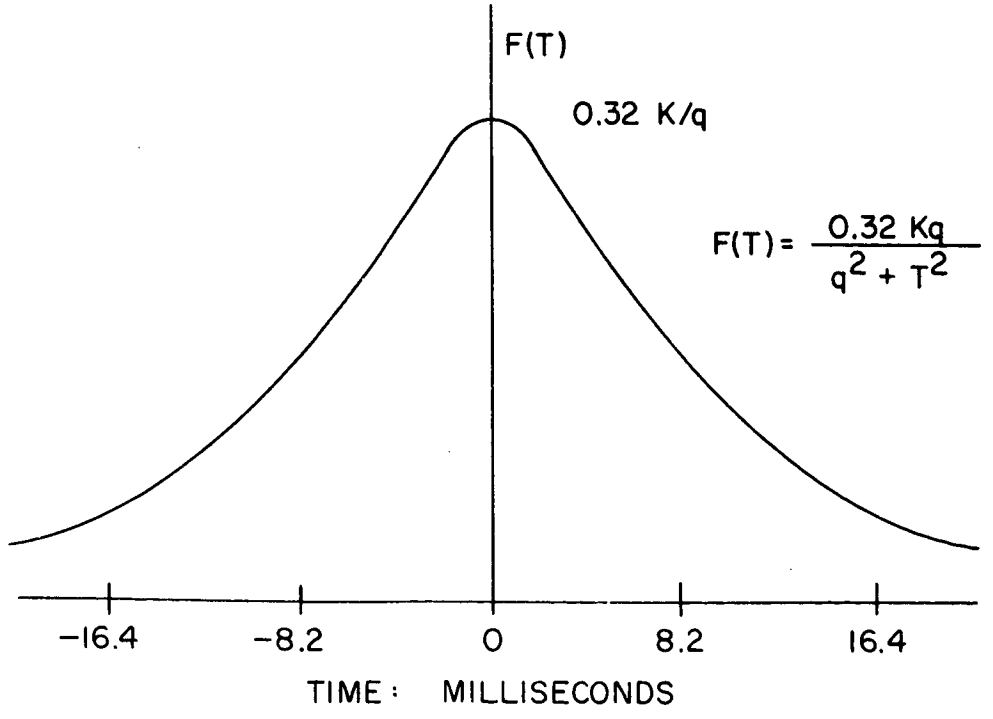

Fig. IV-10(b) Auto-correlation Function of Fading Carrier

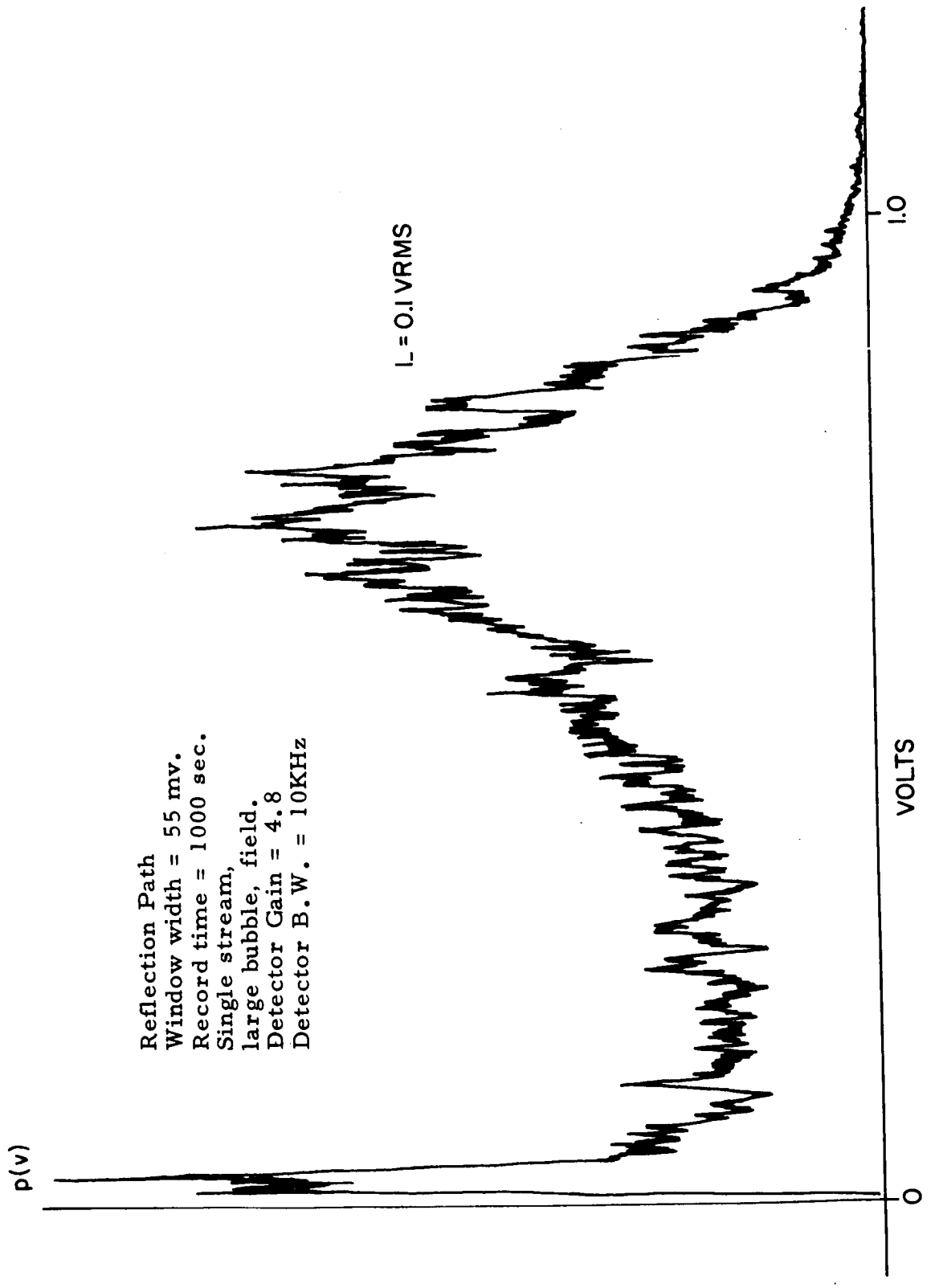

Fig. IV-11 Voltage Probability-Density Function of Fading CW Carrier

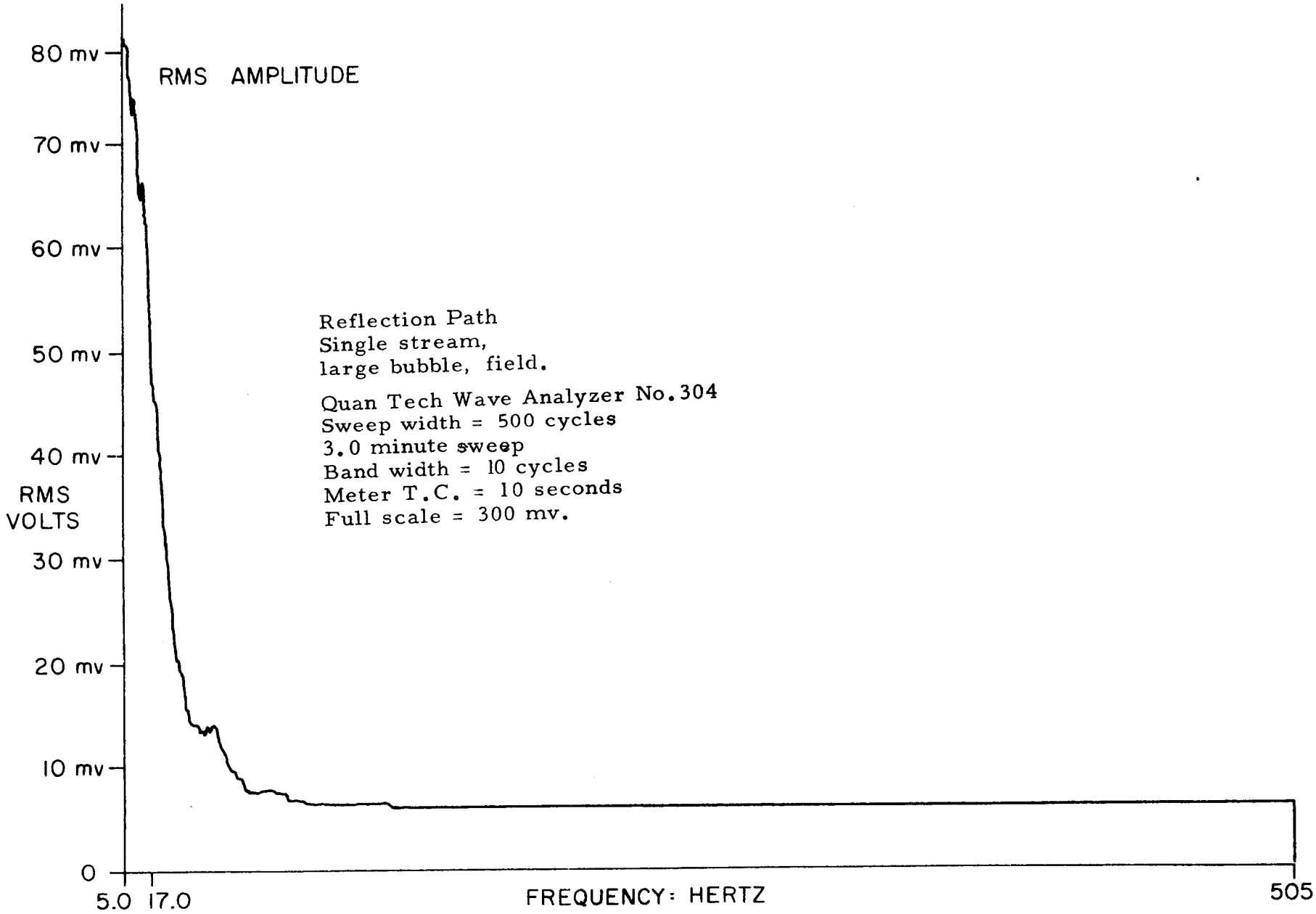

Fig. IV-12 Amplitude-Frequency Spectrum of Fading Carrier

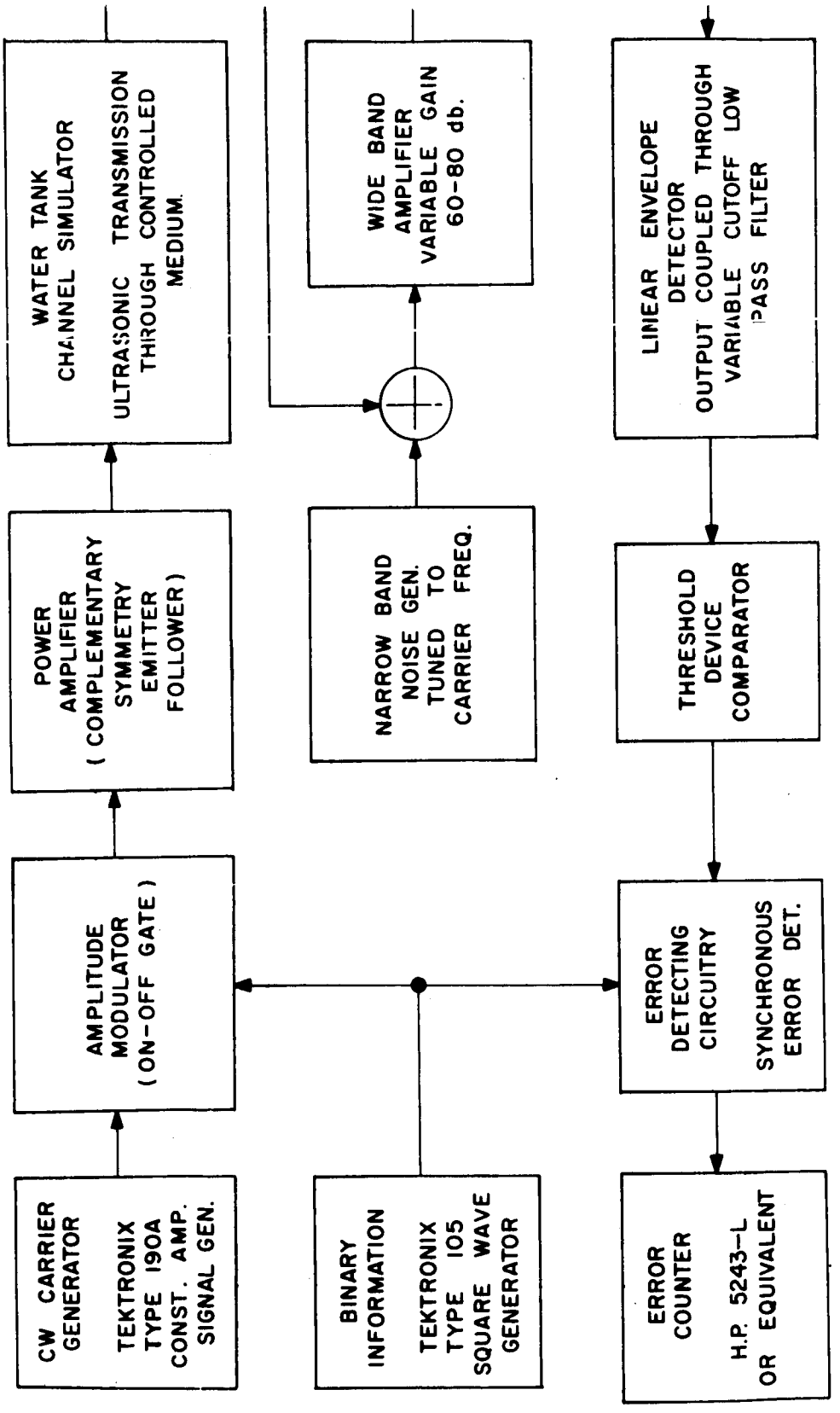

Fig. IV-13 Basic Binary AM Communications System Block Diagram

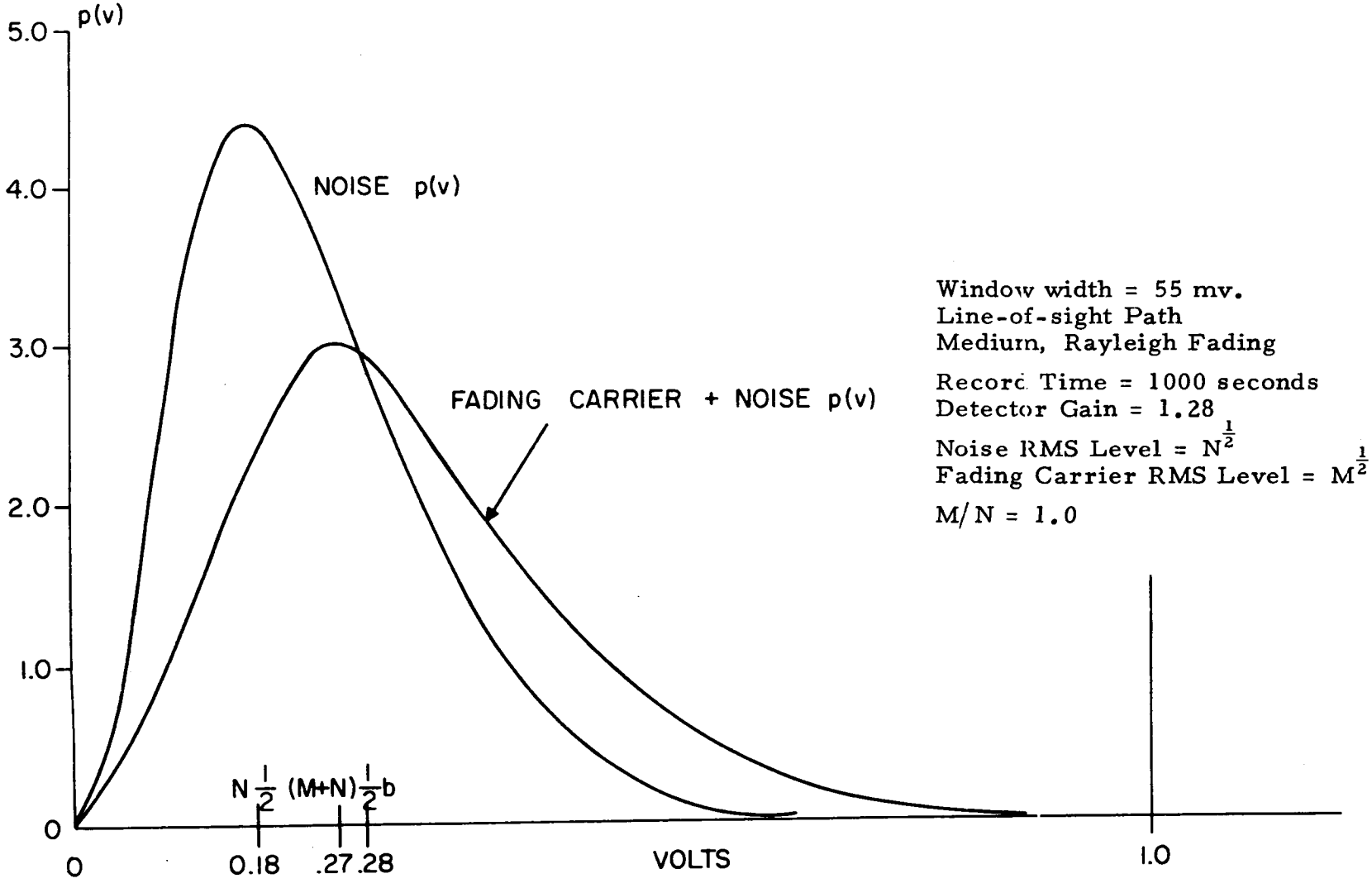

Fig. IV-14 Voltage Probability-Density Function of Noise and Fading Carrier and Noise

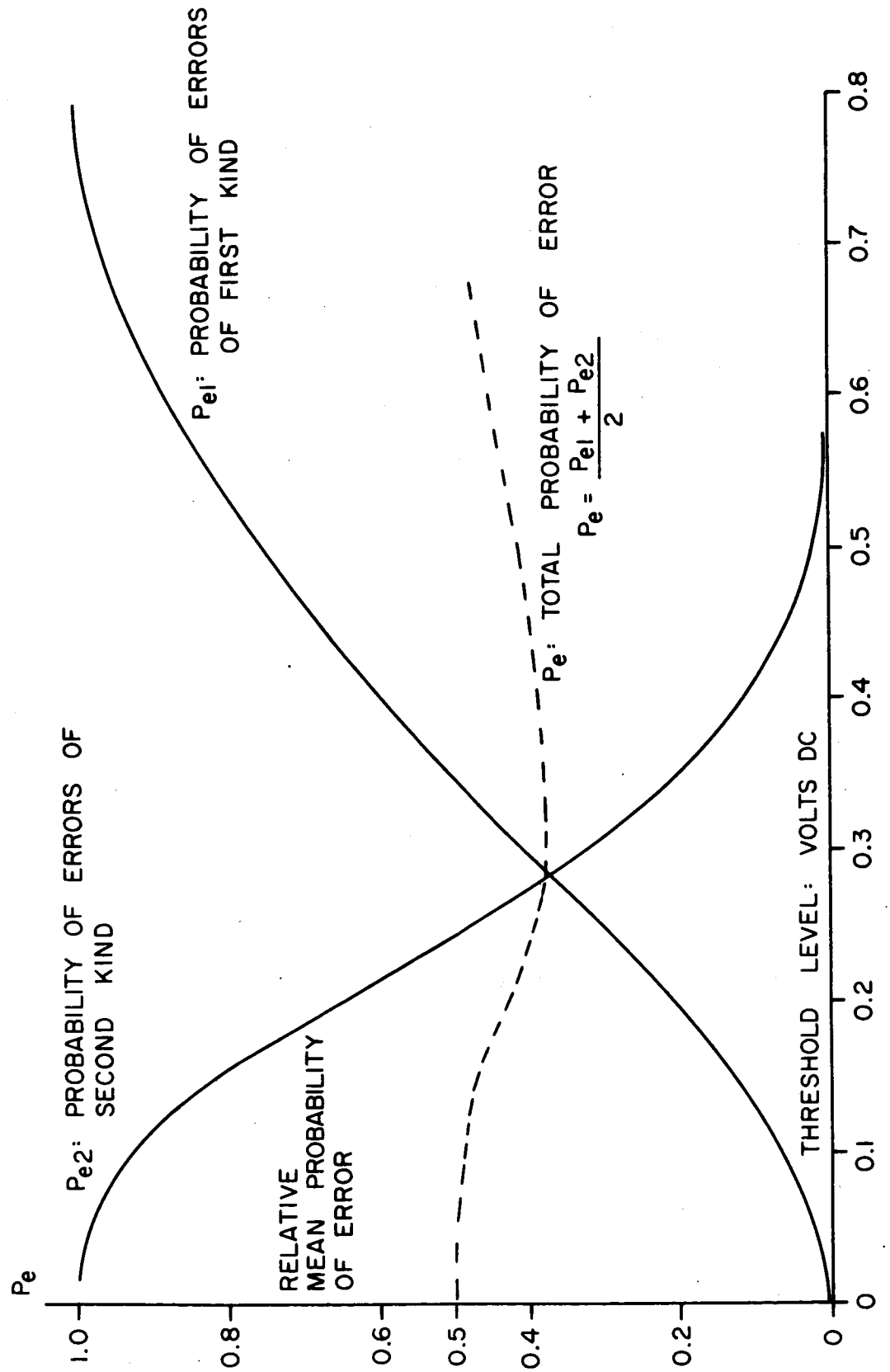

Figure IV-15 Probability of Errors of First and Second Kind versus Threshold Level, V^{th}

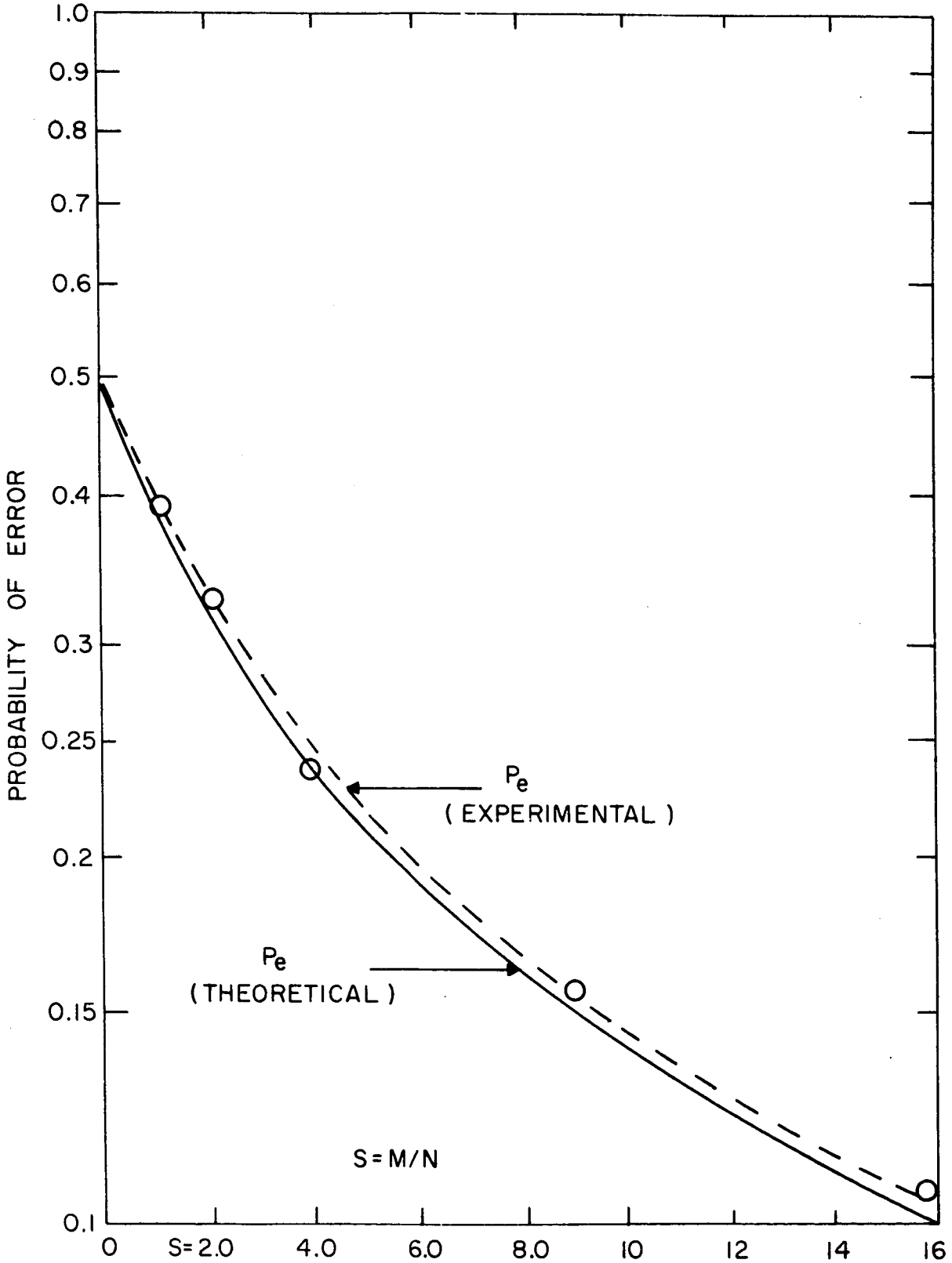

Figure IV-16 Total Probability of Error versus Carrier to Noise Power Ratio, CNR

IVb. Transmission of Binary FSK Signals Through a Fading Channel.

In earlier reports it has been shown how the water tank, channel simulator may be used to test the design of a binary AM communications system. We shall now use this same channel simulator to evaluate the design of a binary FSK communications system where demodulation is accomplished by an FM discriminator.

Figure IV-17 shows the basic binary FSK communications system block diagram. The binary information to be transmitted is in the form of a 1010 sequence since this sequence yields the highest information rate for a fixed bit interval. This binary information is in the form of a square wave, r(t), as shown in the ideal transmitter model of Figure IV-18. Before this square wave is used to modulate the FM transmitter (VCO), it is band-limited to its fundamental frequency, $1\Omega 2T$, thereby reducing the required bandwidth for transmission. The ideal output waveform of the FM transmitter is then shown in Figure IV-18 with center frequency of 4.0MHz and peak deviation, Δf.

In practice, the need for the ideal low-pass filter of Figure IV-18 is eliminated by the use of an Exact, type 301, Function Generator which supplies both square and sine wave synchronous outputs. The sine wave output is used to modulate the FM generator and the square wave output is used to synchronize the error detecting circuitry.

The FM generator is of the voltage-controlled astable oscillator type and its operation may be considered as ideal in this application. The center frequency of the oscillator for zero modulation is 4.0mhz and peak deviations of 500 khz are obtainable. Also, the oscillator accepts modulation rates to 100khz with negligible distortion. Its modulation sensitivity is of the order to 0.27 millivolt/khz deviation. The output of this FM oscillator is passed through a series tuned band-pass filter which accepts only fundamental FM signals.

The above generated FSK signal is now passed through an impedance step-down, power amplifier and fed to the water tank, channel simulator. The channel simulator may be used in any of the modes discussed in Section I to simulate any desired propagation conditions. A fading, noisy channel will be simulated in this Section. The output of the channel simulator will be combined with the output of a noise

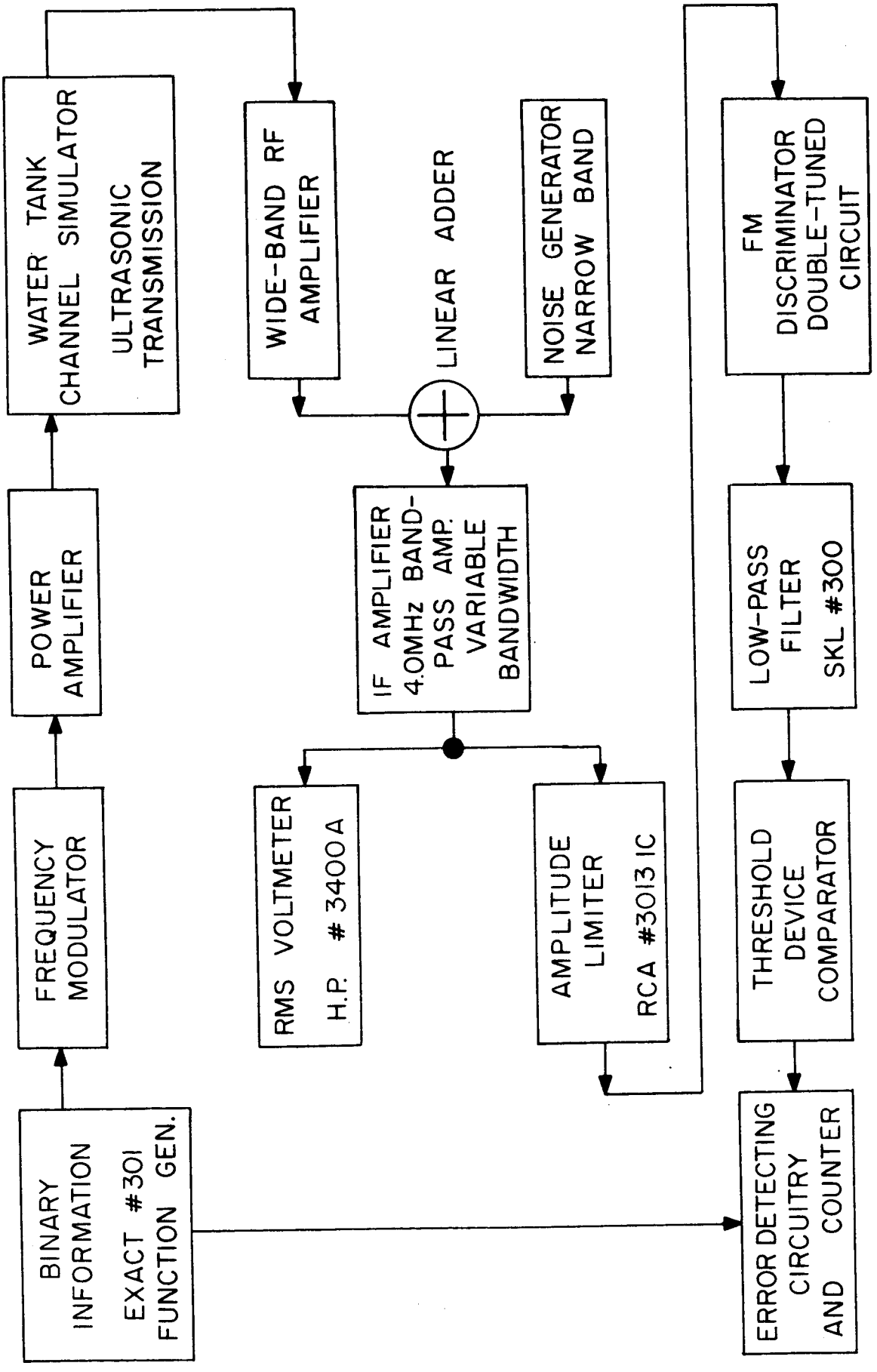

Fig. IV-17 Basic Binary FSK Communications System Block Diagram

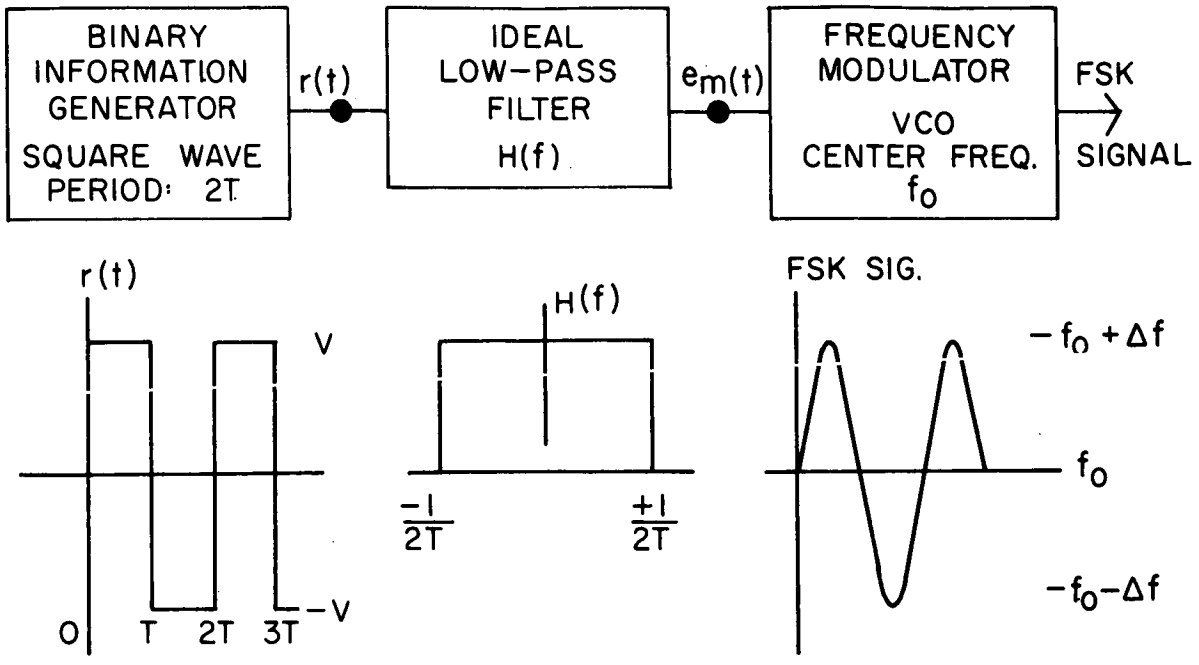

Fig. IV-18 FSK Transmitter Model

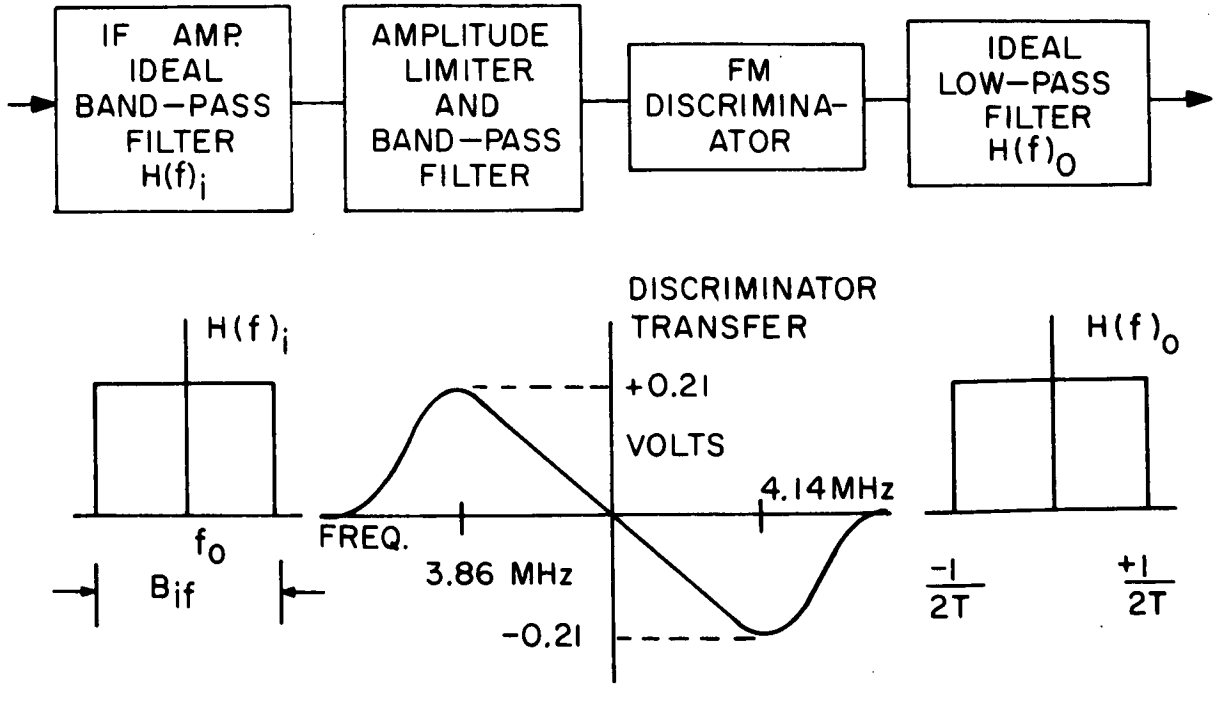

Fig. IV-19 FSK Receiver Model

generator and thus delivered to the receiver input.

As seen from Figure IV-17, the combined received signal (through the channel simulator) plus noise is passed through an IF amplifier. Actually, the IF amplifier here is symbolic of that which would be encountered in an actual communications system at this point; the IF and RF frequencies for this model are the same. The IF amplifier is a simple parallel-tuned circuit of 4. Omhz center frequency and variable bandpass from 40 khz to 200 khz. Thus, the input signal and noise are band-limited at the input to the receiver. From the theory and for the simplifications of calculations, an ideal rectangular band-pass characteristic is assumed for the IF filter; an assumption which appears to be experimentally valid.

The output of the IF filter is then fed to an amplitude limiter whose threshold is 450 microvolts at the carrier frequency. The limiter can handle a maximum input of approximately 2 vrms. Hence, by maintaining the minimum input signal level above 100 millivolts rms in this experiment, we may consider the limiter as nearly ideal. The output of the limiter is again filtered to retain only the fundamental limited signal. The rms carrier to noise ratio, CNR, is measured at the input to the limiter.

An ideal FSK receiver model is shown in Figure IV-19. From Figure IV-19 we see the characteristic transfer function of the discriminator. From the measured transfer charcteristic we see that the center frequency of the discriminator is 4. Omhz and the maximum peak input frequency deviation is 140khz. Hence, the frequency discriminator proves to be the limiting component of the dynamic range of this system. Also, we see that the output of the discriminator is essentially symmetrical with frequency and its peak output voltage corresponding to maximum peak input deviation is 0. 21 VDC.

The output of the frequency discriminator is then passed through a low-pass filter to remove noise signals not in the base-band. The ideal low-pass filter characteristic is shown in Figure IV-19 but in practice this filter will be approximated by a Gaussian low-pass filter of three poles. We shall see that these practical approximations shall not seriously degrade system performance.

The output of the low-pass filter is now continuously sampled by a threshold device which yields a logical (1) at its output when the input is above a threshold level and a logical (0) when it is below. The output pulse train of this comparator is then sampled at mid-band by the error detection circuitry.

Once one has shown that the overall binary FSK communications system closely approximates the theoretical one over a noisey channel, then one may investigate the performance of this system over a fading channel. Since the most common fading channel is one which produces Rayleigh distributed multiplicative disturbances, we shall again simulate the Rayleigh fading channel of Figure IV-6.

As explained in Section I, a Rayleigh fading channel simulation may be obtained by producing random signal reflection over a line-of-sight path. If the bubble field is adjusted for the proper intensity, the resultant signal fading will be Rayleigh distributed and have the power spectral-density and auto-correlation function of Figure IV-7. With the characteristics of the channel known, one can obtain a satistical evaluation of the system performance. Such a theory is set forth in another section of this report.

A suitable method of system evaluation and analysis for the case of transmission over a fading channel is the observation of the received signal distribution functions. In analogy to the procedure of Section I, the conditional probability-density distributions of a received mark or space will be analyzed to yield the average P_e and other insights of system performance.

A simple test of system performance is obtained by simulating the fading FSK signal with the additive noise generator output set to zero. Here, it was seen that the limiter circuit may no longer be considered ideal as errors are recorded by the error counting circuitry in the absence of noise. For an rms carrier level of 0.1 volts, a peak deviation of 50 KHz, and a modulation index = 5, the average error rate was found to be: $P_e = 0.001$. This error rate in the absence of noise indicates that this overall system will be far less efficient over the fading channel.

Figure IV-20 shows the conditional probability density functions

of a received mark and space over the fading channel. Comparison of this plot with the corresponding one for a noisy channel shows that the fading channel produces a "smearing out" of the signal distribution. This phenomena is due to the signal suppression effects when the Rayleigh distributed signal level falls below the noise level. Hence, one sees from Figure IV-20 that this system's efficiency has decreased greatly over the fading channel.

Using the error detection and counting circuitry, and for the transmission conditions listed above, one may obtain values of average P_e versus CNR as shown in Figure IV-21. Here, for comparison, the theoretical P_e of the previous section is also plotted. It is obvious from the Figure that relative increases in CNR yield poor returns in terms of reduced P_e for the fading channel. Indeed, other methods of error reduction (diversity techniques, optimum signal design, etc.) must be considered to obtain low error rates for reasonable values of CNR.

From the results and techniques of this Section, it is apparent that a simulation technique may be used to evaluate system performance whenever system and channel complexity preclude or make difficult a precise mathematical evaluation. Also, using the channel simulator, system parameters can be experimentally optimized for highest efficiency while observing a cause-effect relationship.

In addition to the results shown above, the simulator is currently being used to continue an investigation into intermodulation of the multichannel FM signals transmitted via a time dispensive channel and to investigate the performance of phase locked loops and phase locked loops with fast acting AGC systems as detectors of fading signals. During the coming year preliminary work upon space and frequency diversity will be extended to a full scale effort.

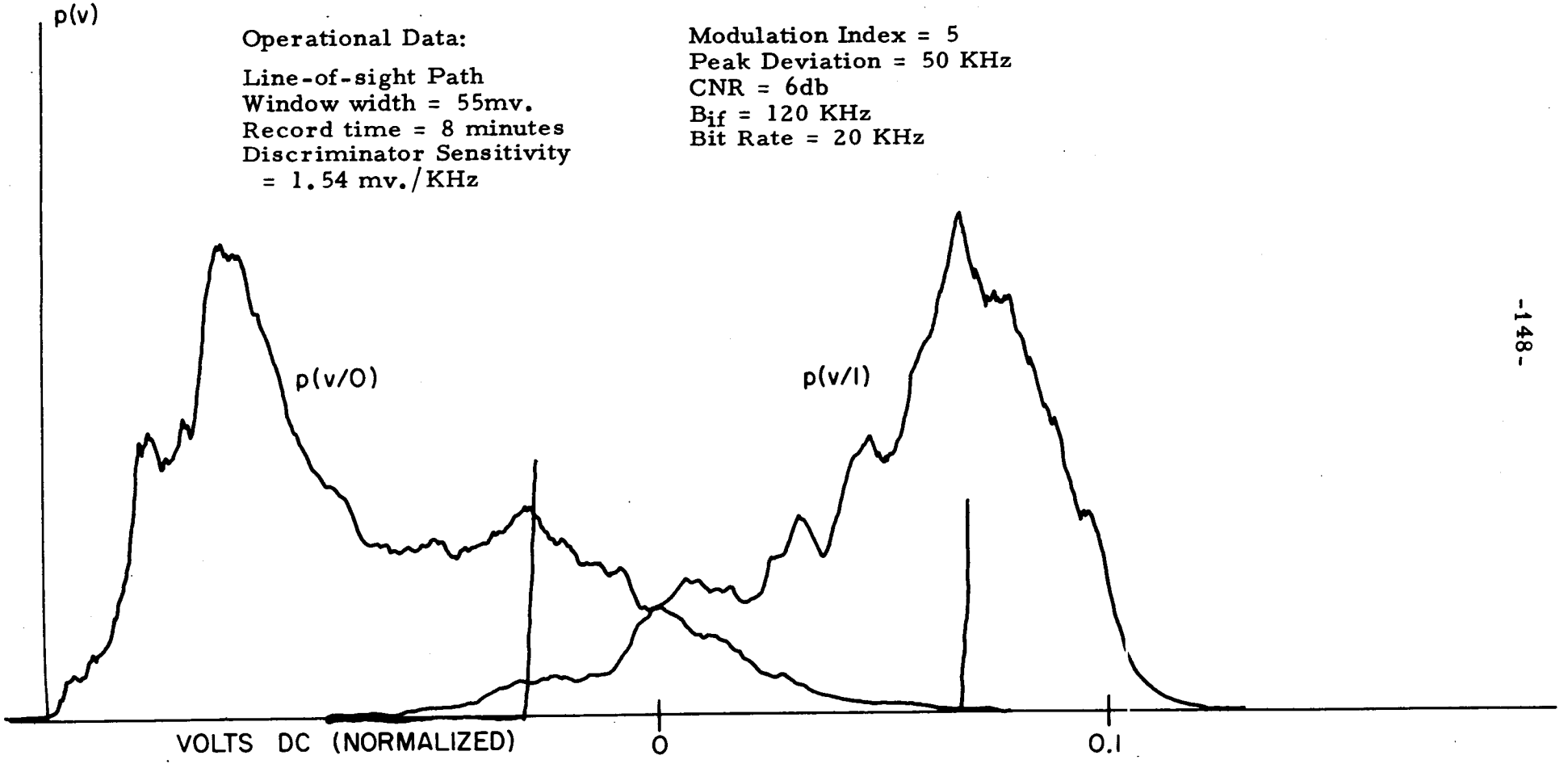

Fig. IV-20 Voltage Probability-Density Function for Conditional Occurence of Mark (1) or Space (0) Over Fading, Noisy Channel

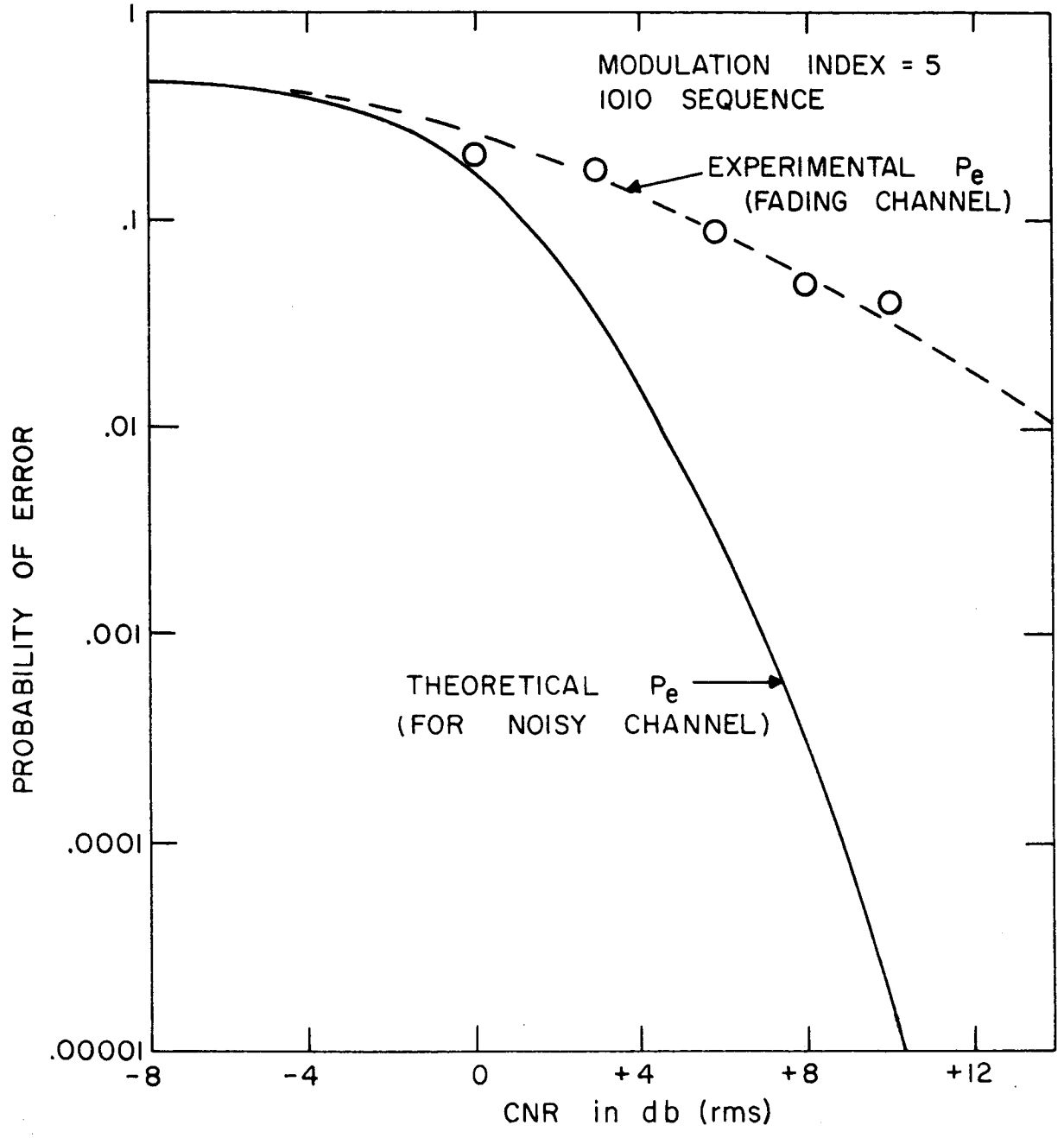

Figure IV-21 Probability of Error vs CNR

REFERENCES

(1) K.K. Clarke, Random Channel Simulation and Instrumentation, Conference Record, First IEEE Communications Convention, Boulder, Colo. June, 1965, p. 623-629.

(2) A.F. Culmone and E.A. Walvick, Binary Transmission in the presence of additive and multiplicative noise, May 1966, Research Report for NSF Grant No. GF 2538- also MSc Project Report, PIB, 1966.

(3) M. Unkauf, Binary system evaluation using a communications channel simulator, MSc Project Report, PIB, 1967.

(4) K.K. Clarke and D.T. Hess - Experiment # 13, "Graduate Communications Laboratory", May 1966 Report for NSF Grant GE2538.

(5) K.K. Clarke, Fading Channel Simulators, Proc. IEEE, Dec.,1966 [Ltrs. to Editor].

V. Transmitters and Repeaters.

A. Intermodulation

A short study was begun to investigate the effects of certain types of nonlinear systems on FM and pulsed signals. In particular, for pulsed signals, one is interested in intersymbol interference introduced by the memory effects of the system. The most common types of nonlinear circuits with memory in space communications are AGC, and travelling wave tubes. Indeed, because of the poor overload characteristics of travelling wave tubes, it is often suggested that a limiter or AGC be used in conjunction with such a repeater. The traveling wave tube repeater may also be used asa transponderf o r deep space ranging and Doppler measurement.

For the case of pulsed signals and an AGC it is possible to develop a fairly realistic model for the study of transients which are vital to the determination of intersymbol interference.

The basic differential equation of the AGC in the active region is given by

$$\frac{dv_o(t)}{dt} + \omega_c v_o(t) = K\omega_c v_o^{-k}(t) v_i^2(t) \qquad \text{(V-I)}$$

where

$v_i(t)$ is the input (r.f.) signal

$v_o(t)$ is the AGC control signal

ω_c is the AGC cutoff frequency $(\frac{rad}{sec})$

K is a constant determined by the AGC logs gain and the reference.

Equation (V-I) is derived by assuming a $(v_o)^{-K}$ variation of AGC control - which is quite realistic and can be fitted to practical AGC characteristics. The equation is in the Bernoulli form and therefore may be converted to a linear equation. This means that the memory can be separated from the nonlinearity. The result is the set

$$\frac{1}{\omega_o}\frac{dz}{dt} + z = K_1 v_i^2(t) \qquad \text{(V-2)}$$

$$f_o(t) = A_o z^{-\frac{K}{2K+1}} \qquad (V-3)$$

K_1 and A_o are (known) constants and $f_o(t)$ is the output (r.f.) voltage.

Equations V-2 can easily be solved for any r.f. input signal for z(f) and the result substituted into (V-3) to find the output r.f. signal.

Several examples have been worked out and preliminary indications are that it is possible to determine intermodulation effects and/or intersymbol interferences using this technique.

B. Travelling Wave Tubes

Just prior to the writing of this report, we received from NAPA, an RCA satellite simulator together with travelling wave tubes. A careful study was made of its operation in order to determine expedient means for the modification as an experimental unit to be used in the investigation of intermodulation effects in AGC, limiters and travelling wave tubes. After some initial difficulty in obtaining the desired output level, it appears that the unit may be operating satisfactorily. Unfortunately, at the time this report is being written, we have not yet procured satisfactory microwave signal sources, detectors etc. As soon as these become available, the experimental work can proceed.

VI - Future Work

The communications group of the Electrical Engineering Department under the auspices of NASA Grant NGR 33-006-020 has been solving several problems dealing with space communications. These problems deal specifically with NASA's satellite communication and tracking of satellites in deep space. The areas of direct concern to us are threshold extension devices, error rate analyses, synchronization problems and channel simulation.

1. Introduction

One of the very important problems facing NASA is the relaying of analog information from satellite to earth. This information can be sent directly or by first converting to a digital sequence and then transmitting the digital information. The problem is further complicated by the fact that many channels are to be relayed back to earth simultaneously. If an analog signal is to be converted to digital, an important question is the type of PCM (i. e. bi-phase or NRZ data, etc.) to be transmitted; whether each channel to be transmitted uses frequency division or time division multiplex techniques; and whether phase or frequency shift keying should be used. In any event, the combined signals are placed on an FM carrier and transmitted through a channel, whose characteristics are not completely known, to earth. The FM signal is then demodulated and the output signals separated. The FM demodulator used is an FM discriminator, Phase Locked Loop, Frequency Demodulator using Feedback or other threshold extension device. Since the signal received at the earth station is deeply embedded in noise a demodulator having extremely low threshold is required. The demodulated signal, if in digital form, must then be detected and reconverted to an analog signal. A problem is then encountered in this phase of the work. A typical detector (decoder) is an integrate and dump circuit representing the "matched filter". However, the noise out of an FM demodulator has a non-gaussian component - spike noise. In addition, the gaussian component of noise is non-white. Under these conditions, the integrate-dump detector is not an optimum detector. Another problem encountered in the detector is the bit synchronization problem. This problem arises because it is not possible to keep the local clock in exact synchronization with the transmitter clock. It should be pointed out that

the synchronization problem here is aggravated by the fact that the digital sequence is embedded in non-gaussian (FM) noise.

While many investigations of threshold extension and synchronization have been made neglecting the non-gaussian and non-white structure of FM noise the Communication Group of P. I. B. is actively engaged in this study[1, 2, 3]. Recent experimental work performed at the Polytechnic Institute of Brooklyn supported under this NASA grant indicates that the non-gaussian character of the FM noise is of paramount importance in determining threshold and error rates.

It must be emphasized that the study of threshold and the existence of low threshold devices as well as the design of low error rate detectors is predicated on the reduction of the spikes occurring at the output of the FM demodulator. Phase locked loops have been built at P. I. B. with thresholds of less than 3DB which is considerably less than that available commercially[4]. In addition we have shown that using an FM discriminator, under conditions of "exact" synchronization (laboratory simulation), the error rate is increased by a factor of 100 over that obtained using a Matched Filter Detector[2]. Theoretical results obtained taking into account the FM character of the noise closely verifies those experimental results.

2. Transmission of Analog Signals

Many signals are transmitted directly in analog fashion by modulating a subcarrier (AM or FM) and multiplexing it with other similar subcarriers (which may be carrying analog or digital data). These subcarriers are then usually modulated on an FM main carrier for transmission. This signal can be demodulated using a main (carrier) FM demodulator followed by subcarrier demodulators. Some of the FM demodulators currently being considered here at the P. I. B. are sub-optimum demodulators as the FM discriminator, Phase Locked Loop[5], Frequency Demodulator Using Feedback[6], and optimum demodulators as the Maximum Likelihood Estimator[6, 7] and Bayes Estimator[8, 9]. We are currently using computer (digital and analog) simulation to determine the behavior of these devices near threshold and to compare their threshold extension capabilities.

Sometimes analog signals are converted into digital form (PCM) for transmission and then reconverted back to analog after detection.

This conversion process results in a threshold effect of its own and depends both on the type of signals used and the nature of the noise coming from the demodulator. Some work has already been begun on determining the relationship between the output signal to noise ratio of the data and the output signal to noise ratio at the main discriminator. The relationship is highly nonlinear. The effect of the spike noise has not yet been investigated and we believe this to be a crucial factor. This investigation is important in designing an optimized overall space communications system which does not have as its weakest link the threshold of one of the subchannels. The PCM demodulator exhibits a threshold effect similar in character to that found in FM demodulators. A study of this effect and how to mitigate it, especially under conditions of high data rate, represents part of the total effort to solve fundamental space communications problems utilizing our recently acquired knowledge of the nature of the FM noise.

3. Transmission of Digital Signals

Most signals are transmitted digitally even if the original signal is analog. Digital signals can be transmitted in many ways; they can be coded using a bi-phase, NRZ, etc., format. Frequency Shift Keying (FSK) or Phase Shift Keying (PSK) of each signal is possible and the resulting signals can be frequency division (FDM) or time division (TDM) multiplexed usually on an FM carrier.

We have already begun to compare these various systems. Again the problem of analysis is the understanding of FM noise, a subject with which we have a great deal of experience. For example, one obvious advantage of TDM rather than FDM transmission is that when a spike occurs it might cause an error in the bit being transmitted (TDM), but might cause many errors if FDM is employed.

The FM demodulators being studied are again the optimum demodulators: Maximum Likelihood Bayes Estimators and Match Filters, and the suboptimum modulators: FM Discriminator, Phase Locked Loop, Frequency Demodulator Using Feedback, etc.

The problems associated with high data rate are, of course, being considered. Thus, the wideband capabilities of these demodulators under conditions of low noise are currently under investigation.

Studies are being conducted to calculate and measure error rates of the demodulated and detected digital signals. This is inherently important when the original signal is digital (e.g. an astronauts heart rate). The error rates are also necessary for determining the performance of the communications links if the original signal is analog (PCM).

4. Synchronization Problems

While much of our error rate analysis and experimentation assumes perfect synchronization, two doctoral students and two masterers students, as well as faculty, have already focused attention to the problems encountered in synchronization. A comparison of various synchronization techniques is in progress. In addition we are attempting to determine the optimum synchronization technique to determine the effect of error rate increase due to imperfect synchronization of the carrier.

The problem of bit synchronization, a similar but distinct problem is also being studied. Narrowband phase locked loops have been constructed which are capable of extracting bit synchronization information from binary signals in FM noise. These devices use spike-detectors to correct errors caused by spikes. Preliminary results show an error reduction of up to 3 to 1 over that obtained using detectors not incorporating these devices. More sophisticated spike detectors are being designed and an "optimal" spike detector is being investigated.

5. Summary of Proposed Work

a. Determine the SNR of optimal and suboptimal FM Receivers.
b. Determine the Error Rates obtained using these FM receivers and compare with the Matched Filter Receiver. Compare FSK & PSK, FDM & TDM, Bi-phase and NRZ.
c. Study the synchronization problem. Compare existing techniques. Determine the optimum synchronization procedure (Bayes receivers for synchronization information using various cost functions).
Study the bit synchronization problem considering FM noise.
d. Study the overall analog communications problem including : FDM, TDM, subchannel thresholds.

It should be noted that a, b, c and d all rely on an understanding of FM noise.

6. Proposed Work Utilizing the P. I. B. Water Tank Channel Simulator

Further work will be undertaken upon the measurement, characterization and control of the channel's properties. Specific items that will be included in this category include probability densities of carriers and envelopes of carriers, the correlation between separate channels with time, space, and frequency as variables, the fading rates obtainable, and the various types of multipath effects obtainable.

In addition to the auxiliary problems of measurement and control the channel will be used for major efforts in the areas outlined below:

a. A Study of error rates in single channel FSK systems using different types of detectors. A correlation between the detector characteristics, the fading characteristics and the error rates.

b. An experimental study of the use of diversity (space and/or frequency) to reduce error rates produced by single channel operation.

c. A continuation of work upon the distortions introduced in multichannel FM when it is transmitted via a time dispersive channel.

VII

Masters Theses & Doctoral Dissertations

Masters Theses

The following Masters Theses were partially supported under this grant:

1. 1966 - Abrams B., and Oberst, J., "Phase Locked Loop Threshold Investigations"
2. 1966 - Callahan, E., "Experimental Study of Noise Spike Generation In Phase Locked Loops"
3. 1966 - Stroh, R. W., "Non-Linear Performance of Near-Optimum Phase Demodulators"
4. 1966 - Sawyer, H.S., "Time of Arrival Measurements"
5. 1966 - Seberg, H.N., "Multilevel Threshold Detection"
6. 1966 - Anioral, A. "Band Limited F.M. Phase Distortion"
7. 1966 - Campbell, T. "Analog Simulation of Foster Seeley Discriminator"
8. 1966 - Chang, F. "FM Intermodulation"
9. 1966 - Corti, F. "A switching Modulator Using MOSFET's"
10. 1966 - Corwin, W. "Amplitude Variations in Phase Locked Loops"
11. 1966 - Dawson, R. "M.O.S. Multivibrators"
12. 1966 - DePompa, J. "Signal to Noise in Transfluxers"
13. 1966 - Dunn, S. "Video Pulse Target Simulator"
14. 1966 - Engle, D. "Interference and Noise in Micrologic Circuits"
15. 1966 - Eskenazi, I. "High Speed Data Transmission"

Masters Theses 1966 continued - 2 -

16.	1966 - Gordon, R.	"The Channel Vocoder"
17.	1966 - Hollis, W.	"F.M. Signal Distortion in Linear Filters"
18.	1966 - Livingston, J.	"Experimental Investigation of a Binary Data Transmission Scheme Using Synchronized Square Wave F.S.K. of Low Index"
19.	1966 - LoCascio, M.	"Design of Wideband Transistor Amplifiers"
20.	1966 - Marks, T.	"Techniques for Product Detection of Signle Sideband Signals"
21.	1966 - Peterala, D.	"Wideband F.M. Generator"
22.	1966 - Pollack, P.	"Analysis and Design of Transistorized A.G.C. System"
23.	1966 - Rosenblum, R.	"Applications of the M.O.S.F.E.T."
23.	1966 - Simpson, R.	"Transistorized TV Receiver"
24.	1966 - Steinman, A.	"Synthesis of F.M. Waves"
25.	1966 - Walvick E. and Culmone, A.	"Binary A.M. Transmission"
26.	1967 - Morartinis, N.	"Design of Amplitude Modulators"
27.	1967 - Yavuz, D.	"F. M. Spectra"
28.	1967 - Negro, V.	"I.G.F.E.T. Electrometer"
29.	1967 - Unkauf, M.	"FSK Via a Simulated Fading Channel"
30.	1967 - Maskasky, J.	"FM Intermodulation In A Fading Channel"
31.	1967 - Yang, M.	"FM Distortion In Linear And Nonlinear Filters"
32.	1967 - Jagodic, M.	"Wideband FM Generator"
33.	1967 - Farrow, M.W.	"Wideband Limiter Circuitry"

Doctoral Dissertations

The following Doctoral Dissertations were partially supported under this grant:

1.	August 1966	- Crepeau, P.,	"Bayes Estimation of FM Signals in Random Fading Channels"
2.	October 1966	- Nelson, E.	"The Response of an FM Discriminator to an FM Signal in Randomly Fading Channels"
3.	December 1966 (Tentative)	- Kreussling, F.	"Information Feedback Communications"
4.	June 1966	- Boorstyn, R.R.	"Realizable Approximations To Optimum Analog Demodulators"
5.	June 1966	- Pickholtz, R.	"Demodulation of Signals Transmitted Through a Random Channel"

VIII Papers Published

The following papers were partially supported under this grant.

1. K. K. Clarke, E. A. Nelson, D. L. Schilling

   "Analysis of an FM Discriminator with Fading Signal plus Additive Gaussian Noise," Proceedings of the 2nd Communication Technology, June 1966.

2. D. L. Schilling and E. Hoffman

   "Demodulation of Digital Signals Using an FM Discriminator" Proceedings of the National Electronics Conference, October 1966.

3. F. Kreussling and D. L. Schilling
   "Application of Feedback to M-ary PAM"
   Proceedings of the National Electronics Conference, October 1966.

4. D. L. Schilling and M. Smirlock
   "IM Distortion of a Phase Locked Loop Demodulator"
   Fourth Canadian Symposium on Communications, October 1966. Accepted for publication in the IEEE Transactions of the Comm. Tech Group.